NUREG/CR-0836
HEDL-TME 79-33
R3

PRESSURE SENSOR FOR USE IN THE LOSS-OF-FLUID-TEST (LOFT) REACTOR

Hanford Engineering Development Laboratory

HANFORD ENGINEERING DEVELOPMENT LABORATORY
Operated by Westinghouse Hanford Company
P.O. Box 1970 Richland, WA 99352
A Subsidiary of Westinghouse Electric Corporation
Prepared for the U.S. Nuclear Regulatory Commission
under Interagency Agreement DOE DE-AC14-76FF02170
NRC FIN No. B6228

Available from
National Technical Information Service
Springfield, Virginia 22161

NUREG/CR-0836
HEDL-TME 79-33
R3

PRESSURE SENSOR FOR USE IN THE LOSS-OF-FLUID-TEST (LOFT) REACTOR

Hanford Engineering Development Laboratory
T.R. Billeter

July 1979

HANFORD ENGINEERING DEVELOPMENT LABORATORY
Operated by Westinghouse Hanford Company
P.O. Box 1970 Richland, WA 99352
A Subsidiary of Westinghouse Electric Corporation
Prepared for the U.S. Nuclear Regulatory Commission
under Interagency Agreement DOE DE-AC14-76FF02170
NRC FIN No. B6228

Printed in the United States of America
Available from
National Technical Information Service
U.S. Department of Commerce
5285 Port Royal Road
Springfield, Virginia 22161

HEDL-TME 79-33
NUREG/CR-0836
R3

PRESSURE SENSOR FOR USE IN THE LOSS-OF-FLUID-TEST (LOFT) REACTOR

T. R. Billeter

ABSTRACT

Tests at temperatures up to 800° F and pressures up to 2500 psig were conducted at Hanford Engineering Development Laboratory (HEDL) to qualify an instrument for measurement of fuel-rod pressure in the Loss-of-Fluid-Test (LOFT) reactor. Operational characteristics of the selected pressure transducers are summarized for a series of static, quasi-static, and transient tests conducted for a period of about 700 hours.

ACKNOWLEDGEMENTS

The author acknowledges the assistance during the described work of C. R. Wandling, D. R. Brietenfeldt and T. M. Fleming.

CONTENTS

FIGURES

FIGURES Cont'd)

FIGURES (Cont'd)

FIGURES (Cont'd)

TABLES

PRESSURE SENSOR FOR USE IN THE LOSS-OF-FLUID-TEST (LOFT) REACTOR

I. SUMMARY AND CONCLUSIONS

Qualification tests have been conducted of a measurement system for determining the pressure of certain fuel rods in the loss-of-fluid-test (LOFT) reactor. Because of physical size (0.35-in. OD by 5.5-in. length) and operational characteristics, an eddy current device was selected as the most promising measurement transducer. The sensor must operate at pressures up to 17.2 MPa (2500 psig) and at temperatures up to 800°F. During the reactor transient caused by loss of coolant flow, sensor temperature and applied pressure will vary rapidly and significantly. Consequently, qualification tests included subjection of the sensor to rapid depressurization, temperature transients, and blowdowns in an autoclave, as well as to calibrations and various slow temperature cycles.

Calibration data show the sensor responds linearly for applied pressure, but with both temperature-dependent sensitivity and zero pressure output signal. Temperature compensation of signal output values was achieved with use of a derived temperature-dependent algorithm to transform the dc output voltage to indicate pressure. Because of the very rapid (up to 100°F/sec) temperature changes imposed, the sensor erroneously indicated pressure by a maximum of 18 percent of reading during some tests. In addition to the influence of magnitude and rate of temperature change on the observed pressure measurement error, a very significant factor pertains to the spatial distribution of the temperature field immediately adjacent to the sensor envelope. As proven during 700 hours of qualification tests, precision and stability of the sensor should be satisfactory for LOFT. Particular responses of each of the three tested units to imposed transient stimulus may be determined by reference to a summary table of acquired data.

On the basis of detailed, lengthy, and severe testing performed with pressure sensors intended for the LOFT reactor, the following conclusions appear warranted:

- All sensors yielded linear signal outputs for increasing pressure up to 2000 psig. Two of three sensors remained linear for pressures up to the maximum of 2500 psig. Zero pressure output and sensitivity must be determined for each sensor by calibrations at specific temperatures. Plotted curves summarize calibration data with a best-fit straight line of appropriate slope and intercept values for each temperature.

- For improved accuracy, a temperature-compensating algorithm must be derived to transform output signal to indicated pressure. The second order polynomial algorithm approximates the temperature dependence of the zero pressure output and sensitivity.

- Each sensor responds with distinctive characteristics to imposed temperature transients. Inaccuracy should be anticipated whenever the applied stimulus results in temperature differences between the two sensor coils. However, for temperature rates up to 100°F/sec, the sensors have exhibited maximum errors less than 18% of reading. Furthermore, the maximum error usually occurs subsequent to reaching the maximum applied temperature rate. Because of this event sequence, quite accurate pressure measurements should result during initial phases of the LOFT blowdown.

- The exact response of the sensor to temperature transients depends upon the rate and magnitude of the imposed temperature excursion and significantly upon the complex spatial temperature field existing adjacent to the sensor envelope.

- One sensor (S/N-01) exhibited data during transient testing suggesting possible mechanical interference between internal moving parts of the sensor. As a result, occasional discontinuities result in the values of indicated pressure during imposed temperature transients (see Figures VIII.31 and VIII.32).

- Temperature variations of only the 16-foot signal cable affect the magnitude of the sensor output signal. The temperature-induced variations of cable characteristics result (see Figure VIII.45 and VIII.46) in nominal errors equivalent to 2% of sensor reading.

- Calibration data remains nearly independent of the immediate surrounding of the sensor. When encapsulated within a metal enclosure for tests in the autoclave, the sensor yielded data (Figure VIII.17) closely resembling data (Figure VIII.13) obtained with a bare sensor.

- All sensors completed at least the initial 500-hour test sequence. During installation into the autoclave one sensor (S/N-02) failed, apparently due to a conductor-to-shield short of the signal cable. Coiling the signal cable for placement in the autoclave appeared to be the cause of failure because of the coincidence of the failure with installation efforts.

- Repair of the cable (of S/N-02) in the area of the connector required dexterity and attention to proper preparation and protection of the brittle conductor wires for soldering. Similar care must be exercised during installation within the LOFT reactor.

- The sensor continued to give stable indications of pressure for periods of 72 hours at temperatures of 650^{0}F and for applied pressure of about 1650 psi. Results shown in Figure VIII.59 confirm the sensor yielded a precise record of the applied pressure.

- Each sensor and associated signal conditioning electronics should be calibrated and subsequently used as an integral measuring unit, thus avoiding measurement errors caused by variations of electronic units.

II. INTRODUCTION

This report summarizes development and qualification testing of pressure measurement instrumentation intended for use in the loss-of-fluid-test (LOFT) reactor. Certain of the nuclear fuel rods in the reactor will be prepressurized. Consequently, during the transient test the gas pressure within those fuel rods will vary rapidly and significantly. One constituent characterizing events within the reactor during loss of coolant is an accurate measurement of fuel rod pressure. Characteristics of candidate pressure sensors, each based on different physical operating principles, were evaluated during initial work phases. Supported by this evaluation, a sensor using eddy current techniques was judged to most nearly satisfy operating and physical characteristics specified for the LOFT pressure sensor.

Two units were initially procured for development tests. Relying on results obtained during those initial tests, a revised sensor was designed and used during subsequent tests of qualification units (four sensors procured). All units have been subjected to multiple iterations of the same series of tests noted below. The first five tests were completed with the sensor installed in a laboratory oven. The sixth test required use of an autoclave. Brief descriptions of each test in the series are presented below.

1. Calibration of the sensor at pressures of atmospheric to 2500 psig for increments of 250 psi and at temperatures up to 800^{o}F.

2. Depressurization from about 1850 psig to atmospheric pressure via a manually operated valve.

3. Temperature transient as caused by flowing cold nitrogen gas over the sensor exterior to decrease its temperature from 650^{o}F to 250^{o}F at maximum rates of at least -10^{o}F/sec. Applied pressure, usually maintained constant at 1850 psig, was occasionally reduced to atmospheric levels.

4. Slow temperature cycle by allowing sensor to cool by natural heat loss from 650°F to 250°F and then reheat to 650°F. Test conducted over a period of about 2 hours and at a constant applied pressure of 1850 psig.

5. Fast depressurization at 650°F as provided by a burst disk rupturing at about 2200 psig (test conducted only once for each sensor).

6. From an initial temperature of 650°F and pressure of 2700 psig, water surrounding a pressurizable enclosure containing the sensor is exhausted as rapidly as possible. Expulsion of water within 15 to 20 seconds creates a minimum sensor temperature of about 350°F. Following the blowdown, water floods the autoclave at a rate determined by the supply pump capacity (3 liters/hr.).

In addition to these tests, the sensors endure a series of vibrations repeated three times. Operating characteristics should remain unchanged due to the imposed loads.

In general, the sensor described in this report should be usable in severe environments up to 2500 psig and 800°F. Although the sensors will survive rapid variations of both temperature and pressure, data output during the transient may not accurately reflect the applied pressure, especially due to temperature gradients existing along the sensor during rapid temperature variations. As an overall purpose, the described work should assure development of a technical specification for procurement of production pressure sensors able to both withstand the LOFT environment and be fabricated by a commercial vendor.

III. SENSOR REQUIREMENTS

Within the instrumented fuel bundle for LOFT, the pressure sensor can be located either as an integral part of the fuel rod or as an attachment to auxiliary structures in close proximity. However, if the pressure sensor is not a part of the fuel rod, a small-diameter tube must be used to transmit the rod pressure to the measurement location. Because of the difference in environment for sensors located inside and outside of the fuel rod, the specifications for each is different, as noted in Table III.1. Sensors located within the fuel rod experience less severe temperature transients, but must be physically smaller. Because of space constraints within the reactor, direct attachment to the fuel rod is the preferred sensor location.

Functionally, the described pressure sensor provides a measurement of fuel pin plenum gas pressure. This measurement is useful for determining fuel pin failure by detecting a loss of pressure in the fuel pin plenum and also for characterizing the rate of depressurization. Sensors placed inside the fuel rod gas plenum must be small enough to fit within a nominally 0.37-inch inside diameter, 0.025-inch wall cladding of the nuclear fuel. The sensor will measure the internal gas pressure of the fuel rod. For much of its service life, the sensor will operate at 2000 psig and 650^{o}F. During imposed transients, the pressure sensor will be exposed to rapid variations of temperature and pressure of the plenum gas.

In addition to the requirements noted in Table III.1, the sensor is expected to withstand vibration loads prevalent during the transient and to have a lifetime of 1000 effective full-power hours.

TABLE III.1

PRESSURE SENSOR PERFORMANCE
REQUIREMENTS AND OPERATING ENVIRONMENT

PERFORMANCE:	
Range	Atmosphere to 17.2 MPa (2500 psig)
Accuracy	3% of reading or ± 172 kPa (± 25 psi), whichever is larger
Resolution	± 69 kPa (± psi)
Response Time	250 msec

OPERATING ENVIRONMENT:	Inside Fuel	External Mount
Flow	None	15 ft/sec, 60 lbm/ft^3
Media	Helium/fission-product gas/ UO_2 water vapor (10 ppm)	LOFT water chemistry
Radiation	2 x 10^{13} n/cm^2 sec 2 x 10^8 R/hr	2 x 10^{13} n/cm^2 sec 2 x 10^8 R/hr
Pressure	Atmosphere to 17.2 Mpa (2500 psig)	Atmosphere to 17.2 MPa (2500 psig)
	$\frac{dp}{dt}$ = 2.4 MPa/sec (350 psi/sec)	17.2 Mpa (2500 psig) 722kPa/sec (105 psi/sec)
Temperature	70 to 650°F 850°F for 100 sec. $\frac{dT}{dt}$ = 10°F/sec	70 to 650°F 800°F for 100 sec. $\frac{dT}{dt}$ = 260°F/sec

IV. CANDIDATE TRANSDUCERS

Because of the demanding characteristics of the required pressure sensor, a detailed appraisal of transducers of distinct operating principle was first conducted. A summary of the resulting appraisal (Table IV.1) shows the major items considered.

As a result of the assessment of the operating and physical characteristics of these sensor types, the small eddy current device (the only continuously operating device able to fit within the fuel rod) became the primary choice for evaluation tests.

TABLE IV.1

PRESSURE SENSING METHODS

METHOD	EDDY CURRENT	STRAIN GAUGE	MICROWAVE	CAPACITIVE	PIEZOELECTRIC
EMBODIMENT	SINGLE OR DOUBLE ELEMENT	UNBONDED, BONDED, SPUTTERED	RESONANT CHAMBER	PROXIMITY OF CAPACITIVE ELEMENT	CHARGE FROM PIEZOELEMENT
TEMPERATURE (^{o}F)	1300	650	1300	NOT KNOWN	750
SIZE, (in.)	0.25 DIA x 5	1 DIA x 3 LONG	2.0 x 1.5 x 2.0 (4 SENSORS)	RELATIVELY LARGE	0.4 DIA x 0.5 LONG
RESPONSE	MECHANICAL	MECHANICAL	MECHANICAL	MECHANICAL	TRANSIENT, NOT STATIC
RADIATION RESISTANCE	SLIGHT DECALIBRATION	UNPROVEN	SAME AS METALS	UNPROVEN	PROVEN (HALDEN)
ATTACHMENTS	ENERGIZING AND SIGNAL OUTPUT CABLE	ENERGIZING AND SIGNAL OUTPUT CABLE	COAXIAL LINE OR WAVEGUIDE	ENERGIZING AND SIGNAL OUTPUT	ONE CHARGE CABLE
AVAILABILITY	RESTRICTED	MANY VENDORS	LIMITED	BOEING DEVELOPED	SEVERAL
SPECIFIC VENDOR	KAMAN SCIENCES	BELL & HOWELL	HEDL	HYTECH, INC.	KRYSTAL, INC.

V. PRIMARY SENSOR DESCRIPTION

The principle of operation of the primary sensor candidate concerns the interaction between a metal plate (target) and the electromagnetic field of an adjacent coil. Proximity of the target and coil affect the impedance of the coil due to eddy current effects. Consequently, a transducer, with relative separation between a coil and an adjacent target dependent upon pressure applied to the transducer, may be designed to yield a signal proportional to applied pressure. Two metal targets, connected via a push rod to a bellows and spring-supported diaphragm, move in unison relative to two adjacent coils. The coils, excited with a 500 kHz signal source, comprise two arms of a balanced four-arm bridge. Pressure applied to the diaphragm causes displacement of the two metal targets relative to the energized coils, thereby changing the coil impedance. The resulting bridge imbalance yields a pressure-dependent signal output which is generated using the signal conditioner shown schematically in Figure V.1. As the maximum displacement of the diaphragm/target assembly approximates .005 in to .007 in., the pressure range of a particular sensor design mainly depends upon physical characteristics of the support springs. Physically, the sensor envelope is 0.23-in. diameter by about 5.5-in. long. However, for the LOFT design, a 0.35-in.-diameter outer shell was attached to the envelope for the purpose of reducing temperature gradients created during the severe temperature transients concomitant with loss of coolant. For development units (Figure V.2), an evacuated, stainless-steel enclosure acted as the thermal barrier. However, during initial evaluations a copper cylinder surrounding the sensor envelope (Figure V.3) proved to be more effective than the evacuated enclosure for reducing temperature gradients; therefore, the copper jacket was used for qualification sensors. Although shown with a 1/4-inch calibration tube as part of the sensor (end opposite signal cable), all except a 0.25-inch length are severed before assembling the sensor into a fuel rod. A 16-foot length of two-conductor, magnesia-insulated, 1/16-inch Inconel-shielded cable connected to signal-conditioning electronics (Figure V.4) acts as the signal transmission cable for the pressure sensor.

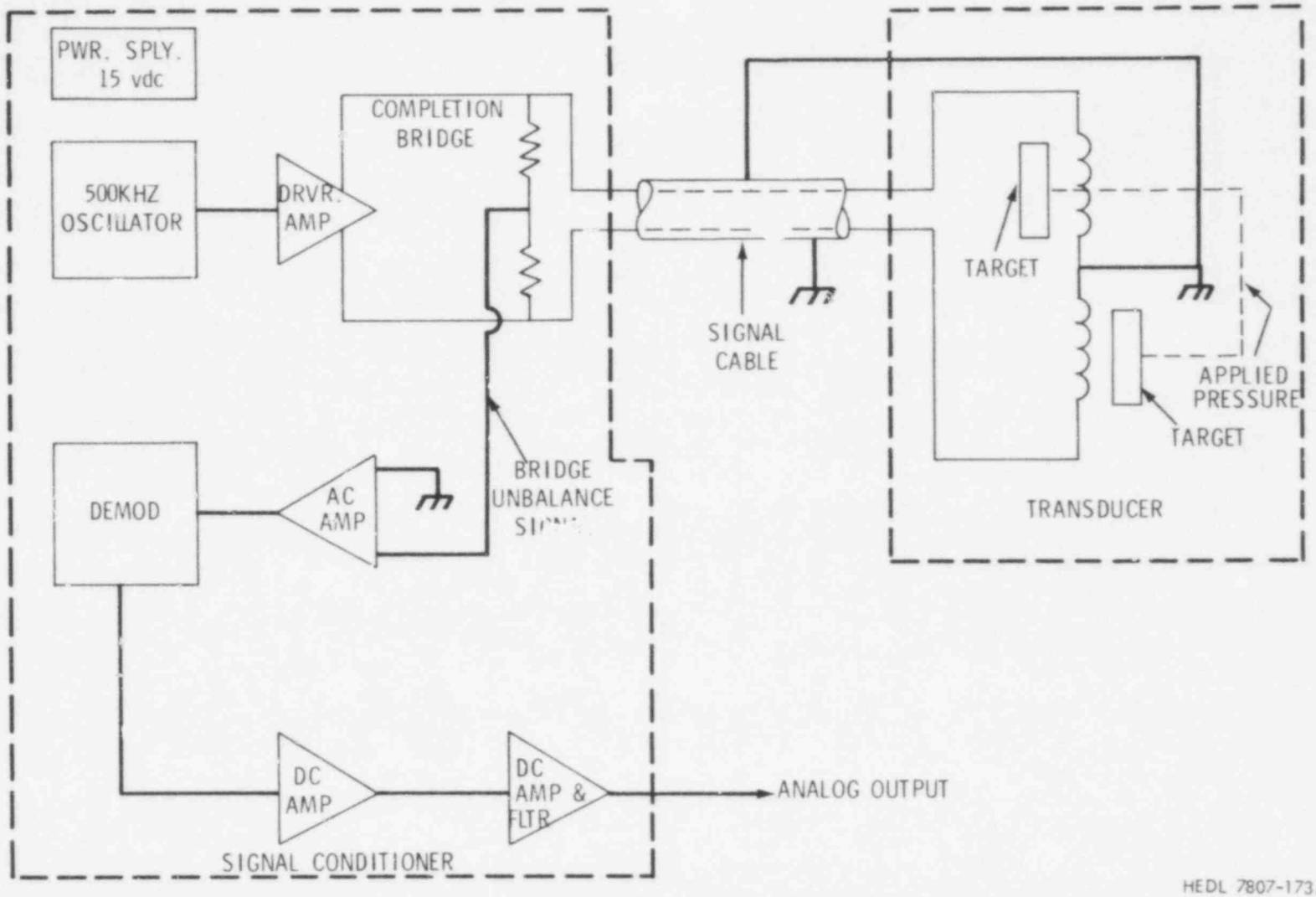

FIGURE V.1 Block Schematic of Complete Pressure Measurement System. (Neg 7808168-3)

FIGURE V.2 Development Pressure Sensor for LOFT.

(Neg 7801658-3)

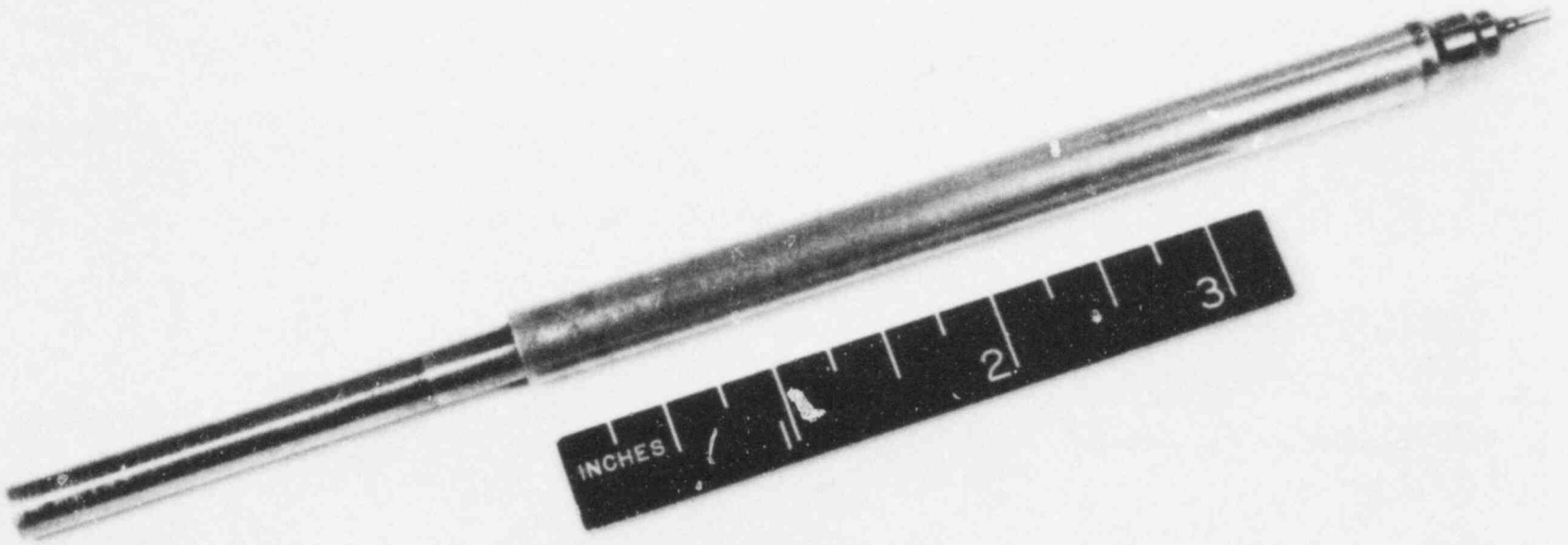

FIGURE V.3 Qualification Pressure Sensor for LOFT. (Neg 7811144-3cn)

FIGURE V.4 Complete Measurement Instrumentation for Qualification Tests. (Neg 7811144-4cn)

VI. TEST PROCEDURE

Qualification testing consists of a 500-hour series of static and dynamic tests conducted in a laboratory oven followed by 200 hours of transient and static tests in an autoclave of 6.4-litre capacity. Vibration of the sensor at critical frequencies concludes the qualification test rigor. During the first 500-hour series, the sensor is immersed in the test environment; in contrast, for autoclave tests the sensor is surrounded by a 7/16-inch OD by 0.368-inch ID by 6.3-inch long stainless-steel cylindrical enclosure which simulates the physical configuration of the nuclear fuel rod cladding.

During tests, data output is acquired and plotted using an HP 3052A data acquisition system. Reference pressure values originate from a Setra Model 204 capacitive pressure transducer and model 301C readout, both maintained at laboratory temperatures and pressures.

Figure VI.1, which depicts the placement of 0.020-in diameter Type K thermocouples on a development-type pressure sensor, shows one thermocouple in contact with the body and another (held on a coolant pipe and rotated about 180^{0} for clarity of presentation) displaced about 1/4 inch from the sensor body. The three coolant lines also appear positioned rotationally at 120 degrees with respect to each other. Except for closure of the clam-shell oven, a qualification pressure sensor installed in the oven facility and ready for testing appears as illustrated by Figure VI.2. To increase credibility of the data output from the pressure sensor selected for the LOFT reactor, a rigorous series of tests was planned for each of the three qualification units. Multiple repetitions of most of the below-described tests were completed for each sensor.

A. TESTS IN OVEN FACILITY

1. Calibration: Each unit is pressurized (and subsequently depressurized) at increments of 250 psi from atmospheric pressure to 2500 psig (as measured with the reference gauge) and for temperatures of 75, 250, 400, 650, and 700°F. Calibrations yielding the dc output signal as a function of applied pressure are conducted as the first test at both the oven facility and the autoclave.

2. Slow Temperature Cycle: Temperature of the sensor is decreased from 650°F to 250°F and then increased to 650°F over a total elapsed time of about 3 hours. Pressure is maintained at 1850 psig and the dc signal output is measured at 5-minute intervals during the test. Data acquired helps to determine sensor stability for imposed slow temperature variations.

3. Fast Temperature Cycle: Flowing cold nitrogen gas along the exterior of the sensor cools it from 650°F to 250°F at rates of at least -10°F/sec. Following the temperature decrease, gas flow stops and the sensor temperature increases to 650°F. Total elapsed time of the test is about eighteen minutes, although the minimum temperature occurs within one minute of test initiation. The sensor output signal measured at two data points per second for the first 74 seconds of elapsed time, and at periodically slower rates thereafter, reflects the effect of applying severe temperature gradients along the exterior of the sensor. Pressure applied to the sensor is maintained constant at 1850 psig for the test period.

4. Pressure Cycle: For a constant sensor temperature of 650°F, pressure applied to the sensor is adjusted to atmospheric pressure, 1850 and 2500 psig. Signal output at each pressure is compared with values obtained when the applied pressure is decreased from 2500 to 1850 psig and then to atmospheric pressure. Repeated periodically throughout the 500-hour test duration, this pressure-cycle test attempts to reveal possible long-term signal drift.

5. Pressure Transient: Except for one test, gas exerting 1850 psig pressure on the sensor is exhausted as rapidly as possible via a mechanically actuated valve. Measurement of the signal output during the pressure release permits evaluation of the time response of the sensor. Significantly, shorter exhaust times occur by placing a burst disk in the pressurizing line. Consequently, for one test a disk rupturing at 2181 psig is used to rapidly reduce applied pressure. In addition to providing data regarding sensor time constant, this series of tests subjects qualification units to multiple fast depressurizations.

B. TESTS IN AUTOCLAVE:

1. Calibration: Each unit is pressurized (and subsequently depressurized) at increments of 250 psi from atmospheric pressure to 2500 psig and for temperatures of 75, 250, 400, and 650^{O}F.

2. Transients in Autoclave: A test environment most closely resembling that expected in LOFT occurs for blowdowns conducted in an autoclave. For two of the test articles, both the sensor and about 14 feet of coiled signal cable reside in the pressure vessel; for the third, only the sensor is placed in the autoclave. Initially at a temperature of 650^{O}F and a pressure of 2700 psig, autoclave water pressure is reduced as rapidly as possible by opening an exhaust valve. As a result, water in the autoclave flashes to steam and exhausts from the pressure vessel. Coincidentally, a very rapid temperature change occurs. 1850 psig pressure applied to the sensor (inside an enclosure which physically simulates a fuel rod) remains nearly constant for this test. Measurement of the signal output provides a basis for determining pressure sensor signal independence of sensor temperature.

C. OTHER TESTS:

1. Vibration Tests: The test unit experiences vibration loads at 40 to 50 Hz of 0.5G for 40 seconds and 2G for 100 milliseconds. Motion occurs along the axis of the sensor. The test unit must survive (as demonstrated by subsequent calibration) three vibration cycles.

2. Irradiation: At least one of the qualification units is placed in a thermal flux reactor to evaluate the stability of the sensor operational characteristics. While in the reactor, pressure applied to the sensor is varied at 250 psi increments between atmospheric pressure and 2500 psig. Signal output measured during the irradiation period should yield repeatable data if the sensor remains impervious to radiation effects. At this date, the irradiation capsule is being fabricated in anticipation of tests in the N-ractor in the near future.

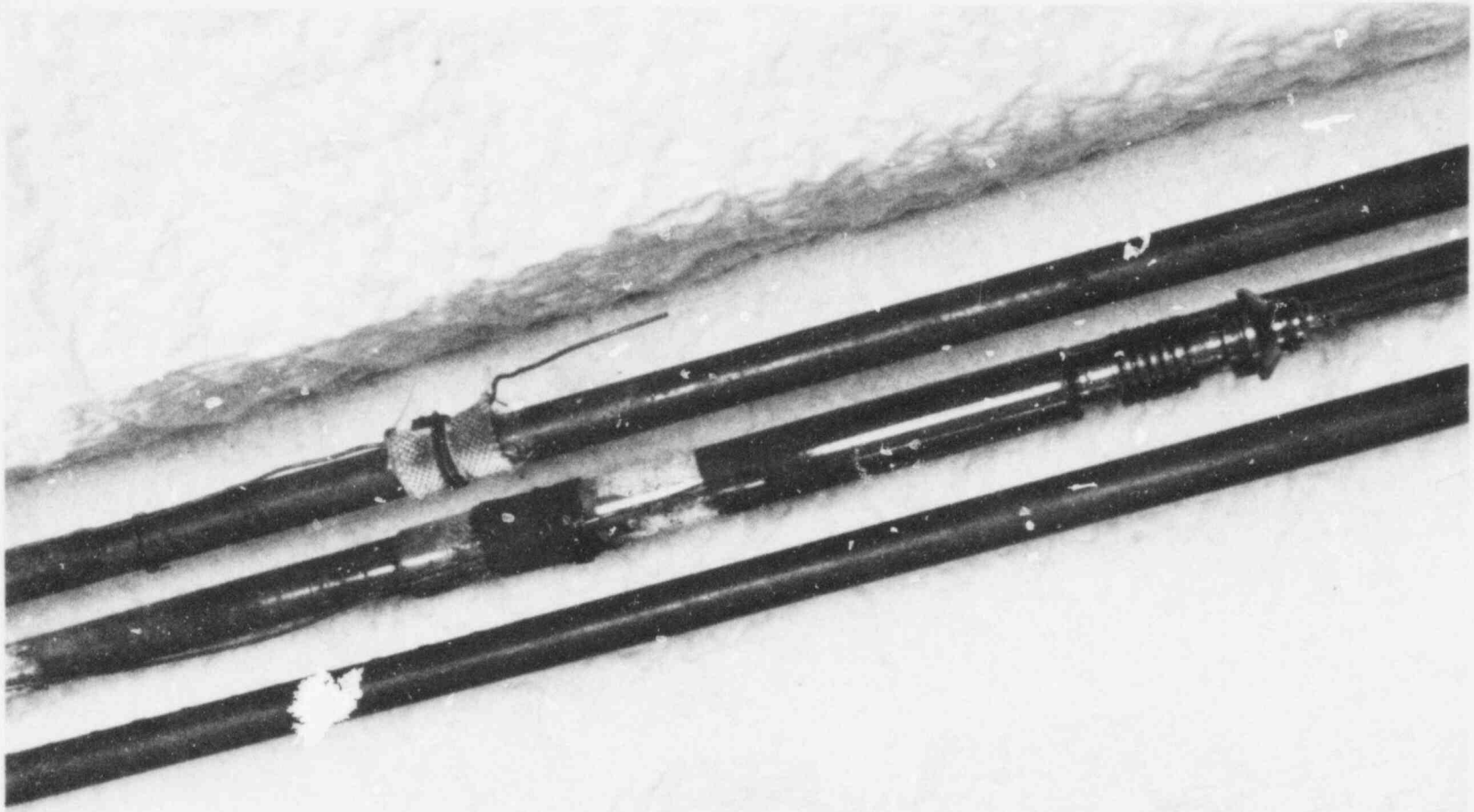

FIGURE VI.1 Thermocouple and Coolant Line Positioning During Tests of Sensor. (Neg 7804573-4)

FIGURE VI.2 Temperature and Pressure Control Unit for Pressure Sensor Qualification. (Neg 7801449-1cn)

VII. TEST FACILITIES

A. OVEN:

During initial tests, qualification units were placed inside a laboratory oven with a 1/4-inch pressurizing tube connecting the test device with the high-pressure argon gas supply. A schematic of the test facility (Figure VII.1) shows components required for performance of the previously described qualification tests. For the fastest depressurization, a holder for a burst disk connects to the pressurizing line at point "A". Pressure variations for calibrations and other tests result from adjustment of the high-pressure regulator at the supply gas cylinder. Inside the tube furnace, the assembly of the test article plus coolant lines, temperature monitors, and other components was oriented as shown in Figure VII.2. The complete oven test facility with a sensor installed appears in Figure VII.3. The outer stainless-steel enclosure has been removed for improved picture clarity. In addition to the oven used for heating the sensor, two adjacent tube furnaces (Figure VII.4) placed collinearly contain the signal cable, which is bent to allow heating of three five-foot sections.

B. AUTOCLAVE:

All qualification units were subjected to 200 hours of tests in a 6.4-liter autoclave. Prior to installation each unit was welded into a pressurizable enclosure to permit independent adjustment of both autoclave and sensor pressure. Also, the enclosure simulates the thermal barrier afforded by a LOFT fuel rod. Next, about 12 feet of signal cable are wound on a 5-inch-diameter mandrel and secured for insertion within the autoclave. However, for sensor S/N-01 only, the signal cable was not coiled and placed inside the autoclave, thereby permitting evaluation of the effects of coiling and subjecting cable to the autoclave environment. Figure VII.5 illustrates components of the test unit mounted within the autoclave head. Fast-response thermocouples measure temperatures within the enclosure near the sensor and also adjacent to the enclosure envelope--essentially the autoclave environment temperature. A schematic illustrating the location of components within the autoclave appears in Figure VII.6.

During blowdowns, pressurized water is exhausted via a manually operated valve. The rate of expulsion of water/steam depends upon the area of the exhaust orifice. Most blowdowns were conducted with maximum attainable exhaust orifice area, although some were rate limited by restricting the exhaust area. For the majority of blowdowns, the exhaust valve was closed and the autoclave feed water pump activated immediately after depressurization. Output signal amplitude variations were measured during the blowdown transient and for the following 15 minutes while water refilled the autoclave. The autoclave and auxiliary equipment employed during the transient tests appear in Figure VII.7.

During time intervals between blowdown tests, the sensor signal output was monitored to determine its stability for relatively long time durations. During these times, sensor temperature and pressure were maintained constant at about 1850 psig and 650^{o}F.

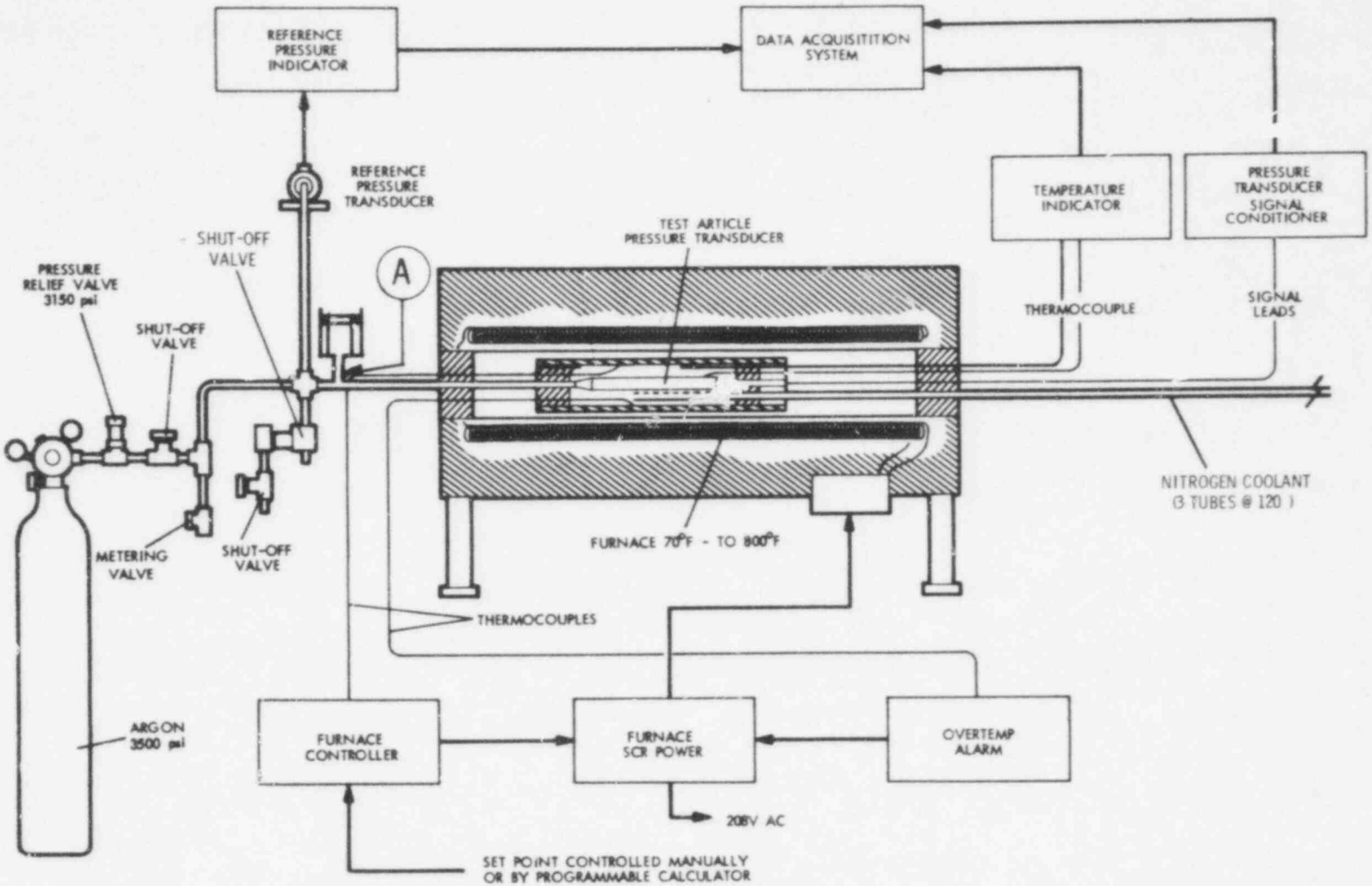

VARIABLE TEMPERATURE FACILITY FOR EVALUATION OF LOFT PRESSURE TRANSDUCERS

FIGURE VII.1 Variable Temperature Facility for Evaluation of LOFT Pressure Sensor. HEDL 7905-091.3

PRESSURE SENSOR TEST ASSEMBLY FOR TEMPERATURE AND PRESSURE TRANSIENTS

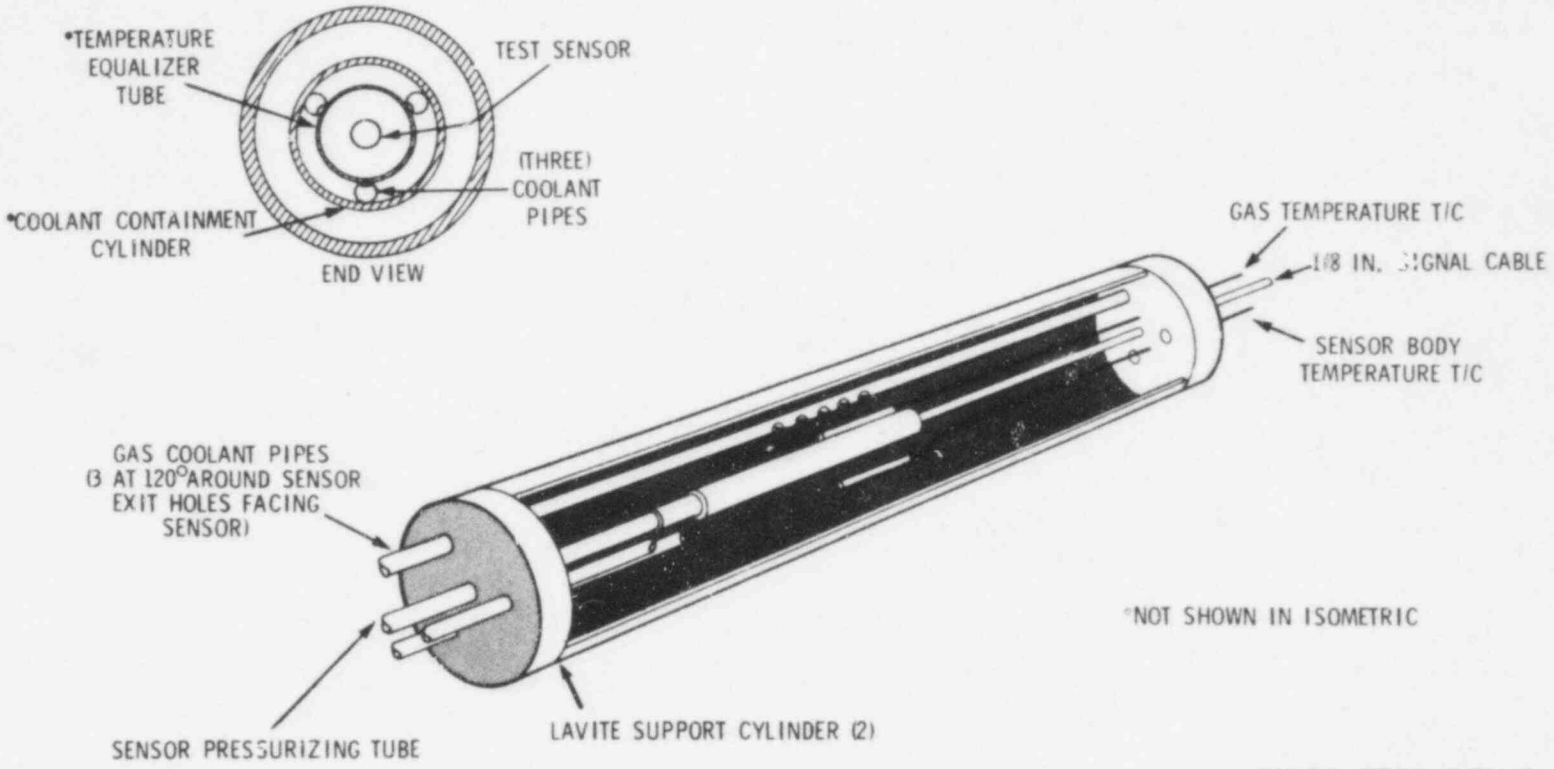

FIGURE VII.2 Pressure Sensor Test Assembly for Temperature and Pressure Transients. (Neg 7308168-6)

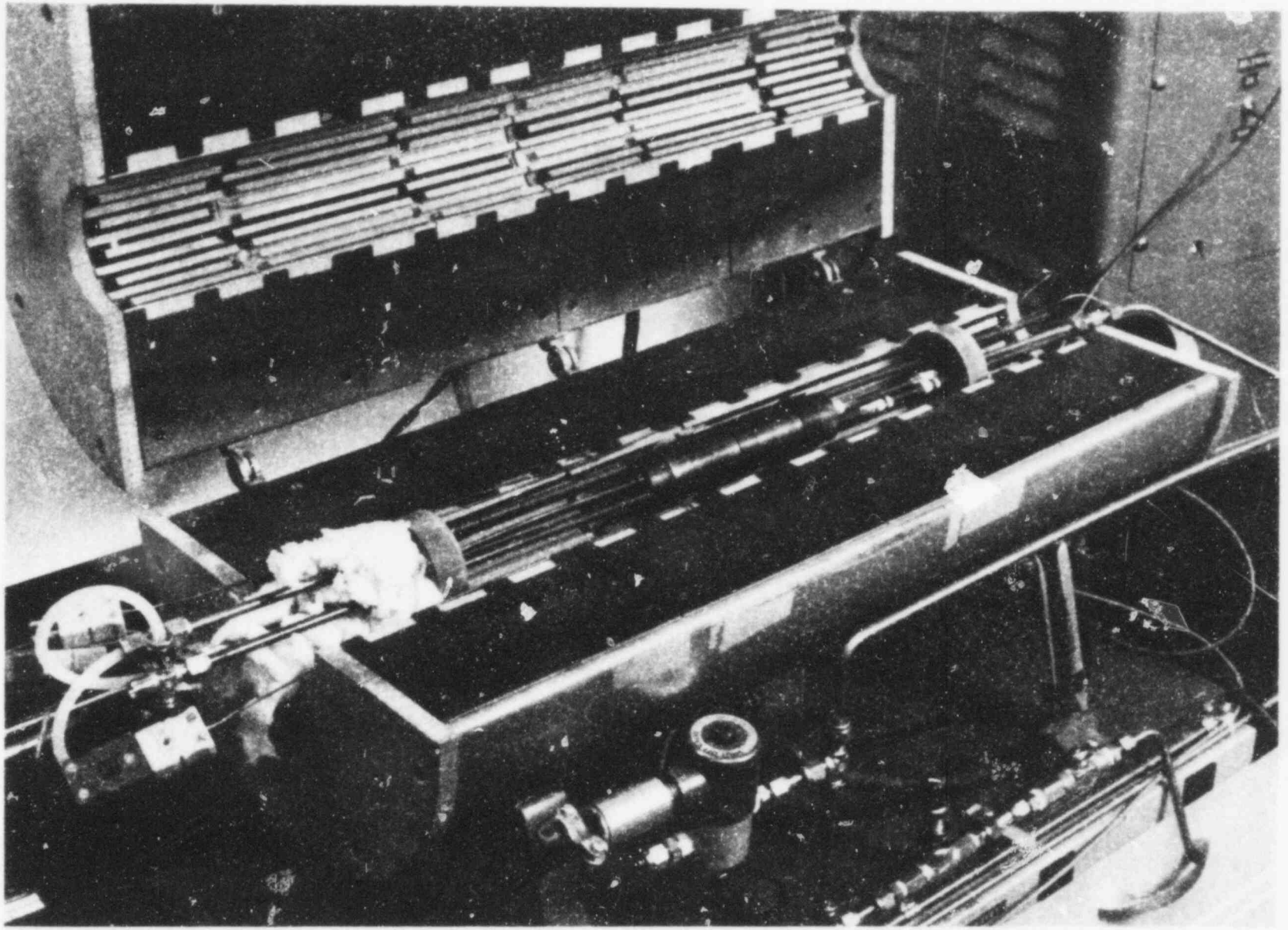

FIGURE VII.3 Sensor Placed in Oven Test Unit.

(Neg 7804573-1)

FIGURE VII.4 Ovens for Controlling Signal Cable Temperature. (Neg 7804573-3)

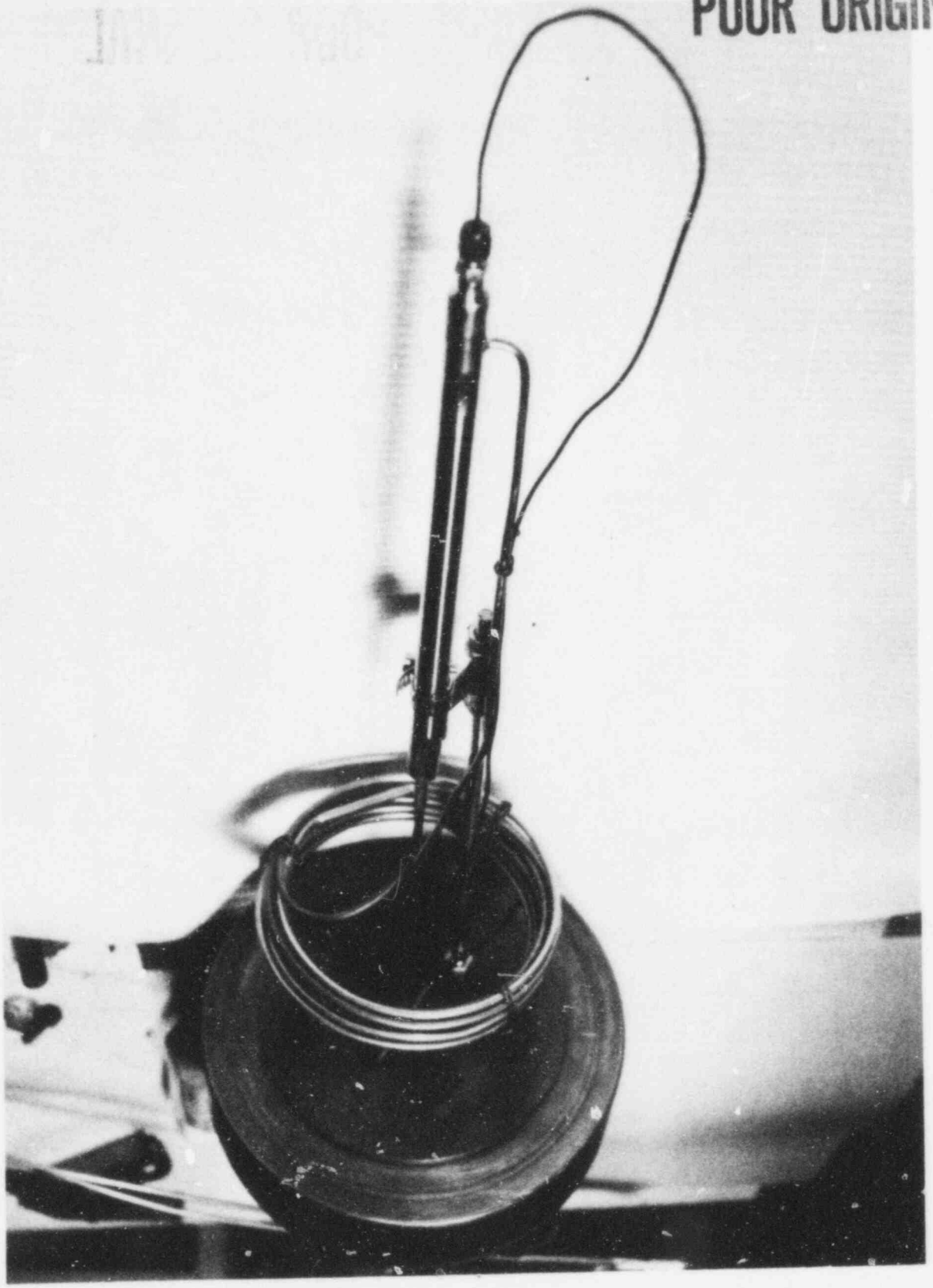

FIGURE VII.5 Encapsulated Sensor and Signal Cable Mounted for Tests in Autoclave. (Neg 7807800-7)

TEST ASSEMBLY FOR EXPERIMENTS IN AUTOCLAVE

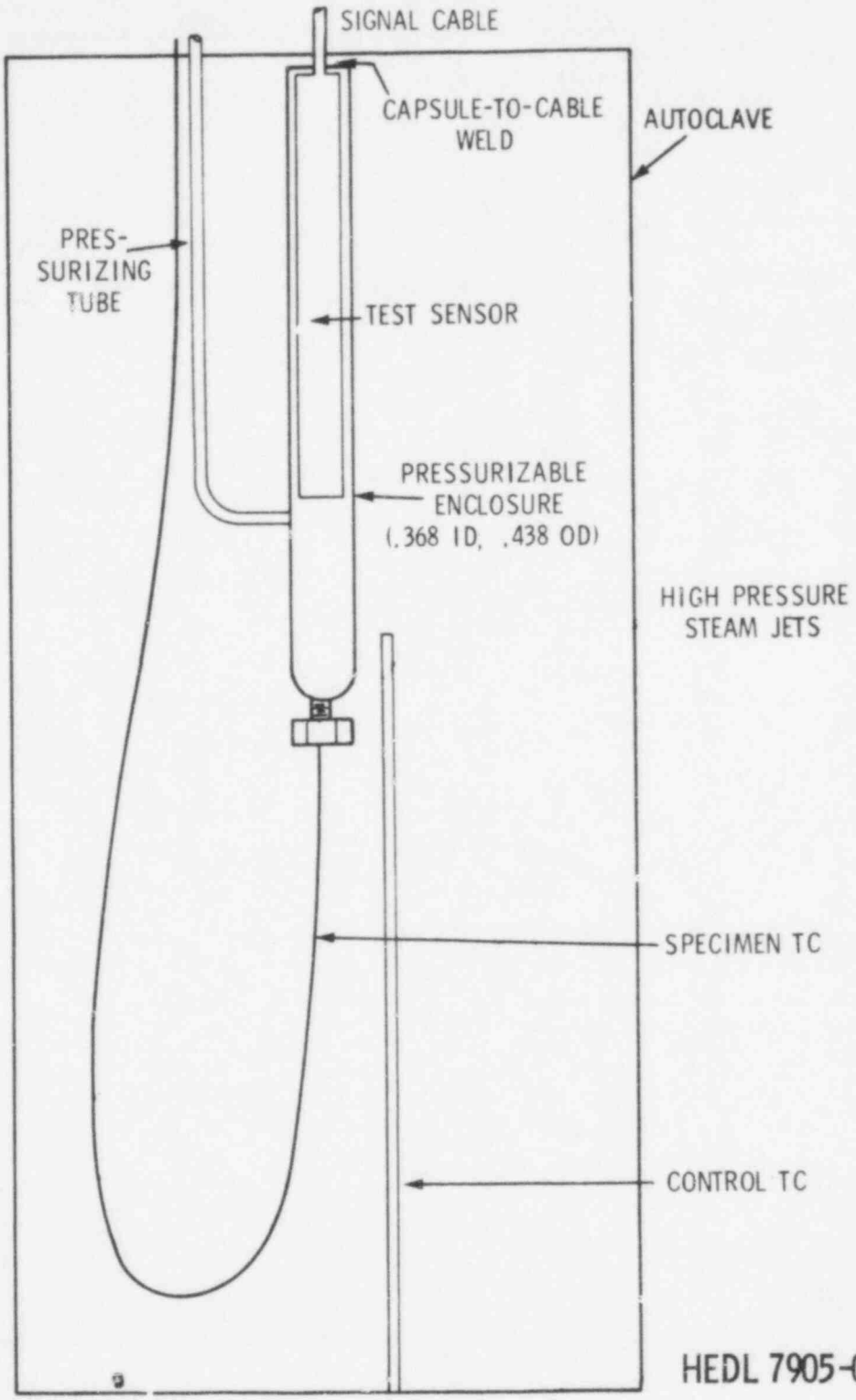

FIGURE VII.6 Component Placement Within Autoclave. (Neg 7808168-2)

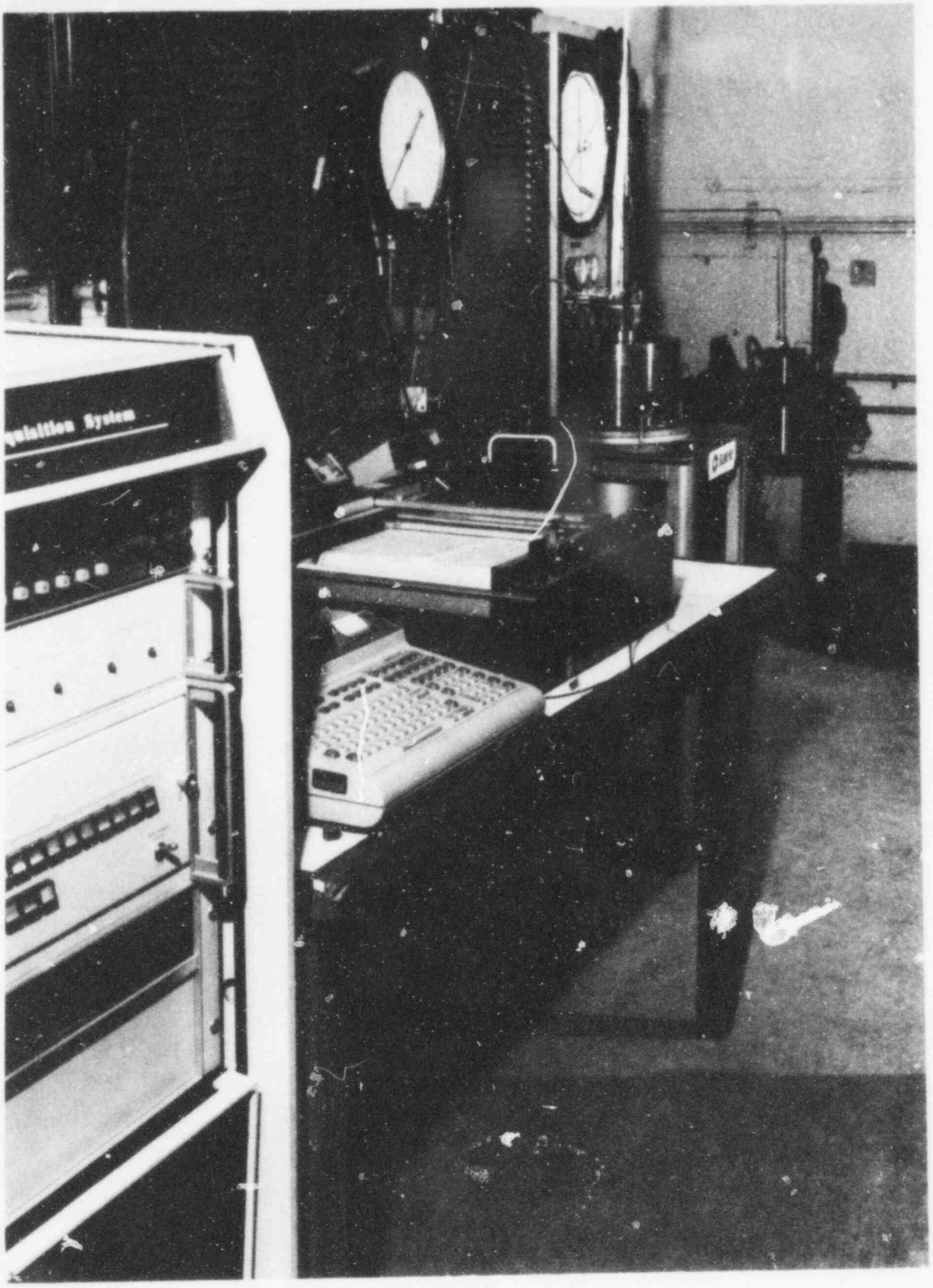

FIGURE VII.7 Instruments for Measuring Sensor Response to Autoclave Transients. (Neg 7900669-1cn)

VIII. TEST RESULTS AND INTERPRETATIONS

Only data typical of the general operational characteristics of the pressure sensor appear in this report, as inclusion of the large volume of acquired data would only, at the expense of considerable bulk, add repetitive evidence supporting conclusions. Data included from each of the three qualification units indicates uniformity of sensor characteristics.

In this report, data acquired during particular tests are grouped together to emphasize general operational characteristics of the sensor type rather than anomalous behavior of each sensor. Information from each sensor has been included, however. As shown in calibration summaries of Figure VIII.1 through VIII.26, each sensor responds nearly linearly for pressure variations to 2500 psig and within the temperature range 75 to 800^{o}F. Except for sensor S/N-01, practically no signal hysteresis occurs for increasing ("*" data points) or decreasing ("+" data points) pressure. Of the tested sensors, S/N-01 exhibited calibration data deviating discernably from the least-squares-fit straight line. S/N-01 responds nearly linearly for applied pressure to 2000 psig and then has steadily decreasing sensitivity for higher pressures. Of the qualification test units, S/N-04 proved least sensitive to pressure variations. At high temperature, sensitivity decreased to about 3 mV/psi. Calibration data obtained at the beginning and end of tests in the laboratory oven show each sensor continues to yield repetitive data after undergoing 500 hours of testing, an indication that long-term signal drift remains limited.

Calibration data from each sensor shows that as temperature increases, sensitivity decreases; however, behavior of the value of zero pressure output signal appears to be a characteristic particular to each sensor. Nevertheless, as the sensor output signal relates in a temperature-dependent way to the applied (reference) pressure, an algorithm was developed for each sensor to transform output signal values to indicated pressure. The algorithm, derived from calibration data, accounts for the variations of sensitivity and zero pressure signal output with temperature. Curves obeying second degree polynomial equations exhibit high correlation with the data as shown by the

variation of sensitivity and zero pressure output signal with temperature depicted in Figures VIII.2 through VIII.25. Transform algorithms derived from, and appearing immediately after, each of the calibration summaries verify that the sensor yielded repetitive calibration data nearly independent of conditions existing during the three different tests. Specifically, these conditions include the following: (1) the sensor only heated; (2) the sensor and cable heated, and, (3) the sensor encapsulated in the pressurizable enclosure and installed inside the autoclave. The derived algorithm (Equation 1) transforms signal output data to indicated pressure as noted on the ordinate of data plots which occur subsequently:

$$P = \frac{E-K(T)}{M(T)} \qquad (1)$$

where P is the indicated pressure, E is the sensor dc output voltage, and K(T) and M(T) are the temperature-dependent values of zero pressure output and sensitivity. Plots of K(T) and M(T) following each set of calibration data relate to coefficients (noted as A0, A1, and A2) on each plot by the general equation

$$K(T) = A_o + A_1T + A_2T^2 \qquad (2)$$

$$M(T) = A_o + A_1T + A_2T^2 \qquad (3)$$

where T is temperature and the values of the coefficients for (2) and (3) are each distinct values.

For slowly varying sensor temperature, the indicated pressure conforms closely with the reference (applied) pressure as shown in Figures VIII.27 to VIII.29. Figure VIII.27 portrays the response of pressure sensor S/N-01 for changes of temperature of $\pm$ 400^{o}F occurring within an elapsed test time of 3 hours. Although an initial measurement error of -8% of reading exists (due to inaccuracy of the transform algorithm), maximum error during the total test duration equals -11% of reading. Each of the sensors exhibited variations of indicated pressure of about $\pm$ 2% of reading for slow variations of temperature between 650 and 250^{o}F.

In contrast, accelerated cooling of the sensor by directing cold nitrogen gas over its exterior results in significant pressure measurement errors. Figures VIII.30 to VIII.42 illustrate typical responses of the three qualification units to rapid cooling. Figure VIII.30 illustrates the response of sensor S/N-01 as its temperature decreases with atmospheric pressure applied. A maximum negative error of 50 psi and a maximum positive error of 75 psi occur at respective elapsed times (after start of test) of 52 seconds and 175 seconds. The errors most likely result from sensor coil temperature differences which effectively unbalance the bridge resulting in a signal output variation. The minimum sensor temperature of 360^{o}F occurs 39 seconds after application of the cooling gas. At that time, interruption of coolant gas flow allows the sensor to reheat to the initial temperature. Data is obtained for a total of about 18 minutes--time for the sensor to return to temperature equilibrium. Alphanumeric notations along the data curve specify the time elapsed after initiation of the test. Note that the rate of data acquisition becomes intermittently slower as the test progresses.

The sensor responds to rapid cooling regardless of the magnitude of applied pressure, as shown by the similarities between the data summaries of Figures VIII.30 and VIII.31. As occurred with zero applied pressure, the sensor yields an indicated pressure less than the applied pressure by 13.7% 52 seconds after test initiation. Maximum rate of temperature change occurs 28 seconds after application of the coolant.

Both S/N-03 and S/N-04 sensors indicate pressure unequal to the applied (reference) pressure for imposed rapid temperature variations. For a time period of 38 seconds, S/N-03 yields values less than the applied pressure by increasing amounts to a maximum of 43 psig. At a later time (after test initiation), the sensor indicates a pressure greater than the applied value, with the maximum positive error of 13.7% occuring at 121 seconds elapsed time. Temperature rates (Figures VIII.35 and VIII.37) during the transients exceed -10^{o}F/sec, the maximum specified for tests of this LOFT instrument. Sensor S/N-04 exhibited error for rapid cooling as shown in Figures VIII.40

and VIII.42. Except for sensor S/N-01, the maximum negative error occurs within 40 seconds and the maximum positive error occurs usually within 170 seconds, both elapsed times after initiation. For S/N-01, only negative error was witnessed, possibly due to inaccuracy inherent in the transform algorithm (note the large negative starting error). Curves showing temperature rates appear immediately following the response summaries. Table VIII.1's summary of test results witnessed during transient tests indicates operational responses to be expected for rapid temperature change. Subsequent to each temperature transient and after reaching thermal equilibrium, each sensor yielded an output signal closely equal to its initial value, an indication that transient tests do not cause permanent signal offset.

Both rapid and relatively slower depressurization of the sensors caused responses shown in Figure VIII.44. In all cases, the sensors respond to the 1850 psi reduction of pressure. The maximum rate of pressure reduction, limited by the size of tubing and valve orifice area along the exhaust path, apparently prevents accurately determining the intrinsic response speed of the sensor; however, even though limited by exhaust capacity, a demonstrated 10 to 90% time response of about 40 to 50 milliseconds easily satisfies the requirement of 250 milliseconds for LOFT use. For comparative purposes, the data traces also show time response of the SETRA reference pressure transducer (specified to respond at a 1000 Hz rate) during depressurization.

For each of the qualification sensors, Figures VIII.45 and VIII.46 depict the very minor signal variations occurring during heat up from 75 to 800°F of 16 feet of signal cable. Ideally, the indicated pressure should remain unchanged, for both the applied pressure and temperature of the sensors remain constant during these tests. Similarities between calibration data for conditions of sensor only and then sensor and cable heated also verify the insignificant contribution to the output signal of heating the signal cable. As used in LOFT, the signal cable will be routed in a compact bundle with many other cables along the structure supporting the fuel assemblies. Consequently, the temperature along the cable will be nonuniform and probably less than the maximum temperature imposed during qualification

tests. Errors attributable to cabling heating effects should therefore be less than witnessed in these tests.

Initial tests in the autoclave include calibration at temperatures of 75, 250, 400, and 650°F. As verifiable from calibration plots (Figures VIII.1 through VIII.26), these data conform closely with calibration data obtained prior to sensor installation in the autoclave. Zero pressure output and sensitivity values derived and plotted immediately after pertinent calibrations yield coefficients for an algorithm used for transforming sensor output data (dc volts) obtained during autoclave blowdowns. Rapid temperature variations during maximum and controlled-rate blowdowns cause the sensors to indicate pressure inaccurately (Figures VIII.47 through VIII.57). For data obtained during a maximum-rate blowdown, maximum errors of +12.5 percent and -8.8 percent (Sensor S/N-01), of +3.5 percent and -11.3 percent (Sensor S/N-03), and of +14 percent and -7.2 percent (S/N-04) of reading occur at times during the transients. The sensors remain within the LOFT specified accuracy limits of 3% for a period of about 13 seconds after initiation of a depressurization which creates temperature change rates up to -100°F/sec, ten times as severe as expected to occur at the pressure sensor location during transients in the LOFT reactor. Even for controlled blowdowns, the temperature change rates were up to 25°F/sec and the sensor indicated pressure deviated by less than ± 3% of reading as shown in Figure VIII.51. Pressure measurements higher by 192 psi and lower by 57 psi than the applied pressure were observed during the test duration.

Tables VIII.1 and VIII.2 summarize data obtained for the transient tests used as examples in this report. Because of the small initial errors for tests in the autoclave, the derived transform algorithm for each sensor accurately related output signal and indicated pressure. In contrast, the algorithm used for S/N-01 during temperature transients in the oven facility yielded relatively large initial errors. Of significance, regardless of comparative temperature rates, errors observed during tests in the autoclave were generally less than those caused by coolant gas in the oven facility.

TABLE VIII.1

ERRORS INDUCED BY TEMPERATURE TRANSIENTS

Sensor Serial No.	S/N-01	S/N-03	S/N-04
Ref. Figure	VIII.32	VIII.34	VIII.40
Start Error	-7.6%	-1.3%	-1.6%
Maximums	-16% @ 48 sec.	+13.7% @ 121	+16.8 @ 96 sec.
1-3% Error	>151 sec; <195 sec	<60 sec; >277 sec	<38 sec; >210 sec
Max. Temp Rates	-29^{o}F/sec; +12^{o}F/sec	-11^{o}F/sec; +3^{o}F/sec	-23^{o}F/sec; +6^{o}F/sec
Comment	no positive error		
Ref. Figure	VIII.31	VIII.38	VIII.42
Start Error	-7.5%	-2%	-1.5%
Maximums	-13.7% @ 52 sec.	+12% @ 168 sec.	+15.4% @ 88 sec.
3% Error		<57 sec; >400 sec.	<40 sec; >210 sec.
Max. Temp Rates	-21^{o}F/sec; +12^{o}F/sec.	-10^{o}F/sec; +5^{o}F/sec	-14.5^{o}F/sec; +7^{o}F/sec
Comment	no positive error	signal output discontinuity during test.	

1078 057

TABLE VIII.1 (Cont'd)

Sensor Serial No.	S/N-01	S/N-03	S/N-04
Ref. Figure	VIII.30	VIII.36	
Start Error	+19 psig	-1.1%	
Maximums	-50 psi @ 52 sec.	+13% @ 85 sec.	
	+75 psi @ 175 sec.		
3% Error	not applicable	<31 sec; >244 sec.	
Max. Temp Rates	-20°F/sec;	-13°F/sec;	
	+4°F/sec	+4°F/sec.	
Comment	0 psig applied		

TABLE VIII.2

ERRORS INDUCED BY TRANSIENTS IN AUTOCLAVE

Sensor Serial No.	S/N-01	S/N-03	S/N-04
Ref. Figure	VIII.47	VIII.53	VIII.55
Start Error	+1.2%	0.1%	-0.7%
Maximums	-8.8% @ 19 sec.	-11.3% @ 21 sec.	-7.2% @ 15 sec.
	+12.5% @ 72 sec	+3.5% @ 62 sec.	+14% @ 56 sec.
3% Error	12 sec.	13 sec; 39 sec.	13 sec; 128 sec.
Max. Temp. Rates	-68°F/sec;	-86°F/sec;	-70°F/sec;
	+22°F/sec	+45°F/sec	+28°F/sec
Ref Figure	VIII.49	VIII.51	VIII.[illegible]7
Start Error	+1.5%	0.8%	-0.6%
Maximums	-8.1% @ 19 sec	± 3%	-3% @ 20 sec.
	+13.5% @ 66 sec.		+10% @ 61 sec.
3% Error	12 sec.		20 sec; 117 sec.
Max Temp. Rates	-65°F/sec;	-26°F/sec;	-24°F/sec;
	+21°F/sec	+60°F/sec	+22°F/sec

This further emphasizes the importance of minimizing temperature gradients in the sensor vicinity. In the autoclave, the pressurizable container enclosing the sensor provides a thermal mass tending to reduce gradients near the sensor.

Calibrations (Figure VIII.26) obtained just before removal of the sensor from the autoclave correlate closely with initial calibrations (Figure VIII.23), thereby implying sensor stability for environments created within the autoclave. Each of the qualification units exhibited differing response to autoclave blowdown. However, for all imposed test conditions, none of the test units exhibited measurement errors greater than 18% of reading for applied pressures above 500 psig.

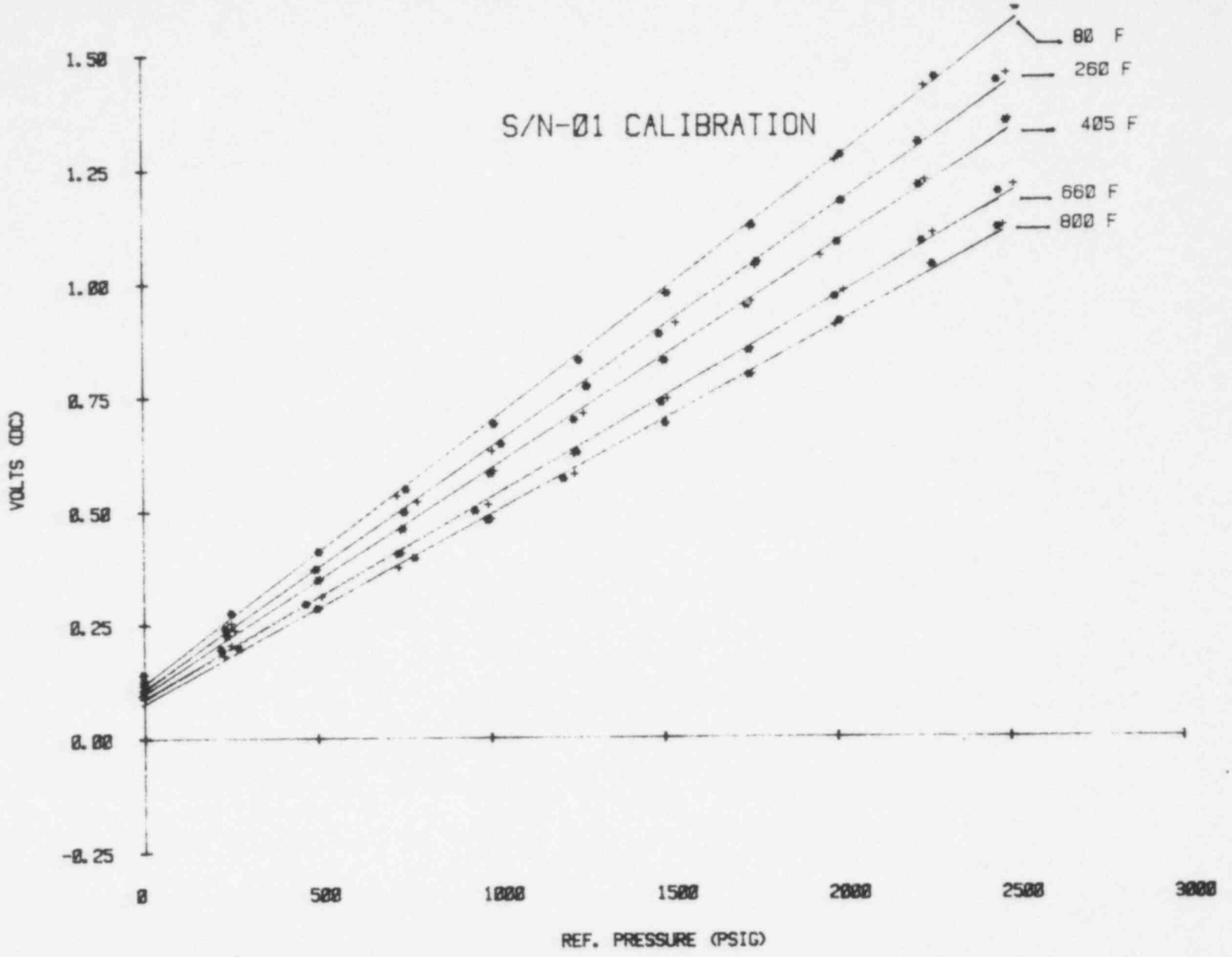

FIGURE VIII.1. First Calibration With Only Sensor Heated.

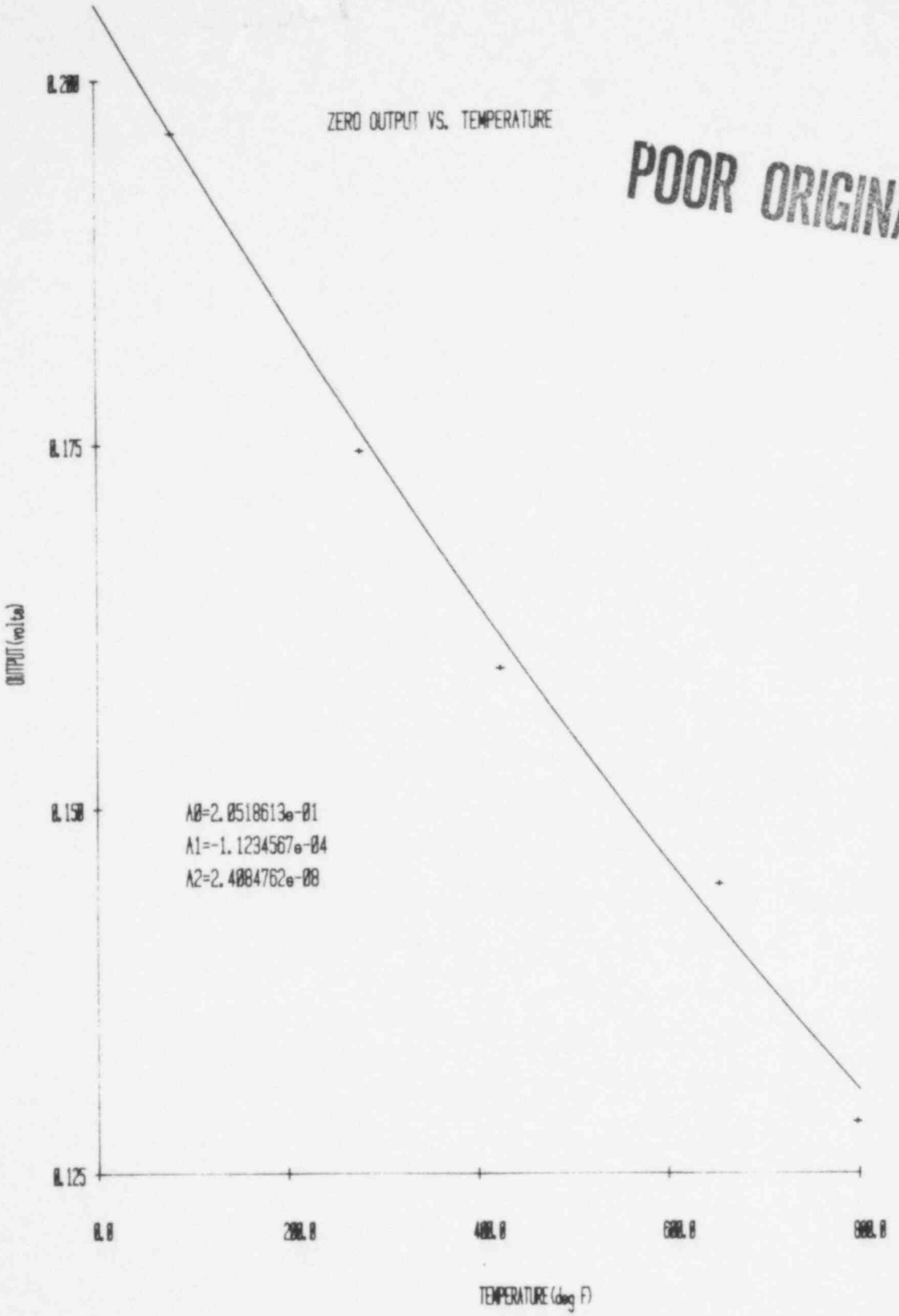

FIGURE VIII.2 Zero Pressure Output for Calibration of Figure VIII.1.

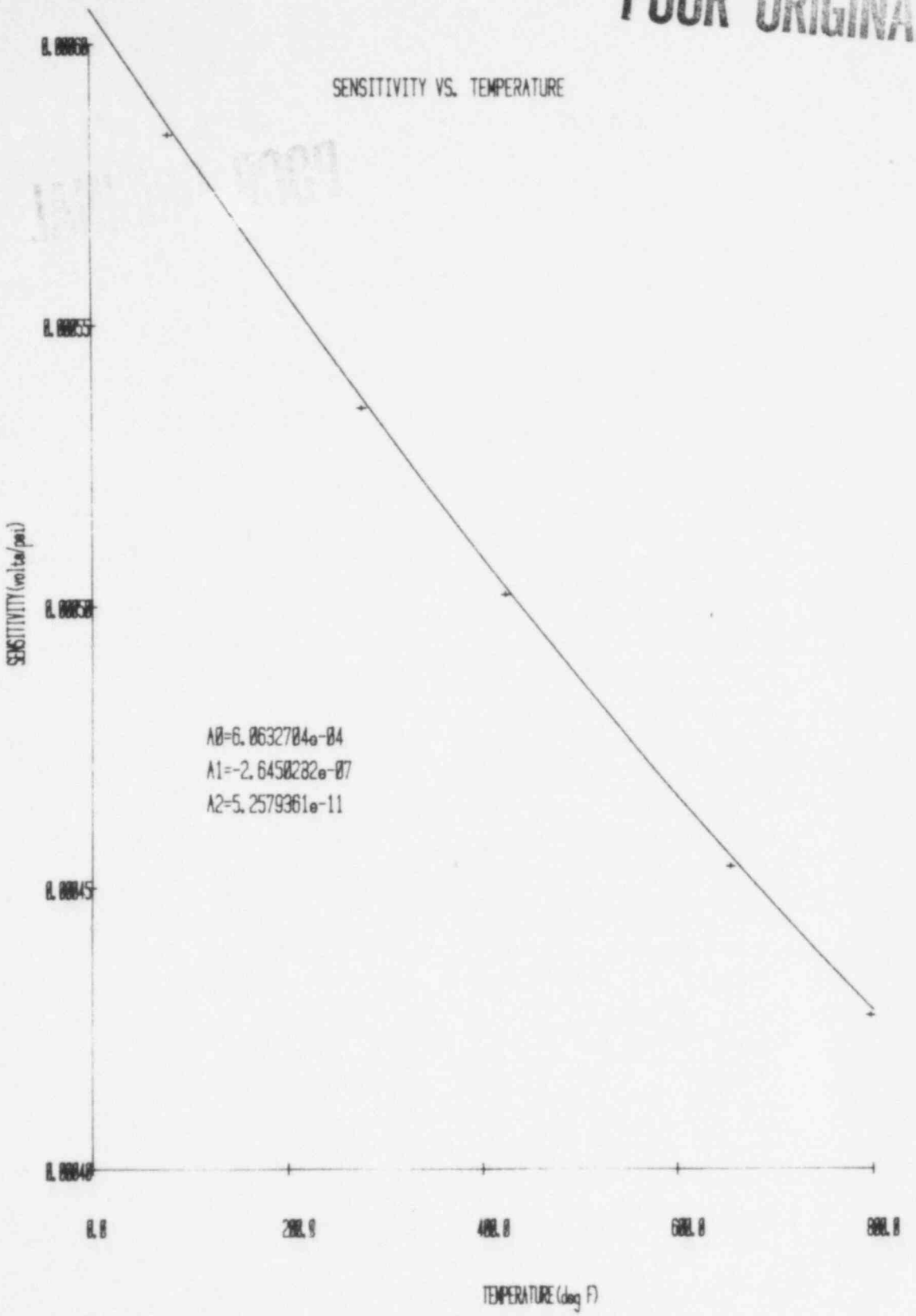

FIGURE VIII.3 Sensitivity for Calibration of Figure VIII.1.

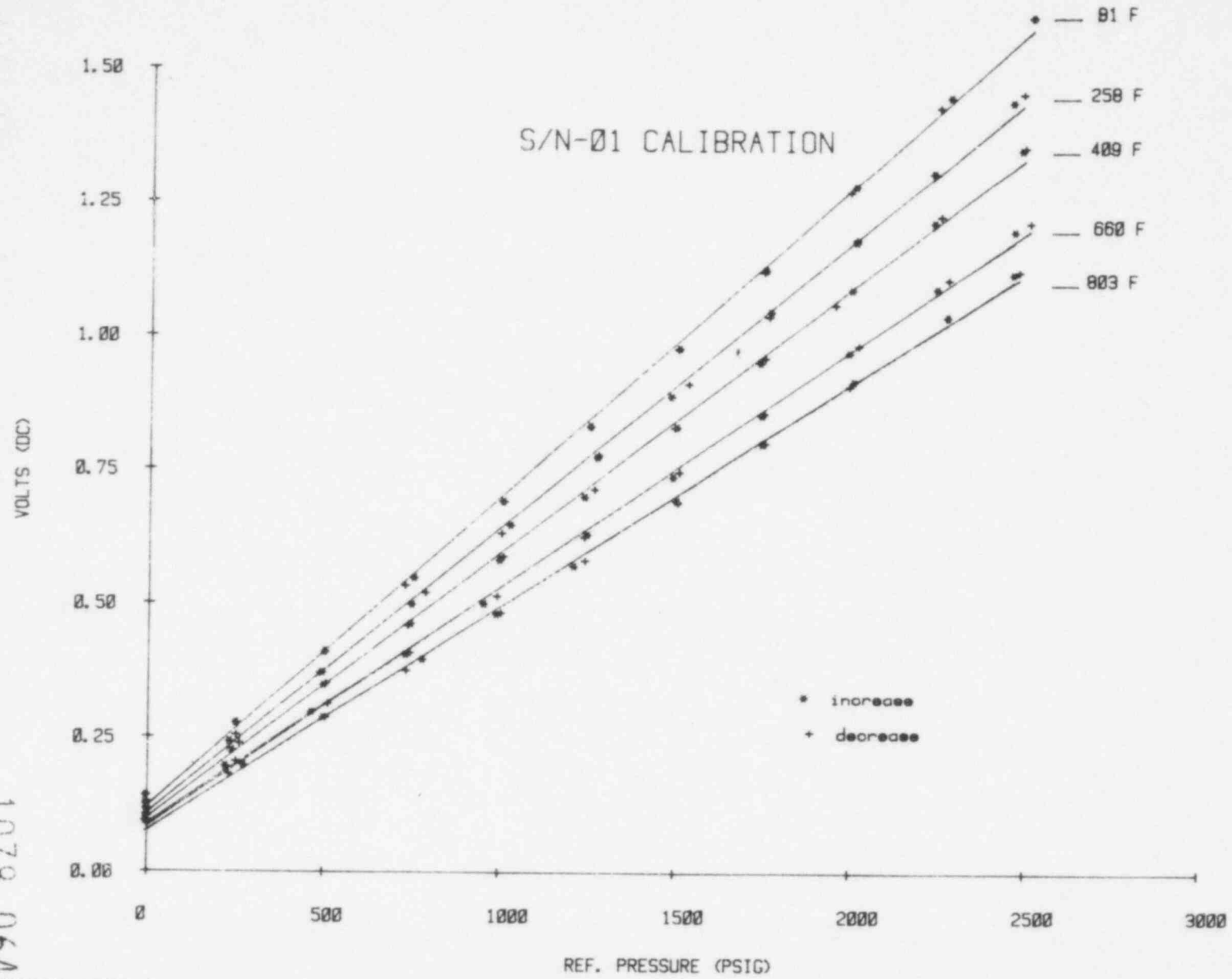

FIGURE VIII.4 Calibration with Sensor and Signal Cable Heated.

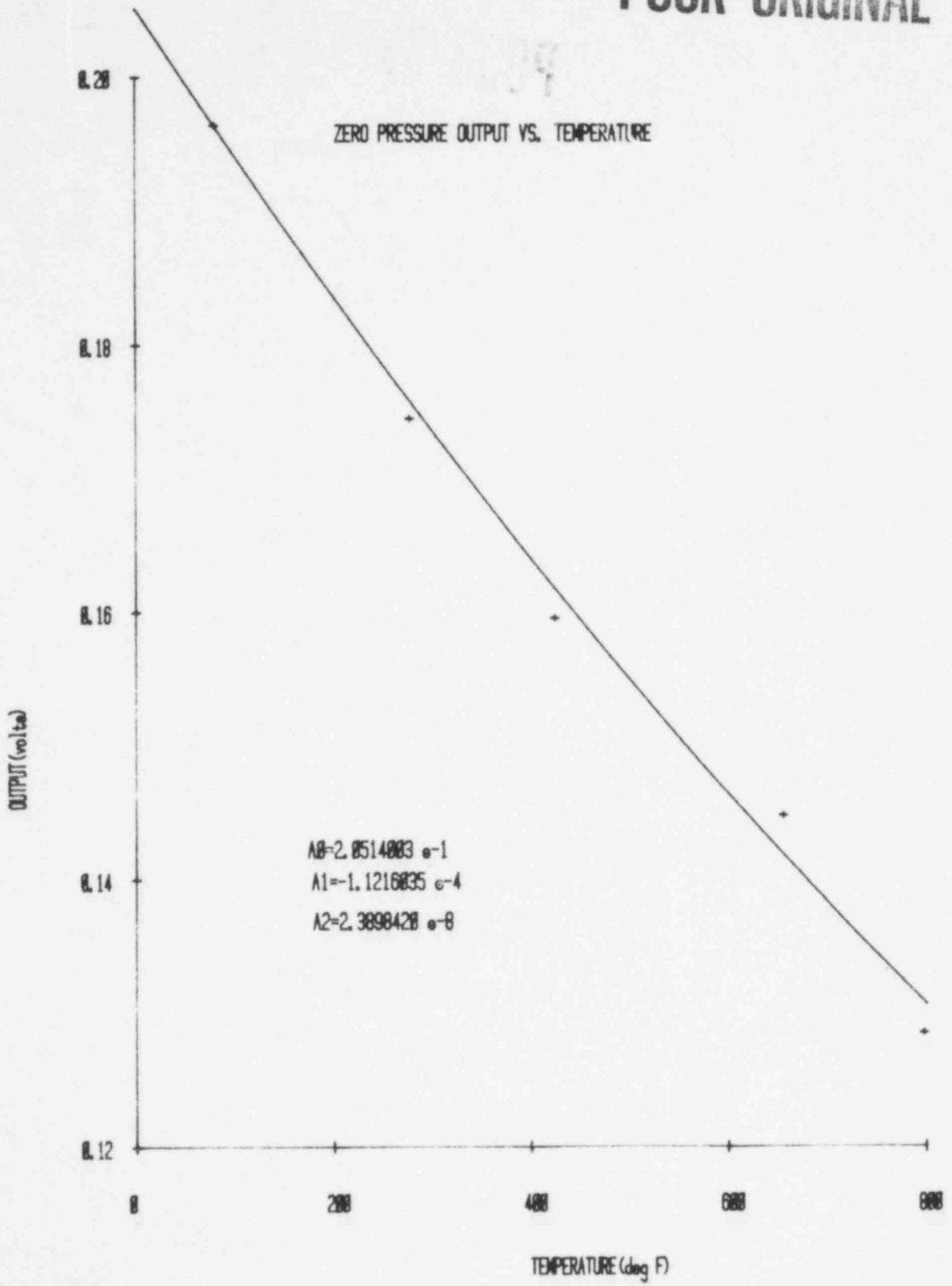

FIGURE VIII.5 Zero Pressure Output for Calibration Data of Figure VIII.4.

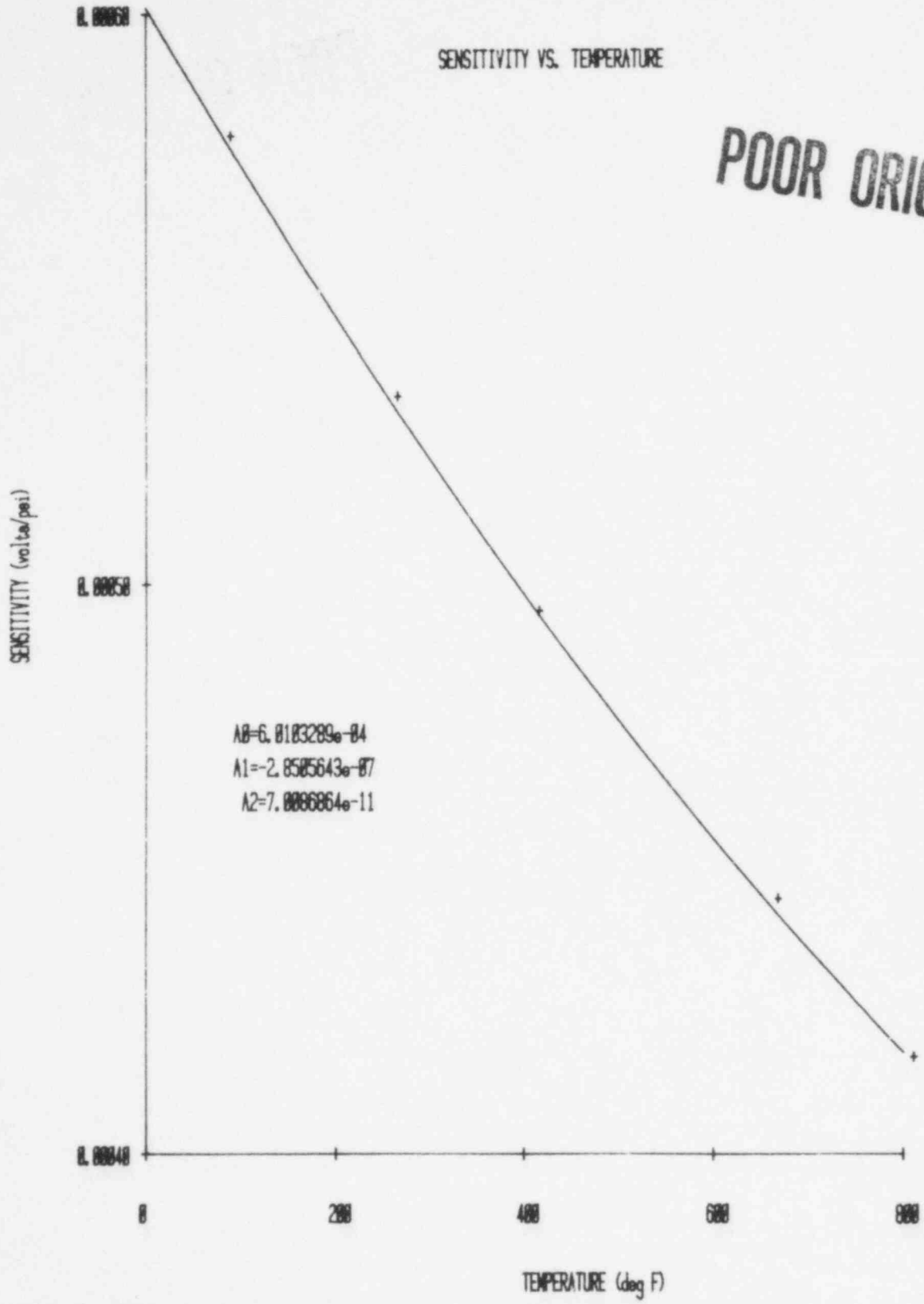

FIGURE VIII.6 Sensitivity for Calibration of Figure VIII.4.

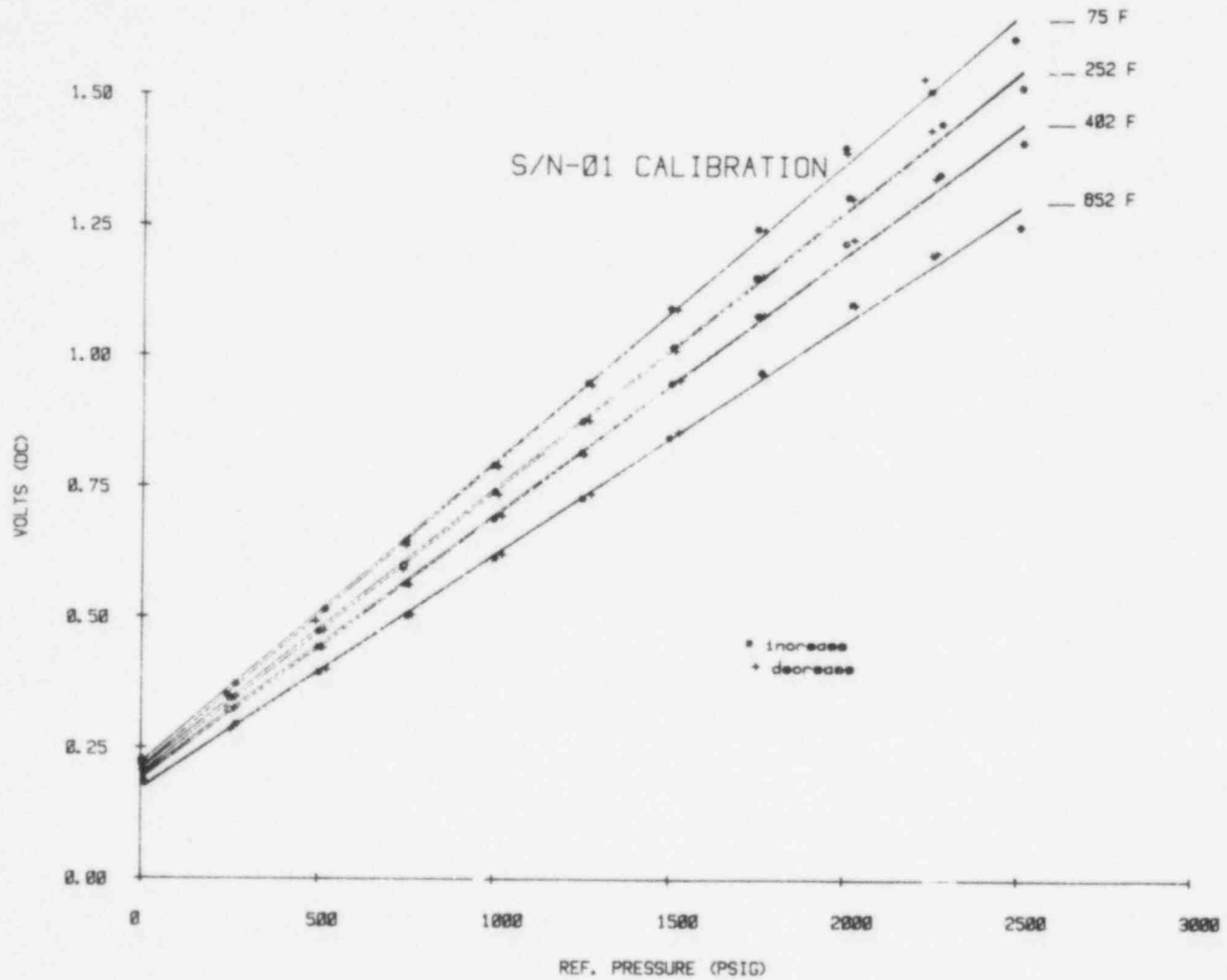

FIGURE VIII.7 Calibration for Sensor and Signal Cable Installed in Autoclave.

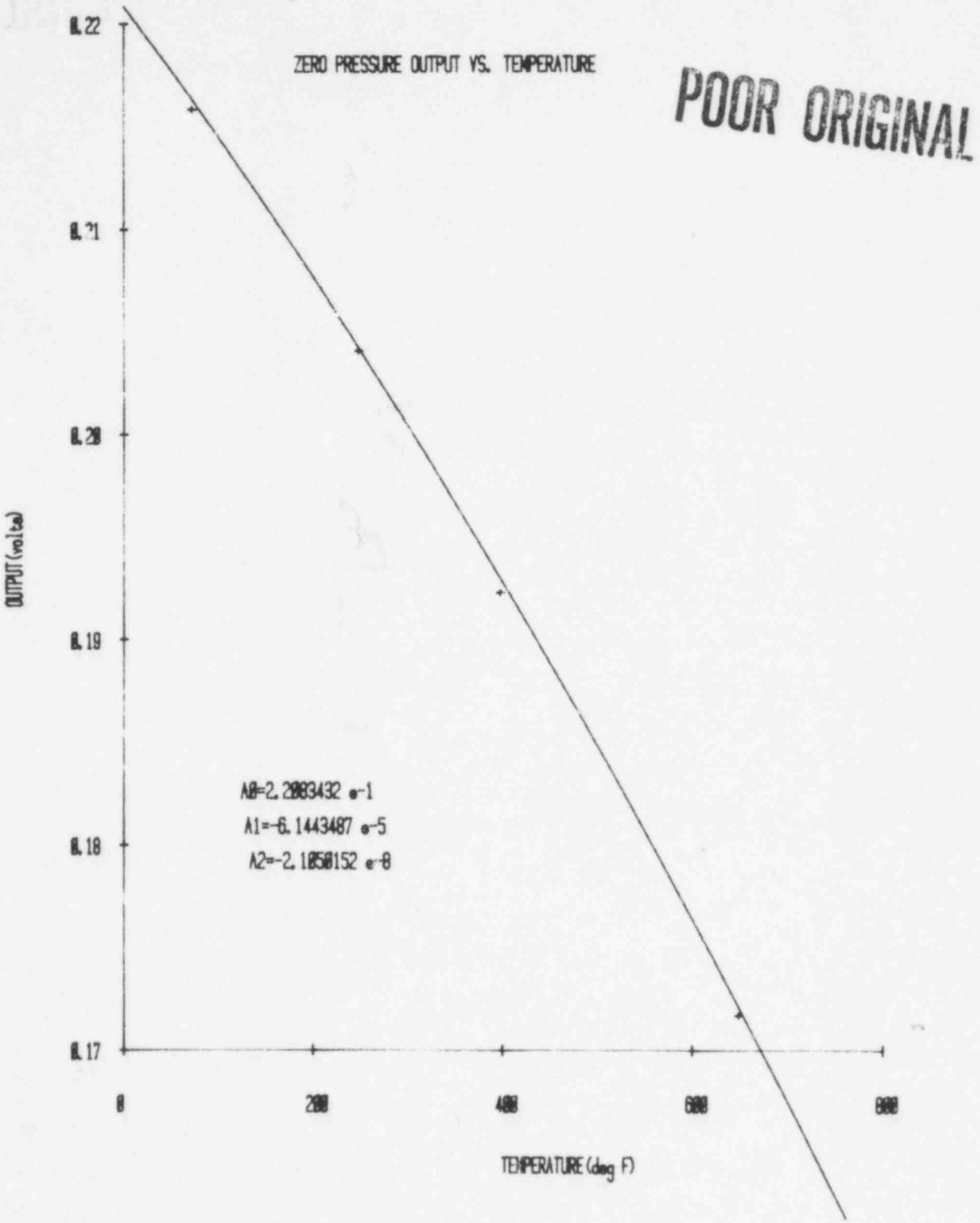

FIGURE VIII.8 Zero Pressure Output for Calibration of Figure VIII.7.

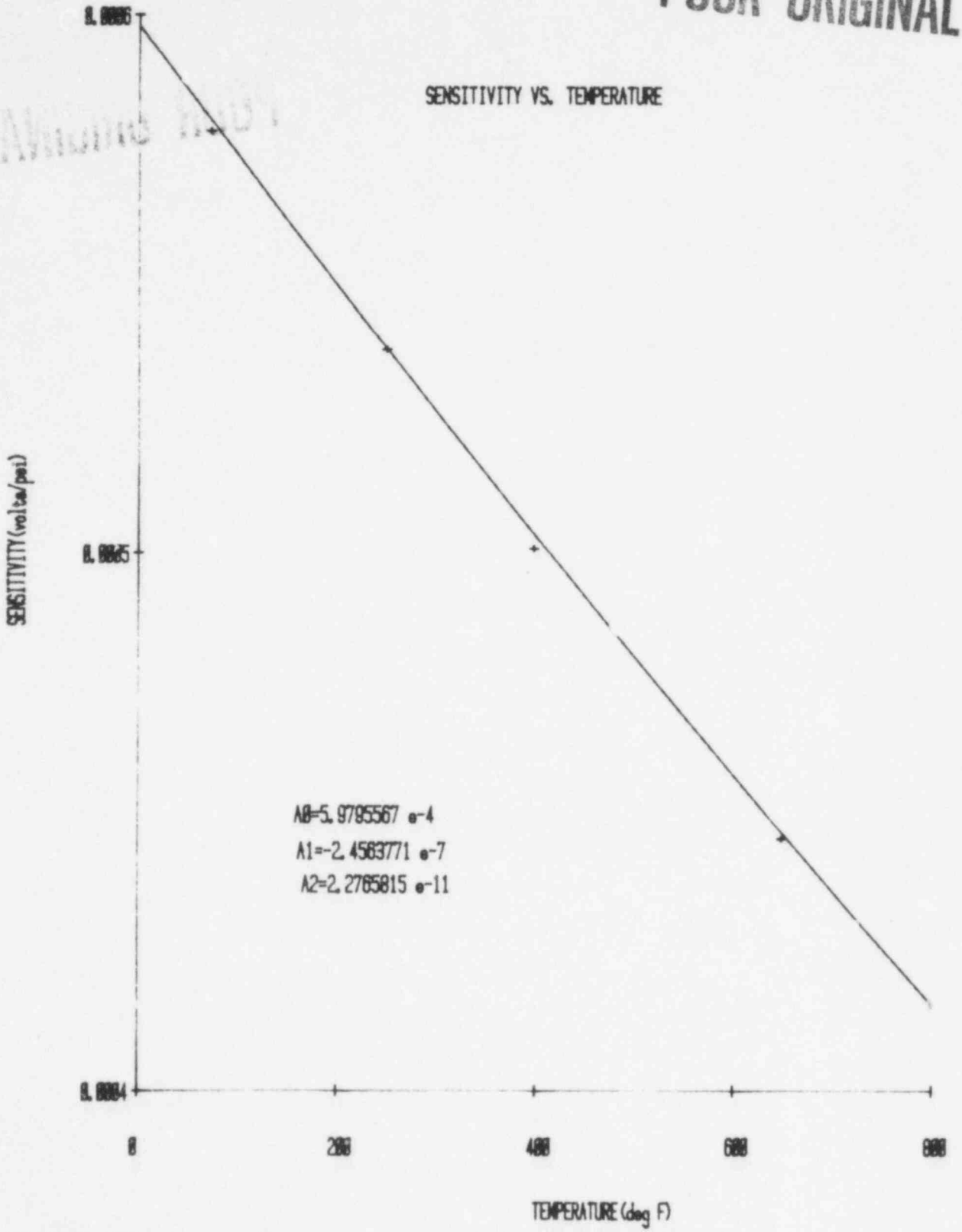

FIGURE VIII.9 Sensitivity for Calibration of Figure VIII.7.

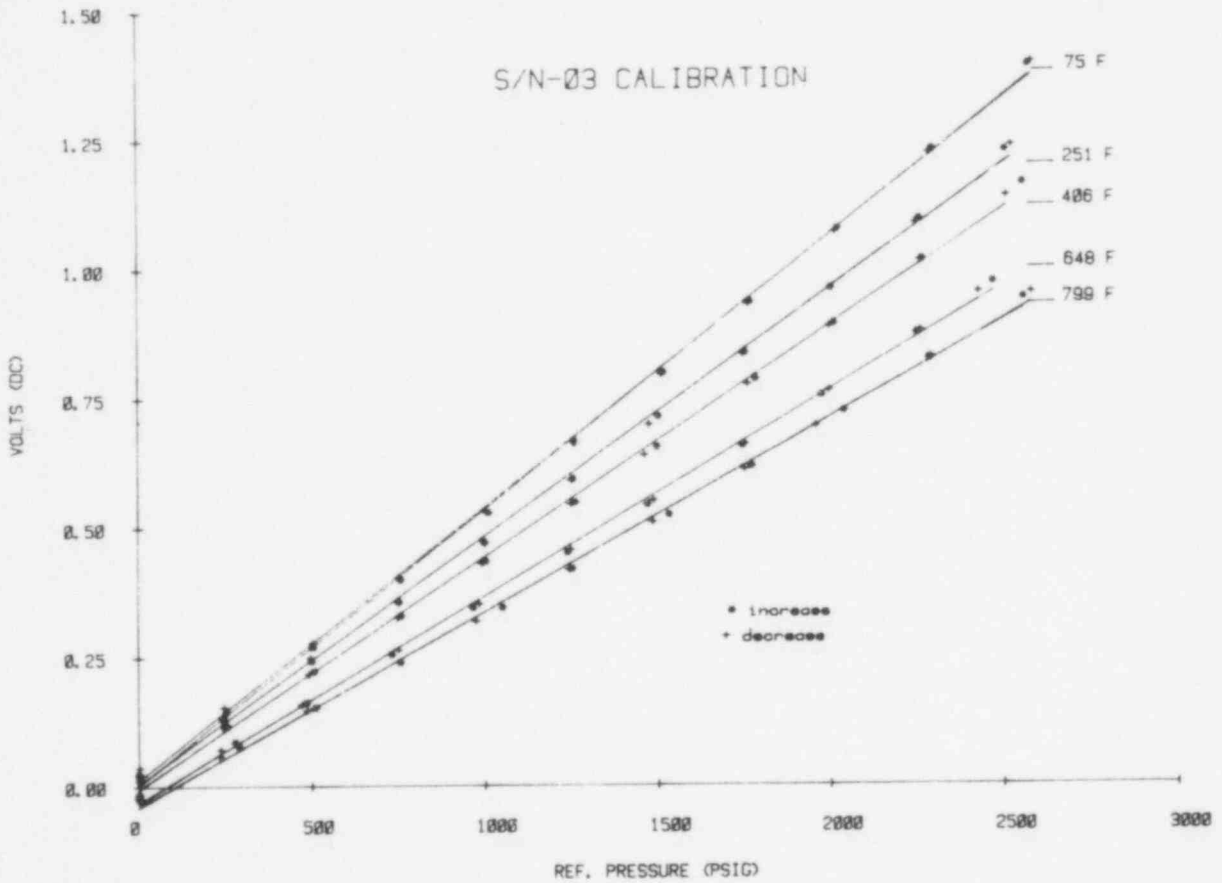

FIGURE VIII.10 First Calibration With Only Sensor Heated.

1078 070

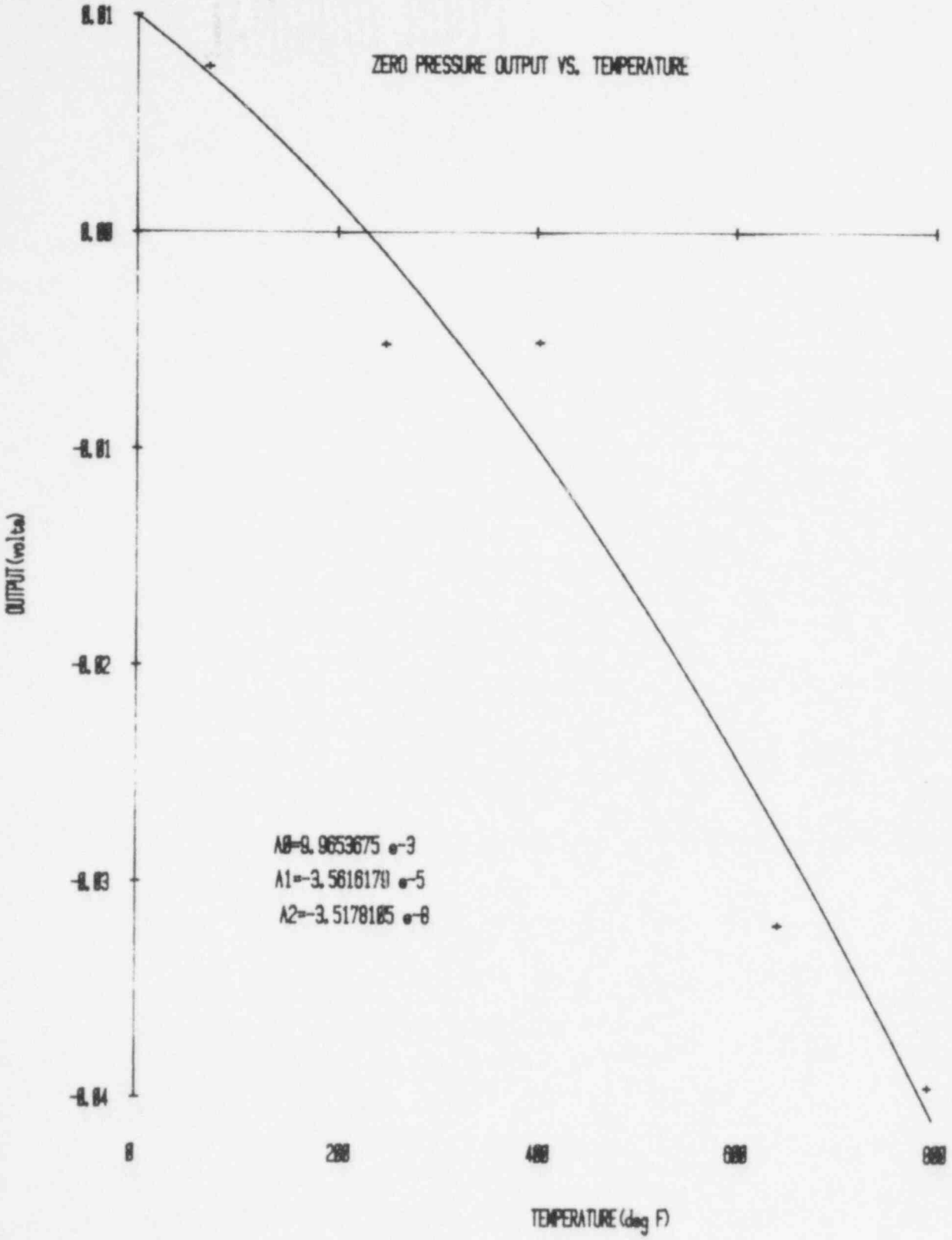

FIGURE VIII.11 Zero Pressure Output for Calibration of Figure VIII.10.

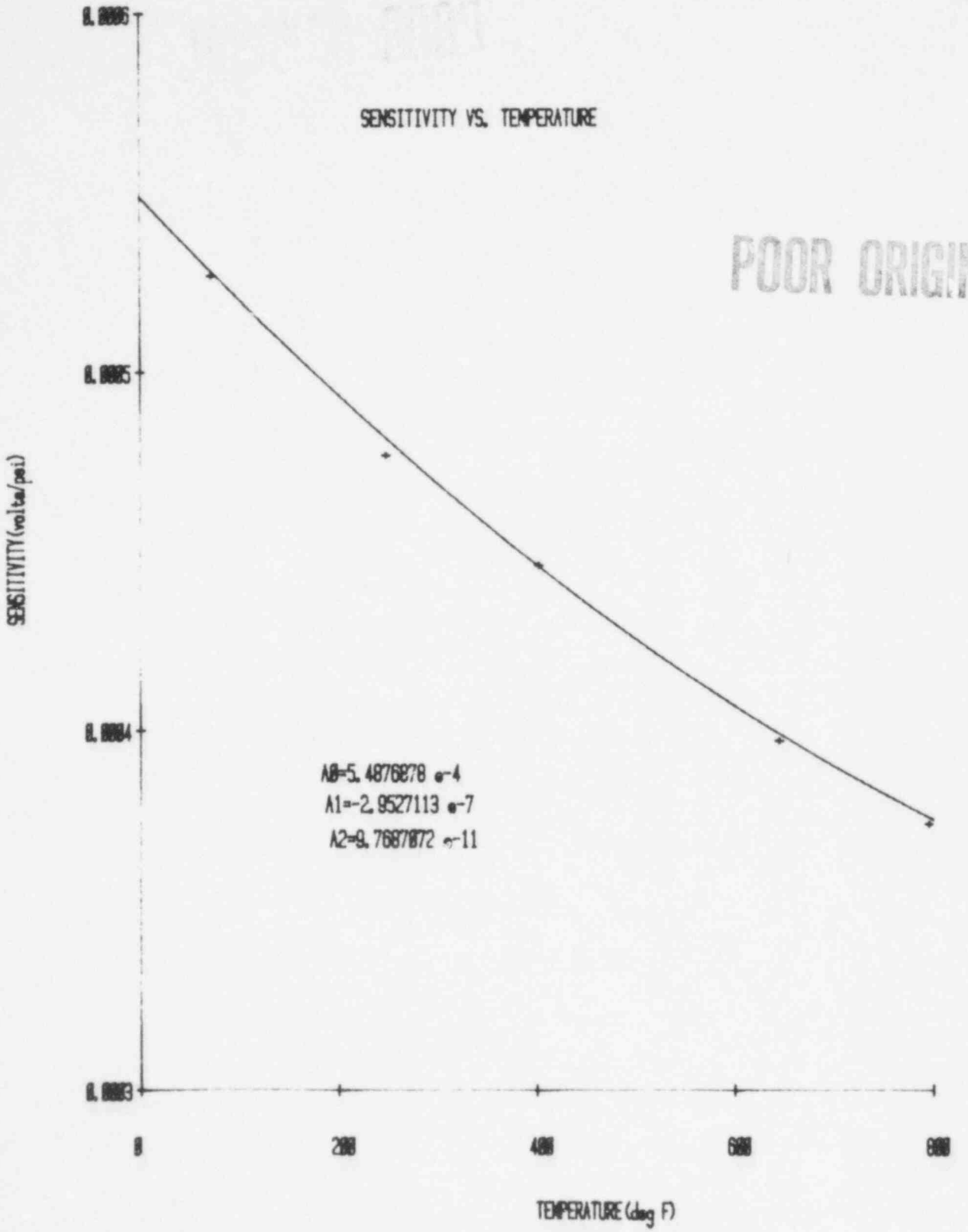

FIGURE VIII.12 Sensitivity for Calibration of Figure VIII.10.

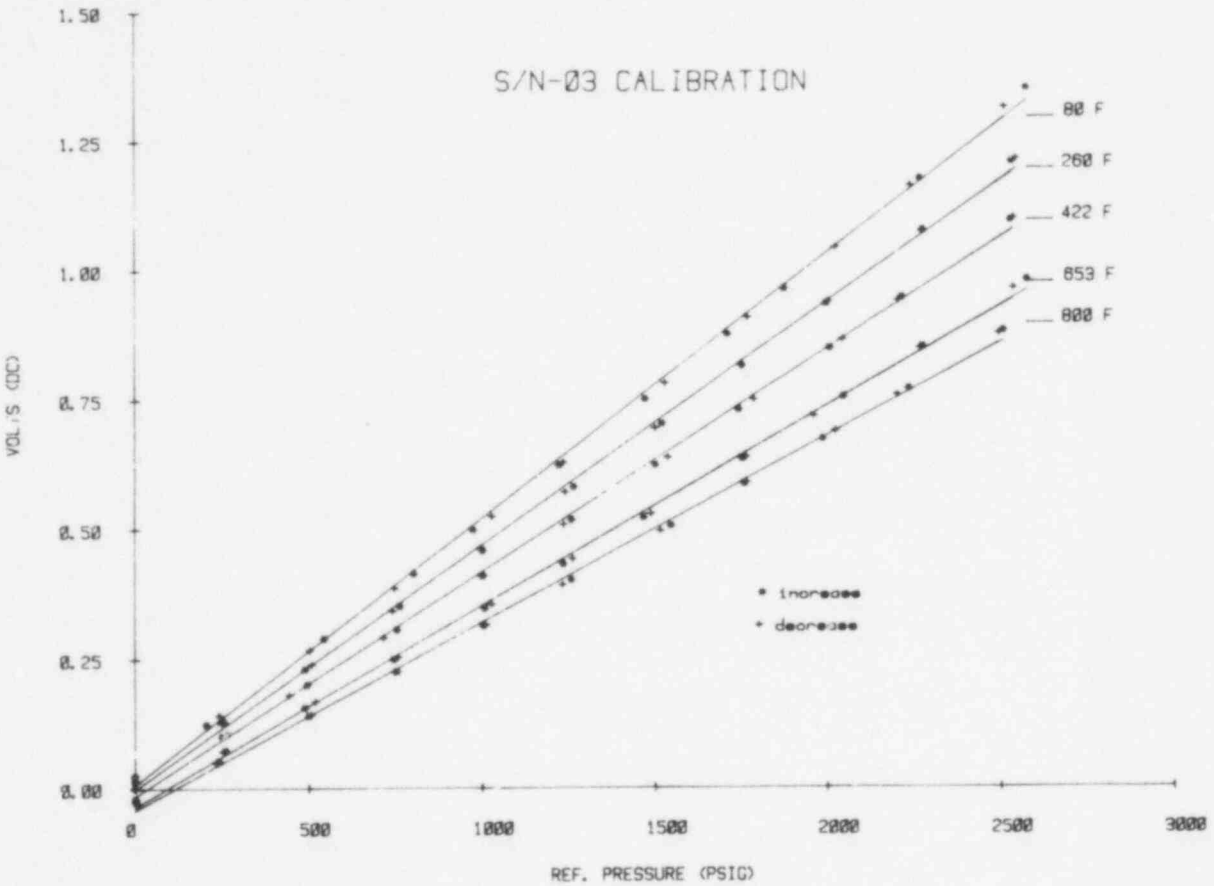

FIGURE VIII.13 Calibration with Sensor and Signal Cable Heated.

1078 0/3

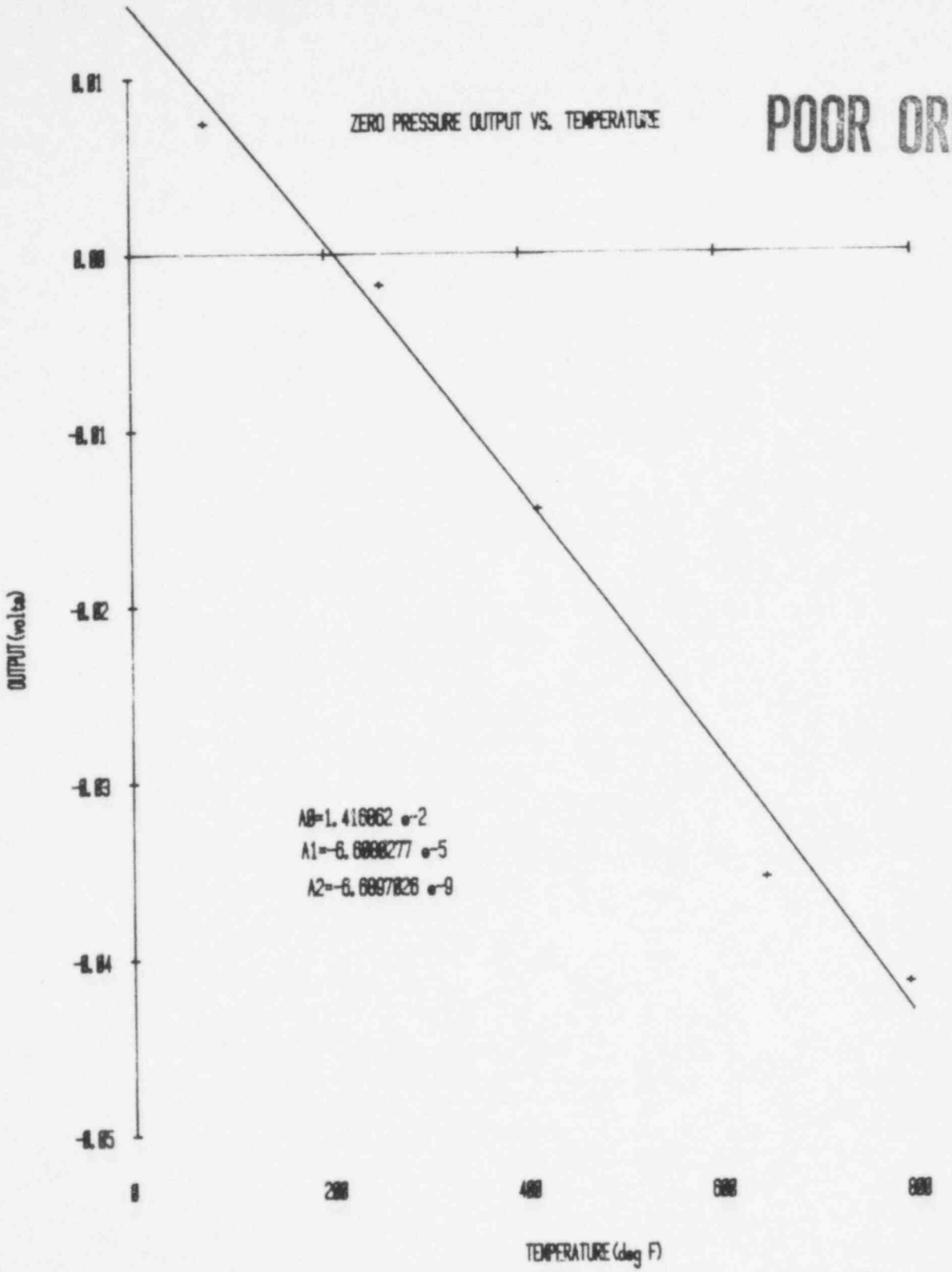

FIGURE VIII.14 Zero Pressure Output for Calibration of Figure VIII.13.

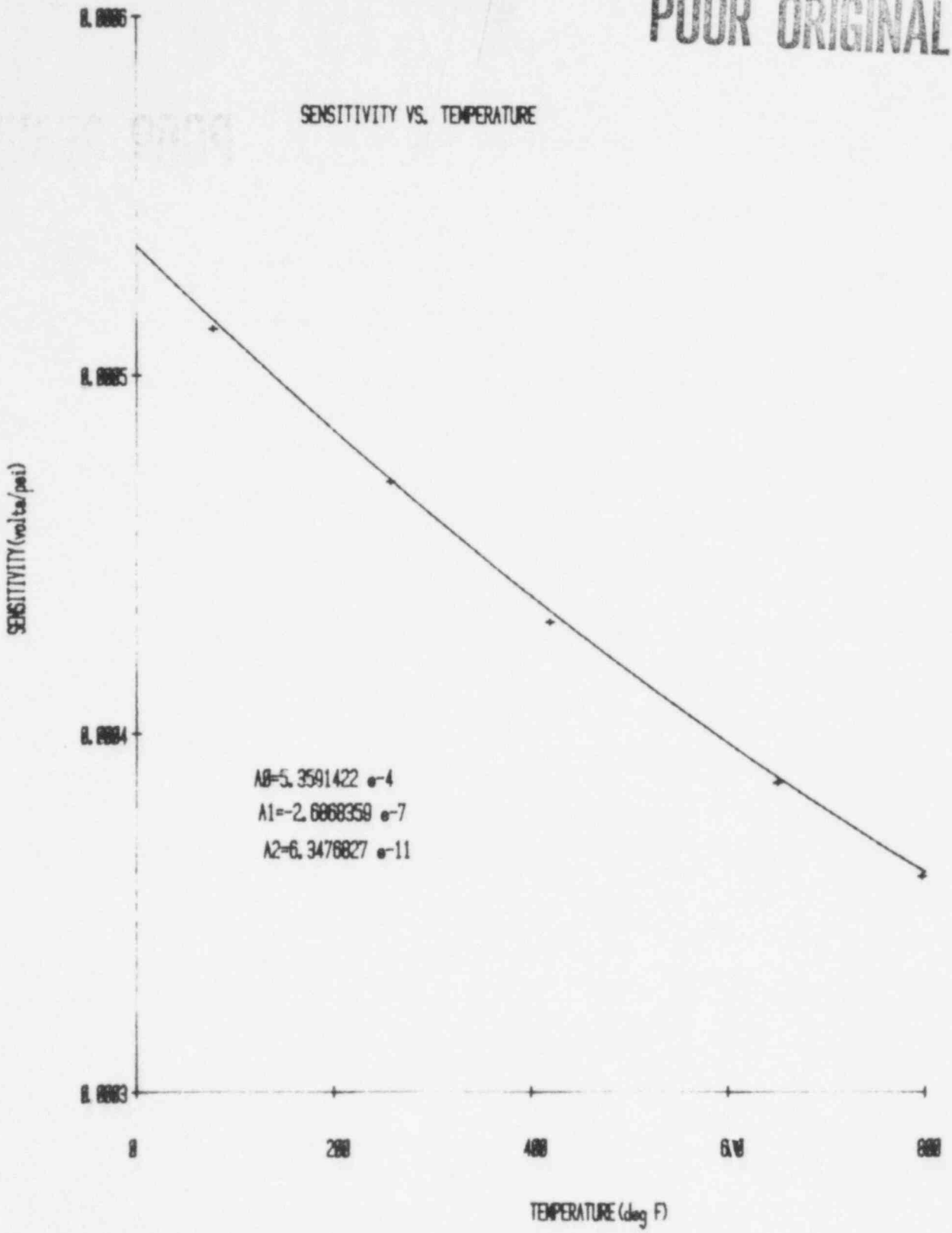

FIGURE VIII.15 Sensitivity for Calibration of Figure VIII.13.

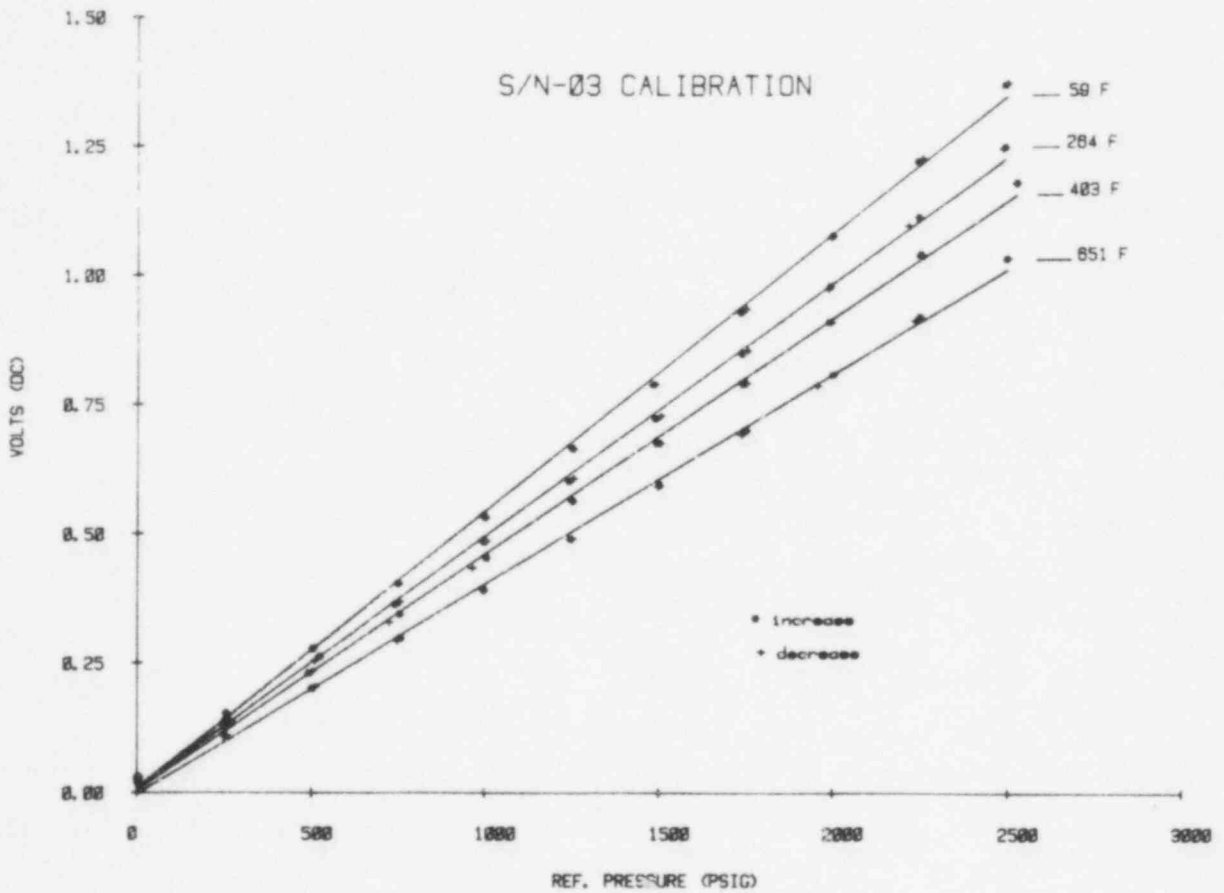

FIGURE VIII.16 Calibration With Sensor and Signal Cable Installed in Autoclave.

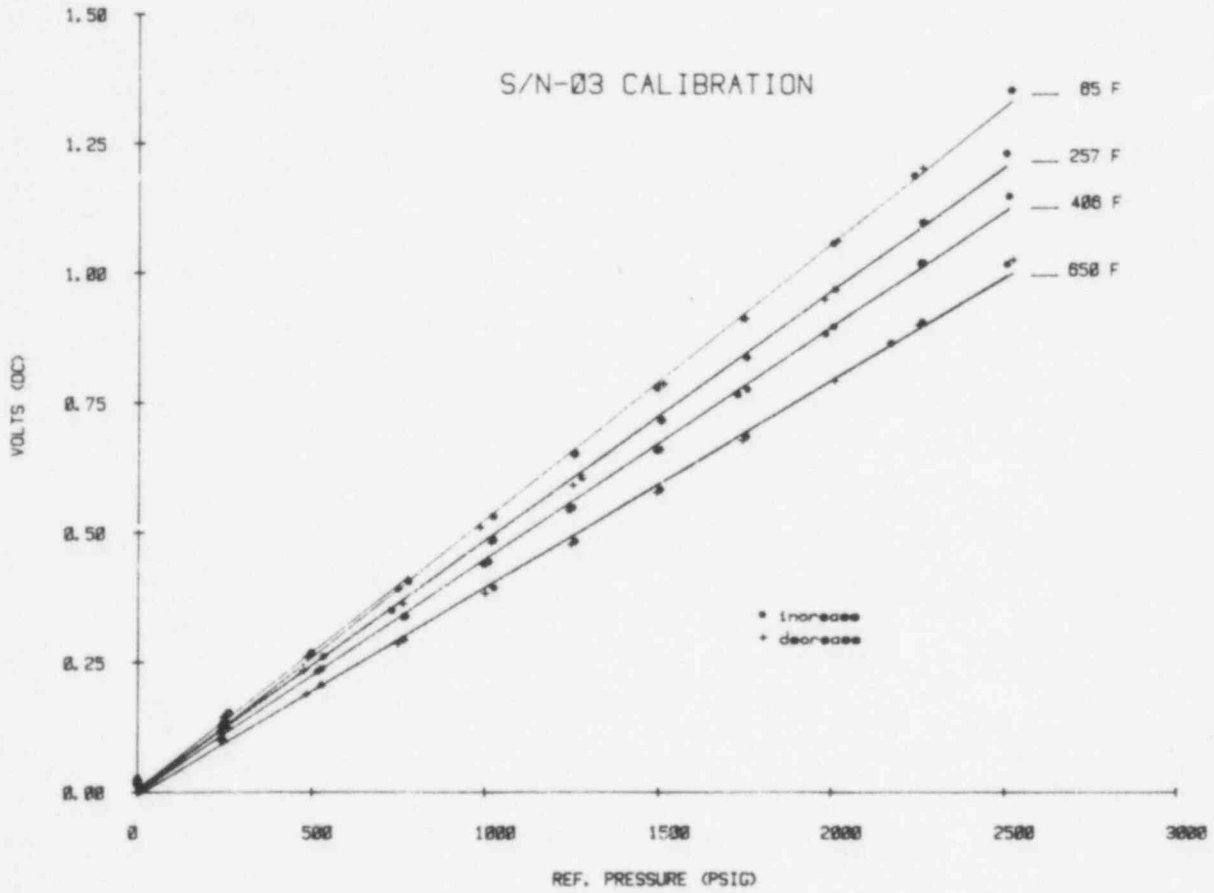

FIGURE VIII.17 Calibration After Blowdowns With Sensor and Signal Cable Installed in Autoclave.

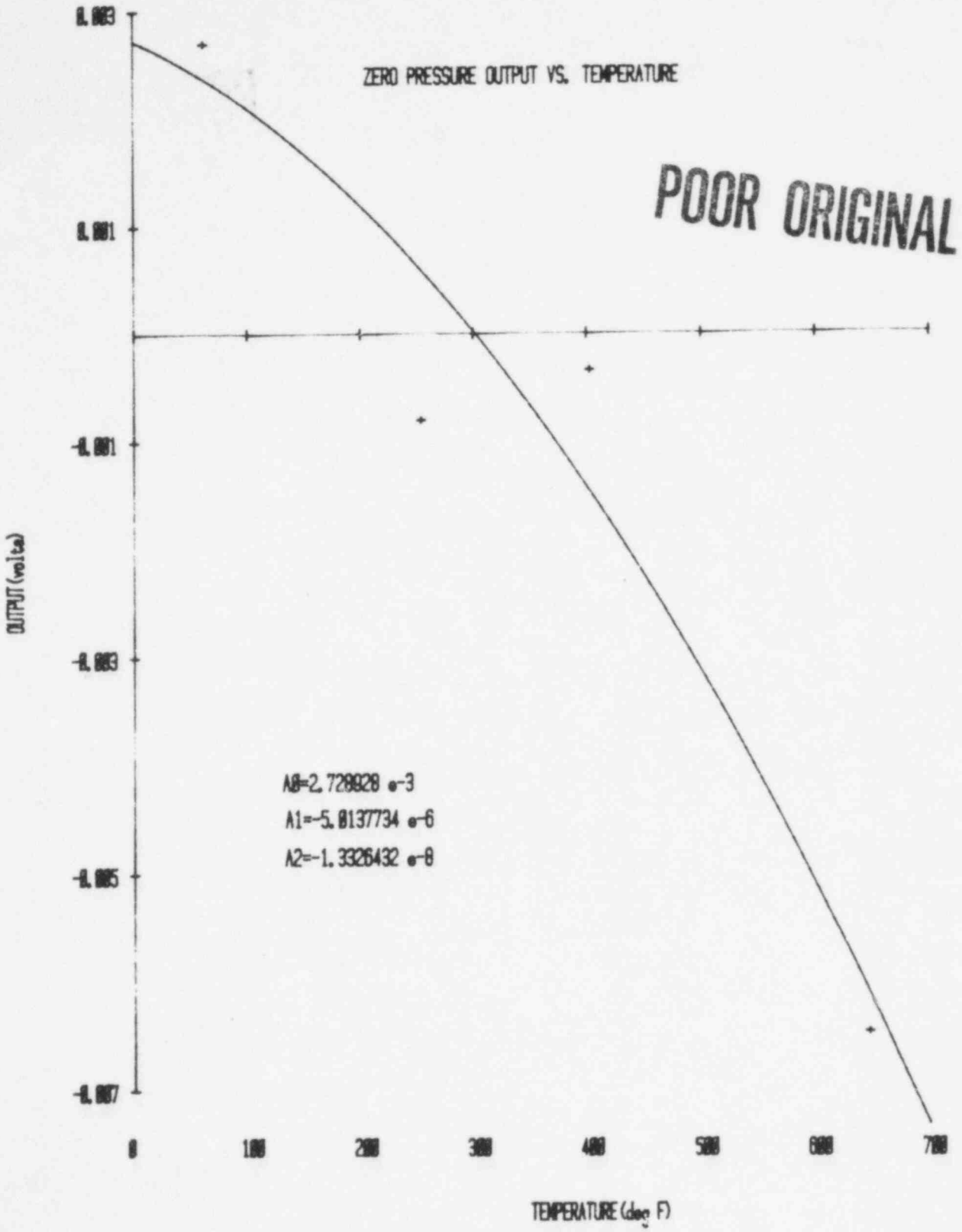

FIGURE VIII.18 Zero Pressure Output for Calibration of Figure VIII.17.

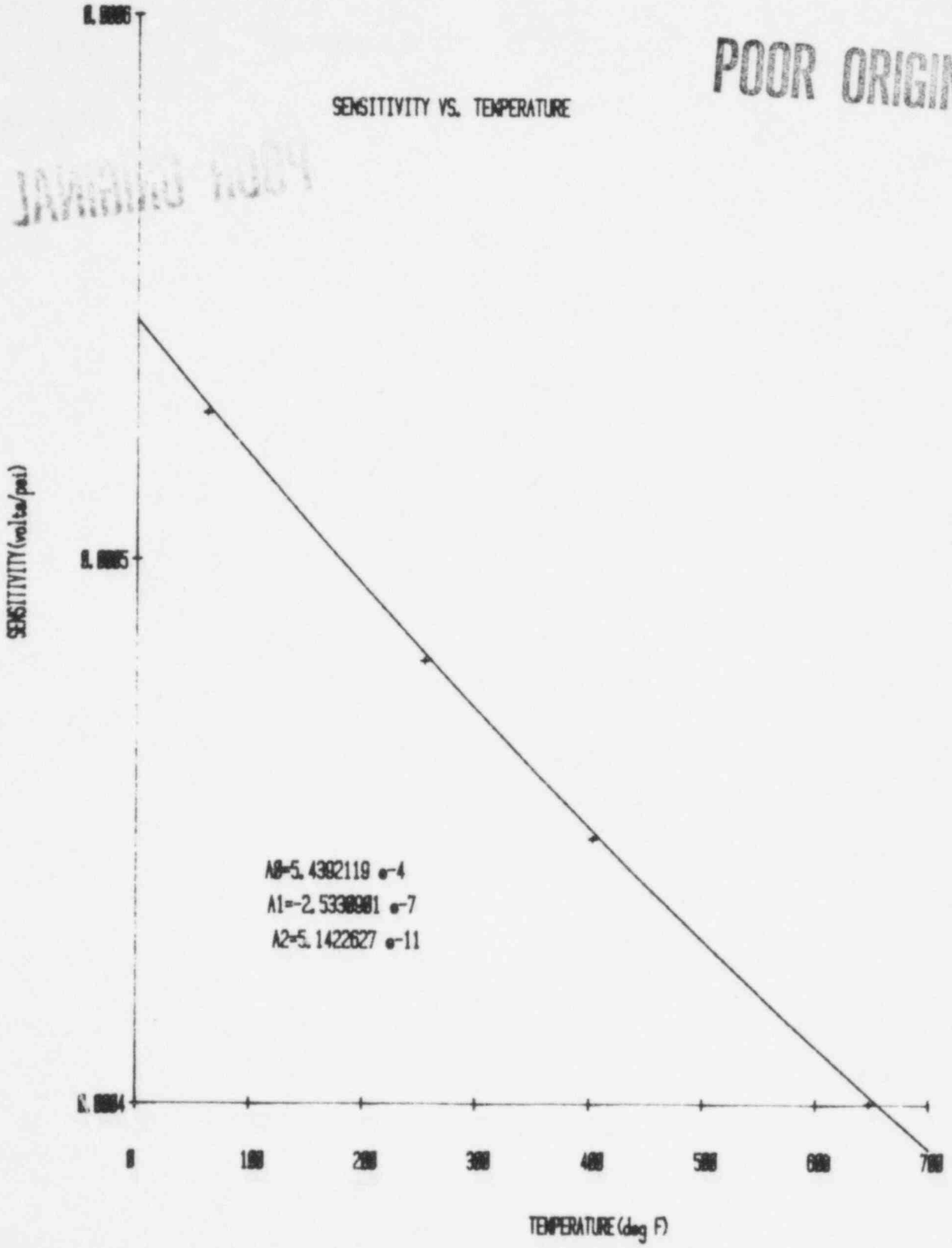

FIGURE VIII.19 Sensitivity for Calibration of Figure VIII.17.

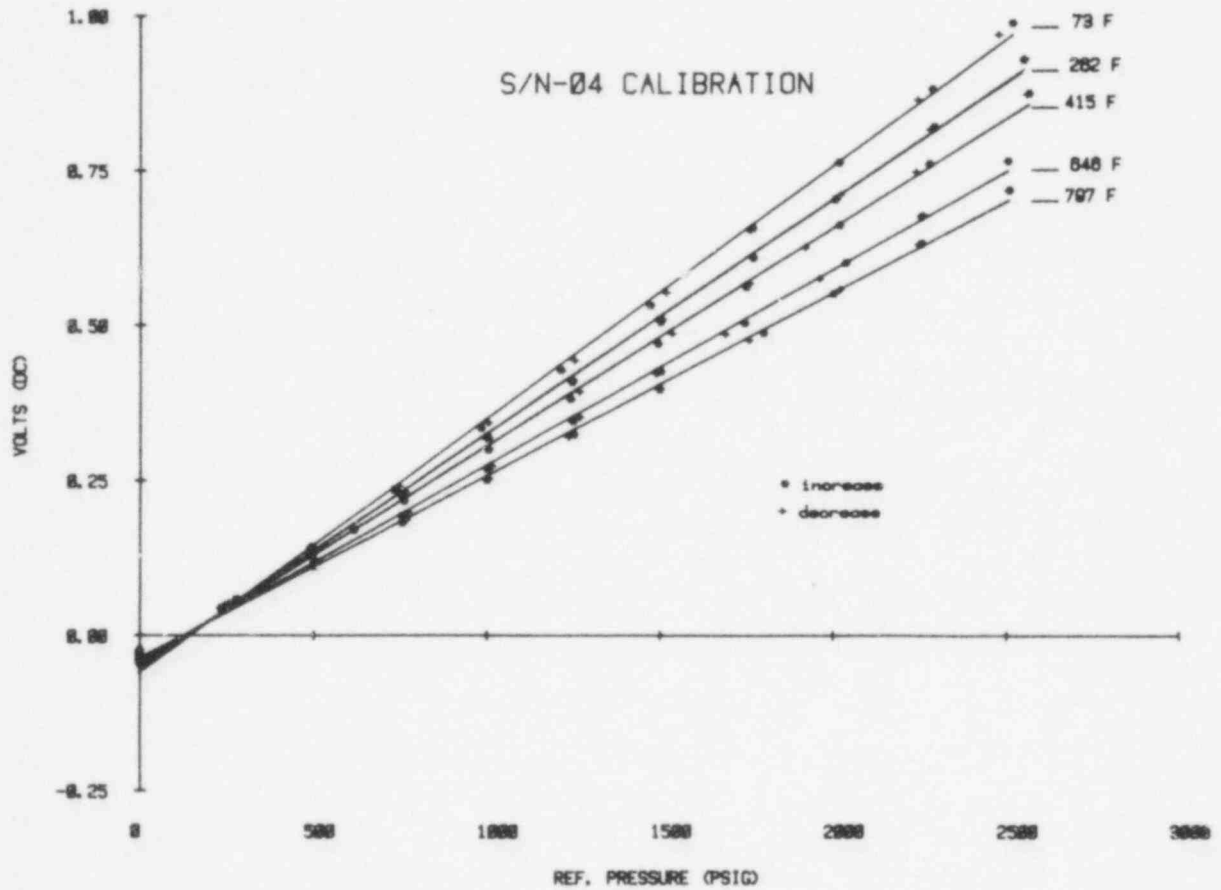

FIGURE VIII.20 First Calibration With Only Sensor Heated.

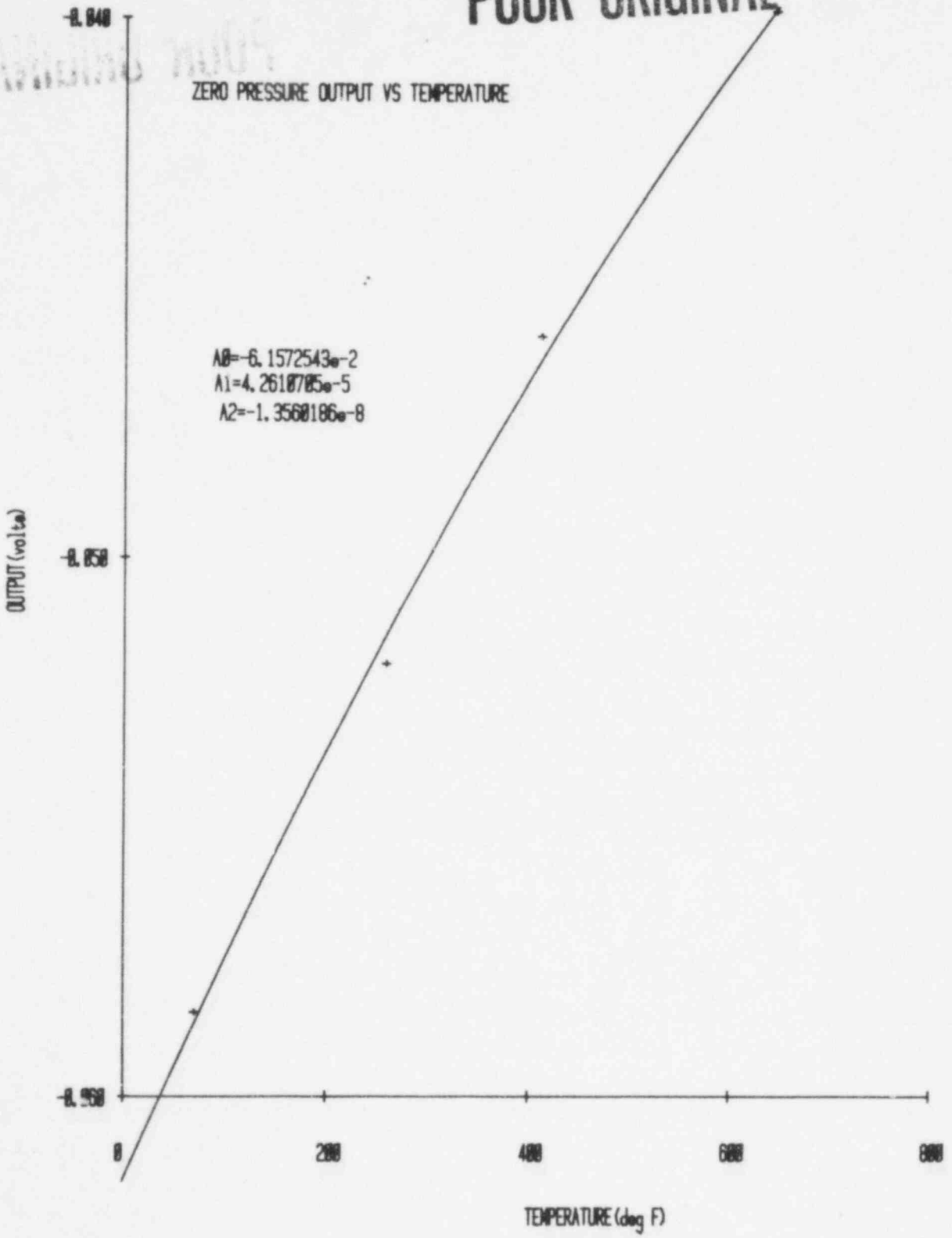

FIGURE VIII.21 Zero Pressure Output for Calibration of Figure VIII.20.

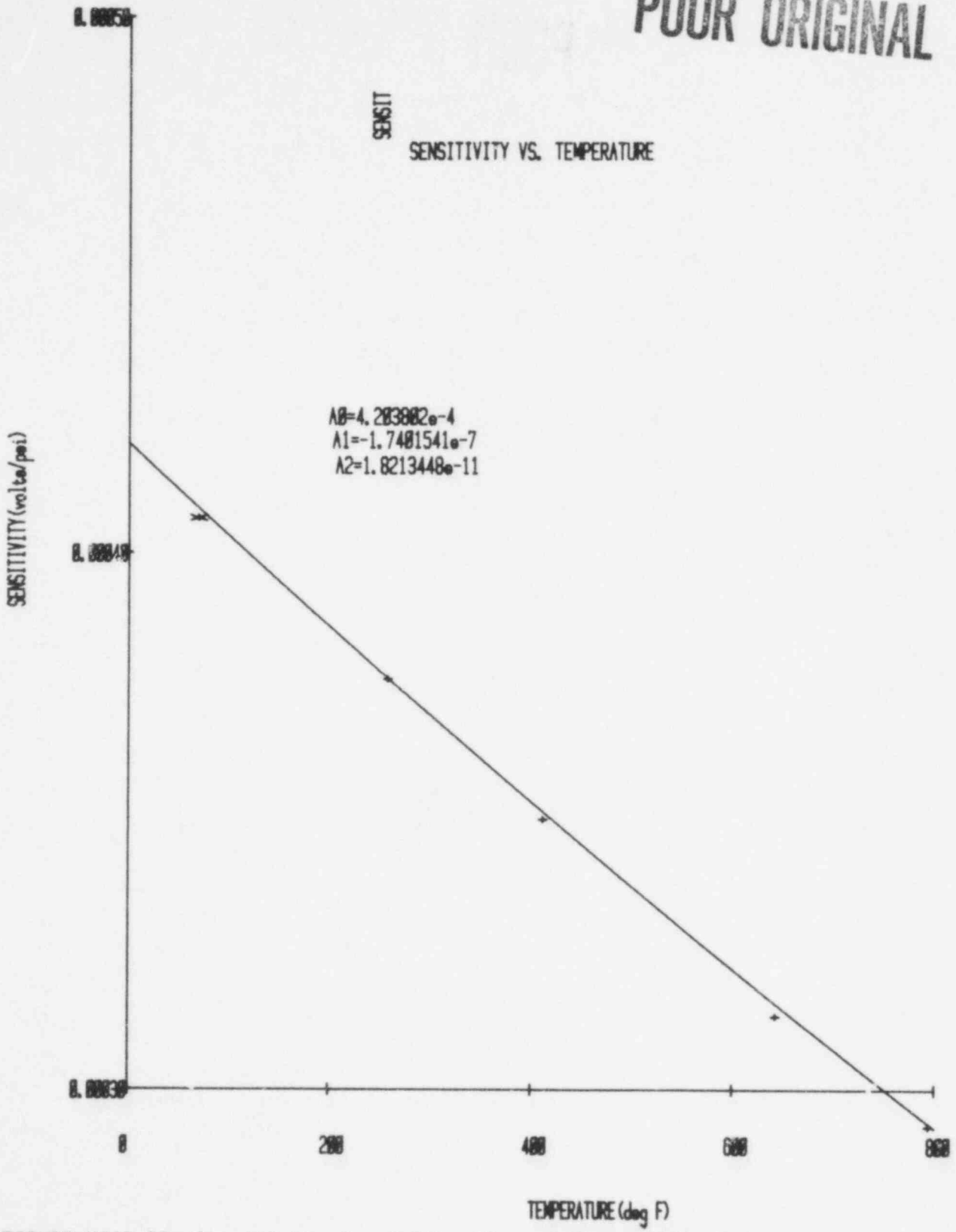

FIGURE VIII.22 Sensitivity for Calibration of Figure VIII.20.

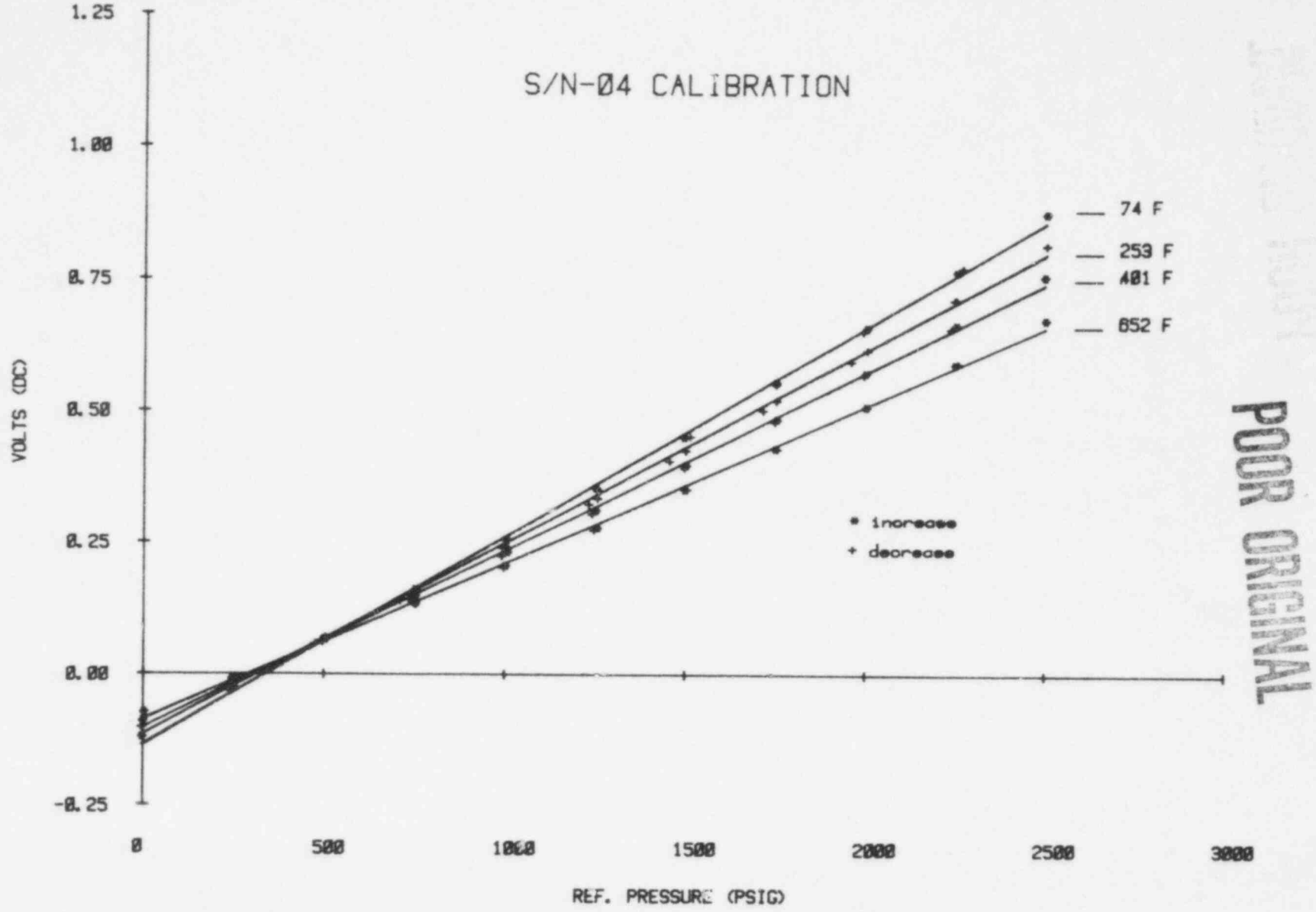

FIGURE VIII.23 Calibration With Sensor and Signal Cable Installed in Autoclave.

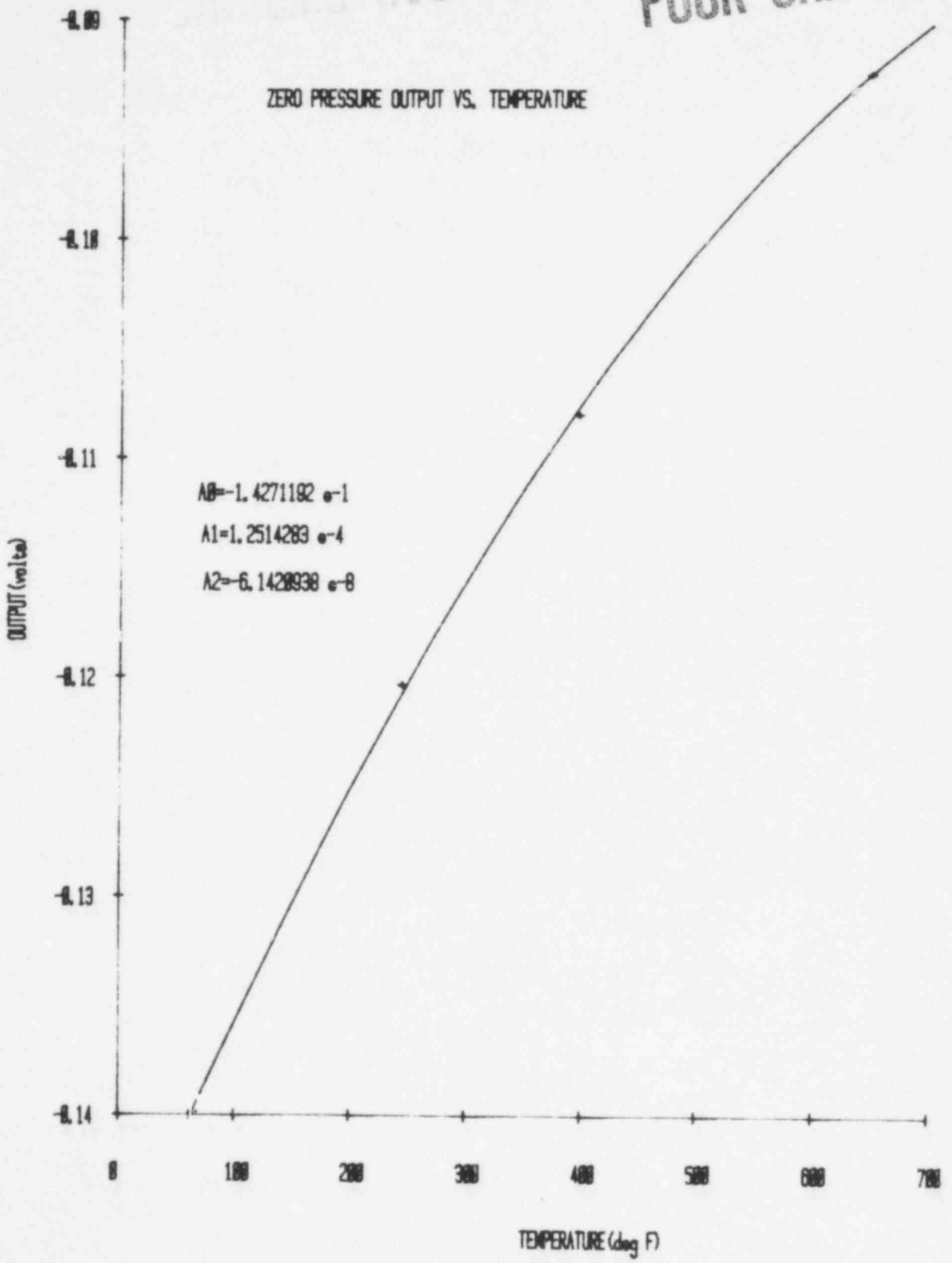

FIGURE VIII.24 Zero Pressure Output for Calibration of Figure VIII.23.

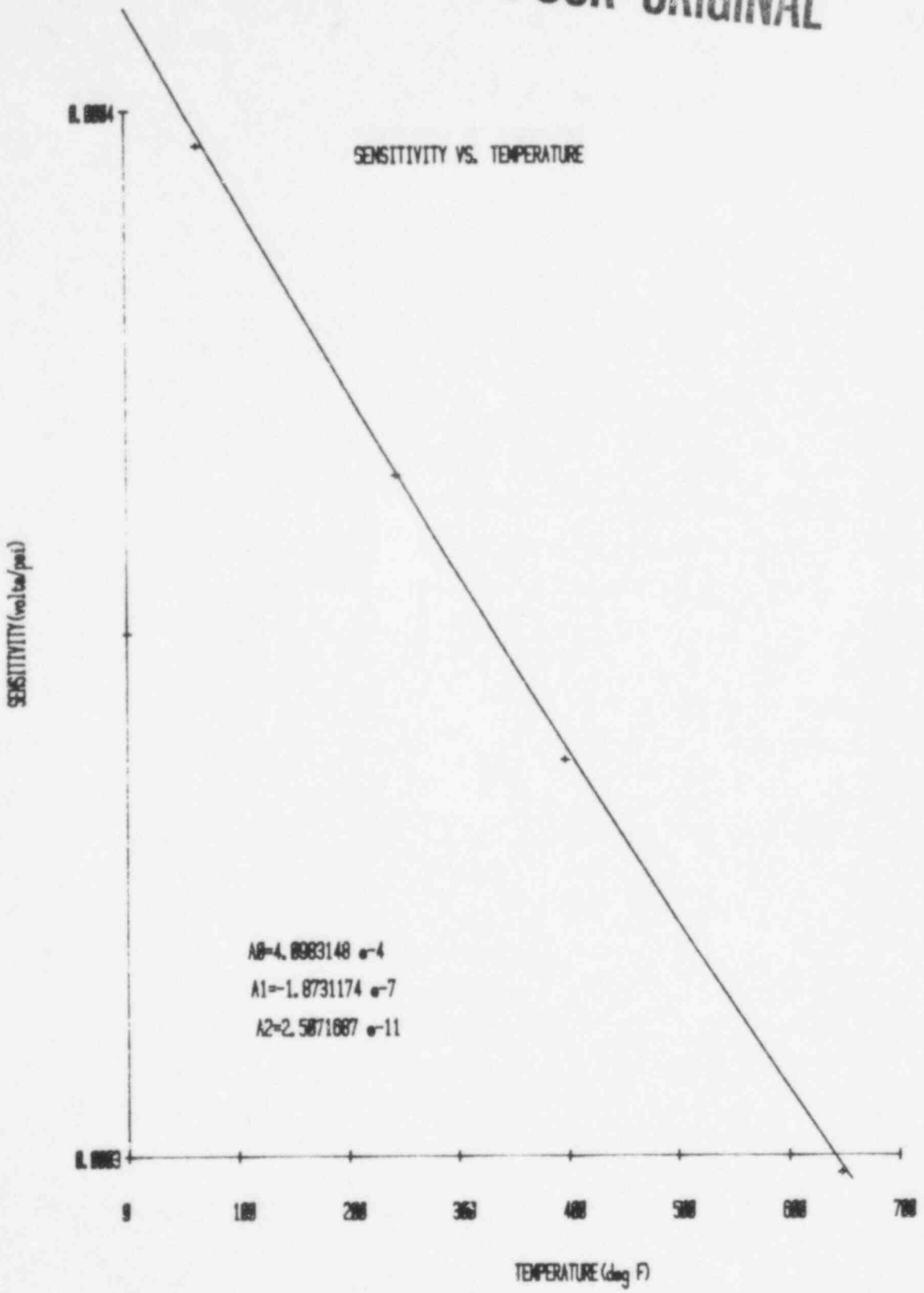

FIGURE VIII.25 Sensitivity for Calibration of Figure VIII.23.

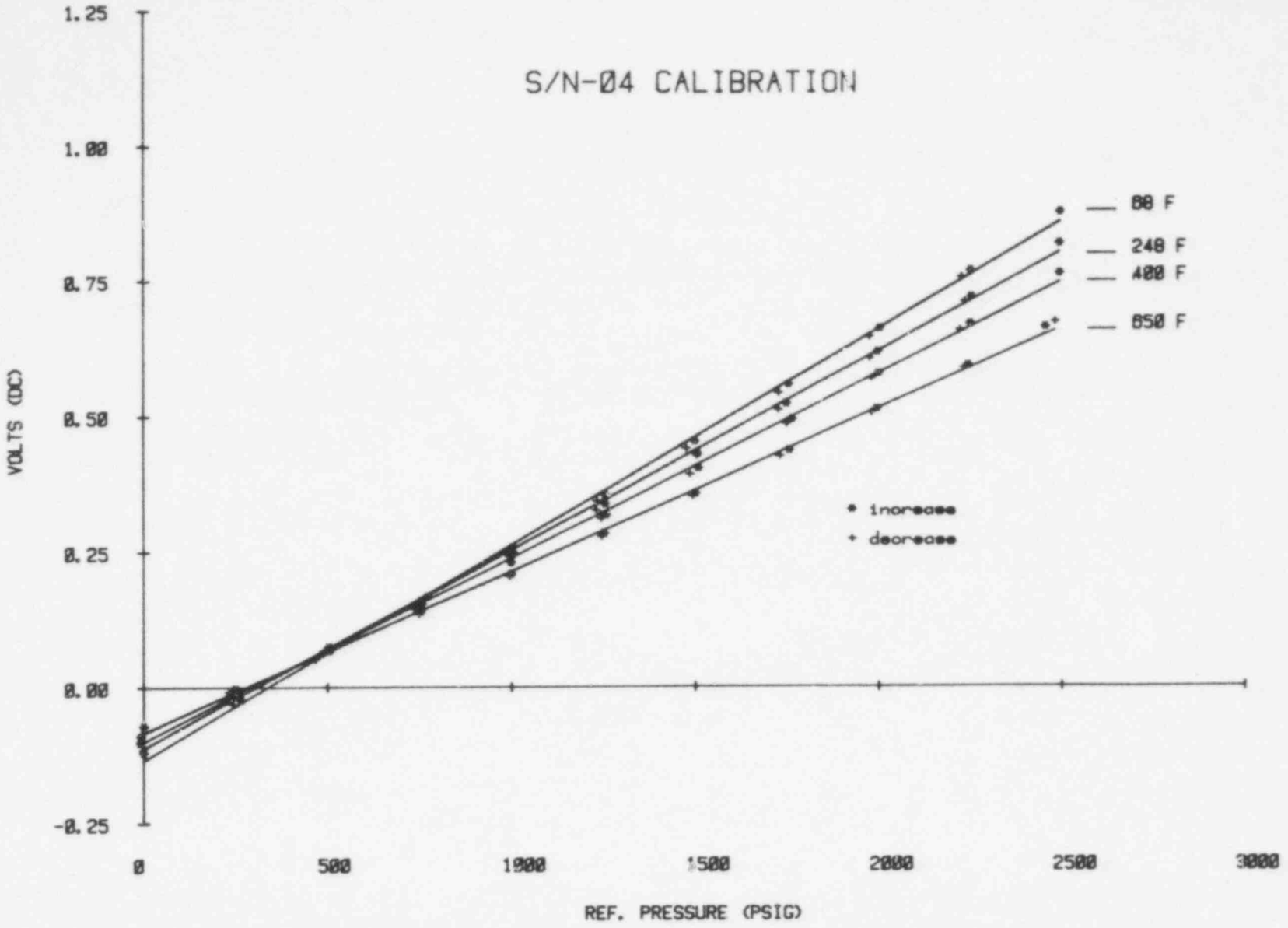

FIGURE VIII.26 Calibration After Blowdowns With Sensor and Signal Cable Installed in Autoclave.

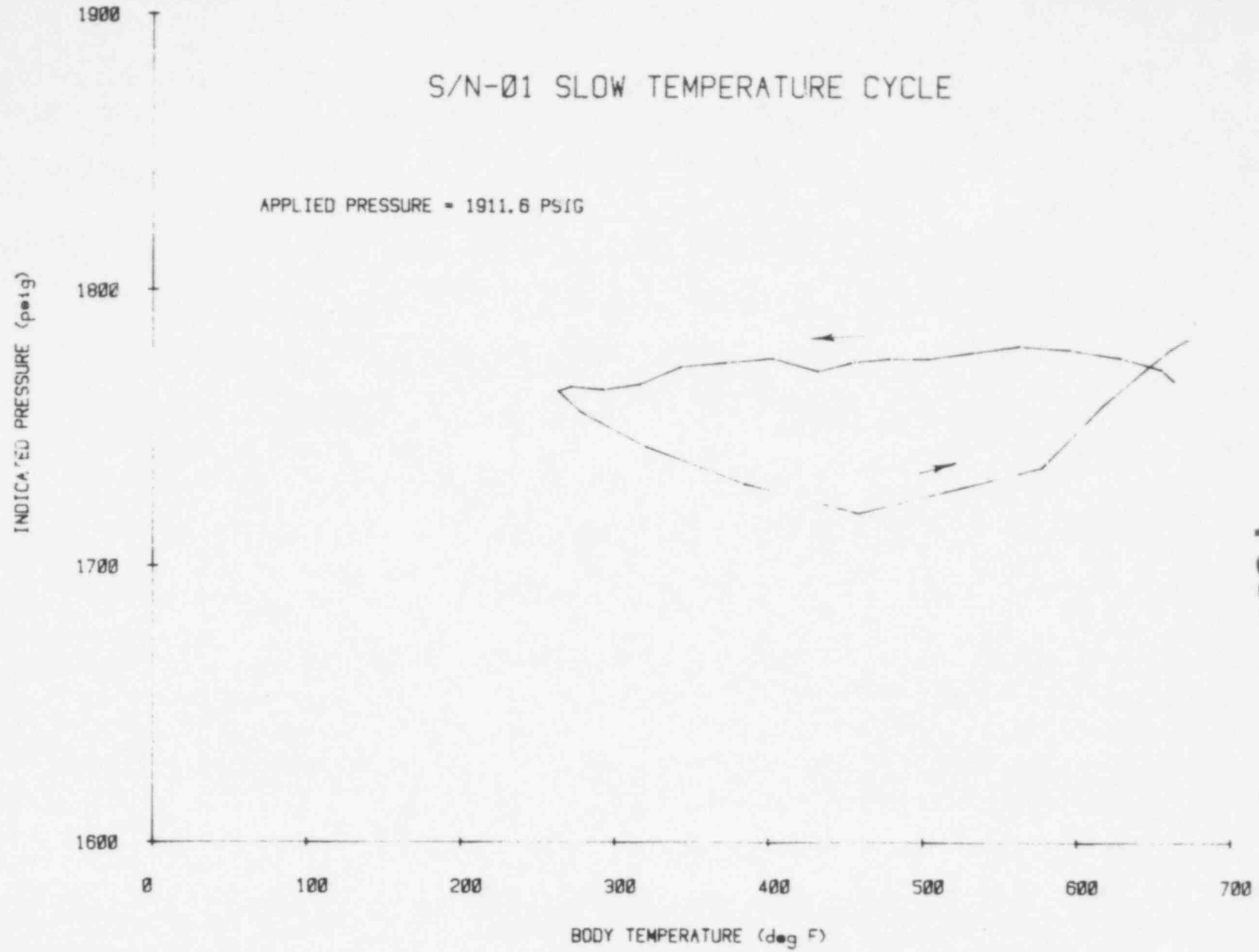

FIGURE VIII.27 Sensor Response for Slowly Varying Temperature.

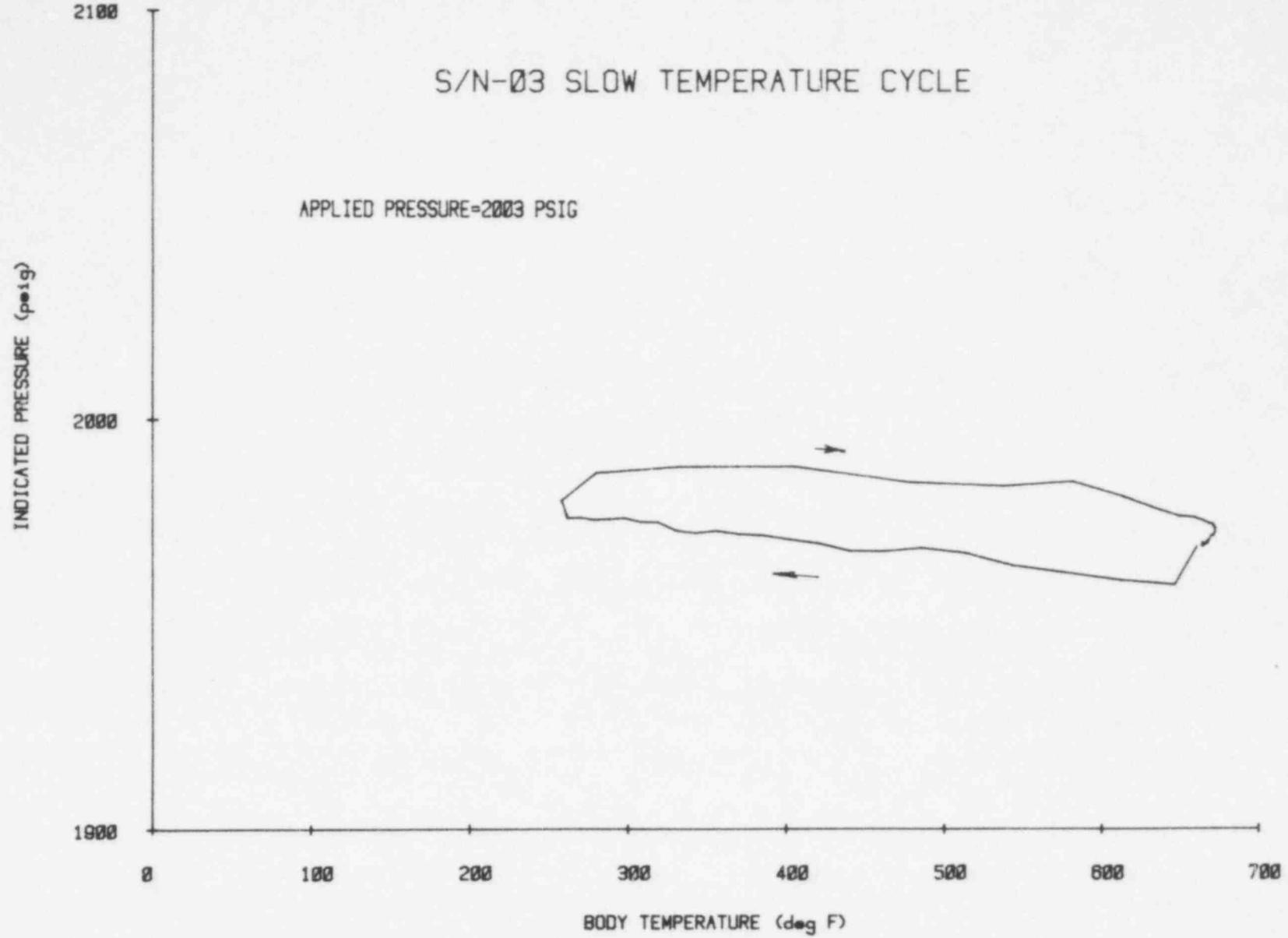

FIGURE VIII.28 Sensor Response for Slowly Varying Temperature.

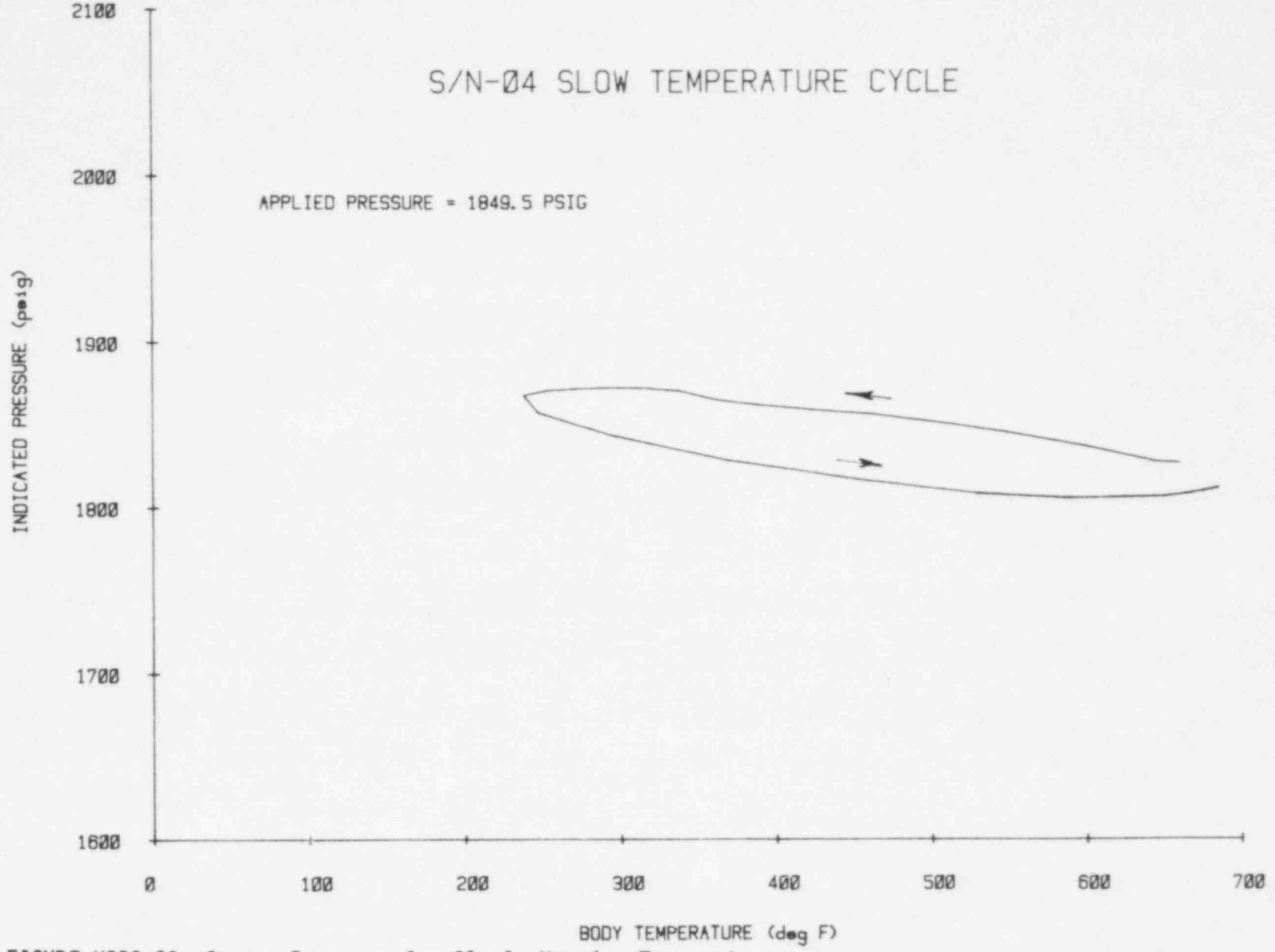

FIGURE VIII.29 Sensor Response for Slowly Varying Temperature.

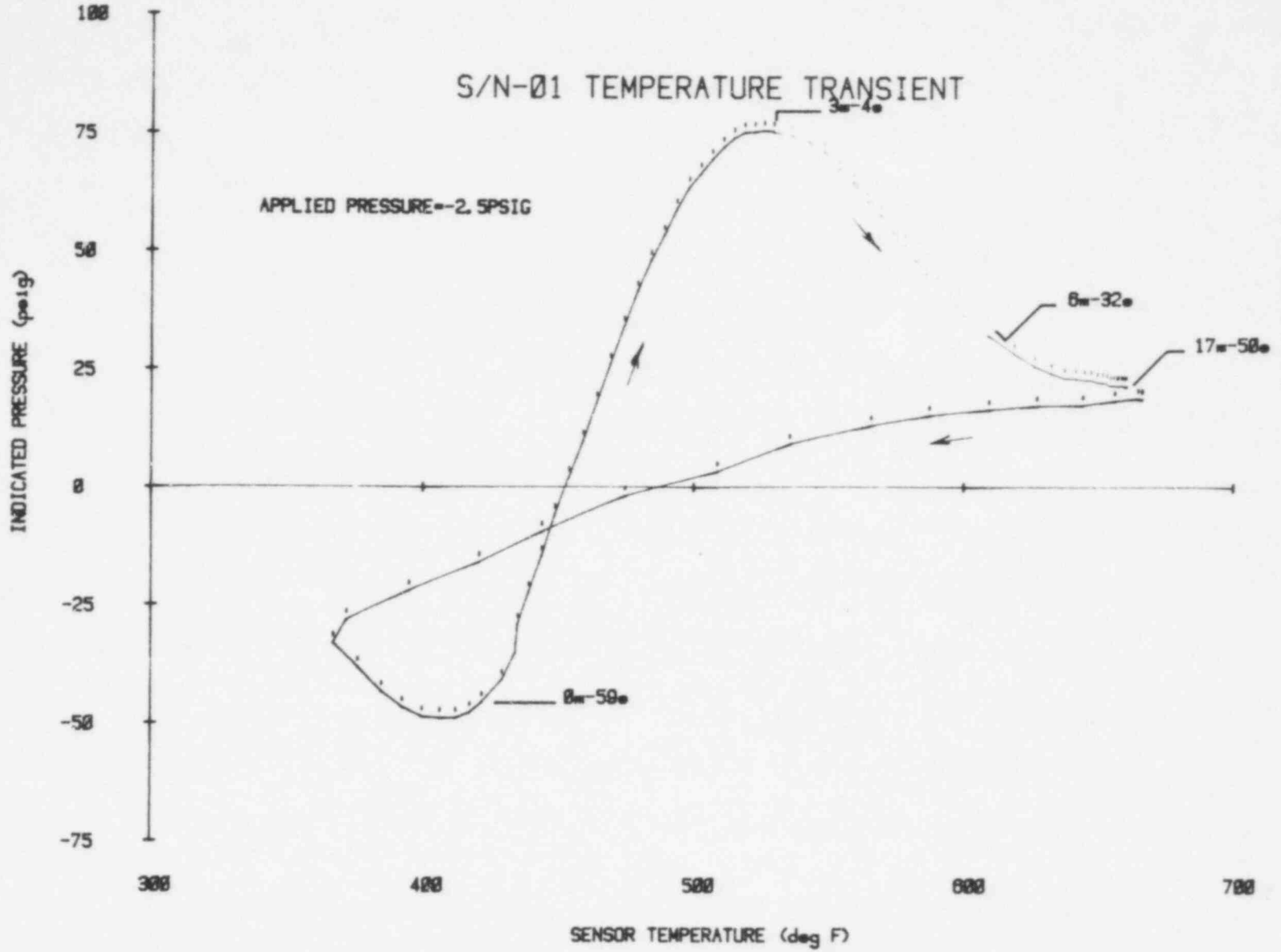

FIGURE VIII.30 Sensor Response for Rapid Cooling (Elapsed Time Shown).

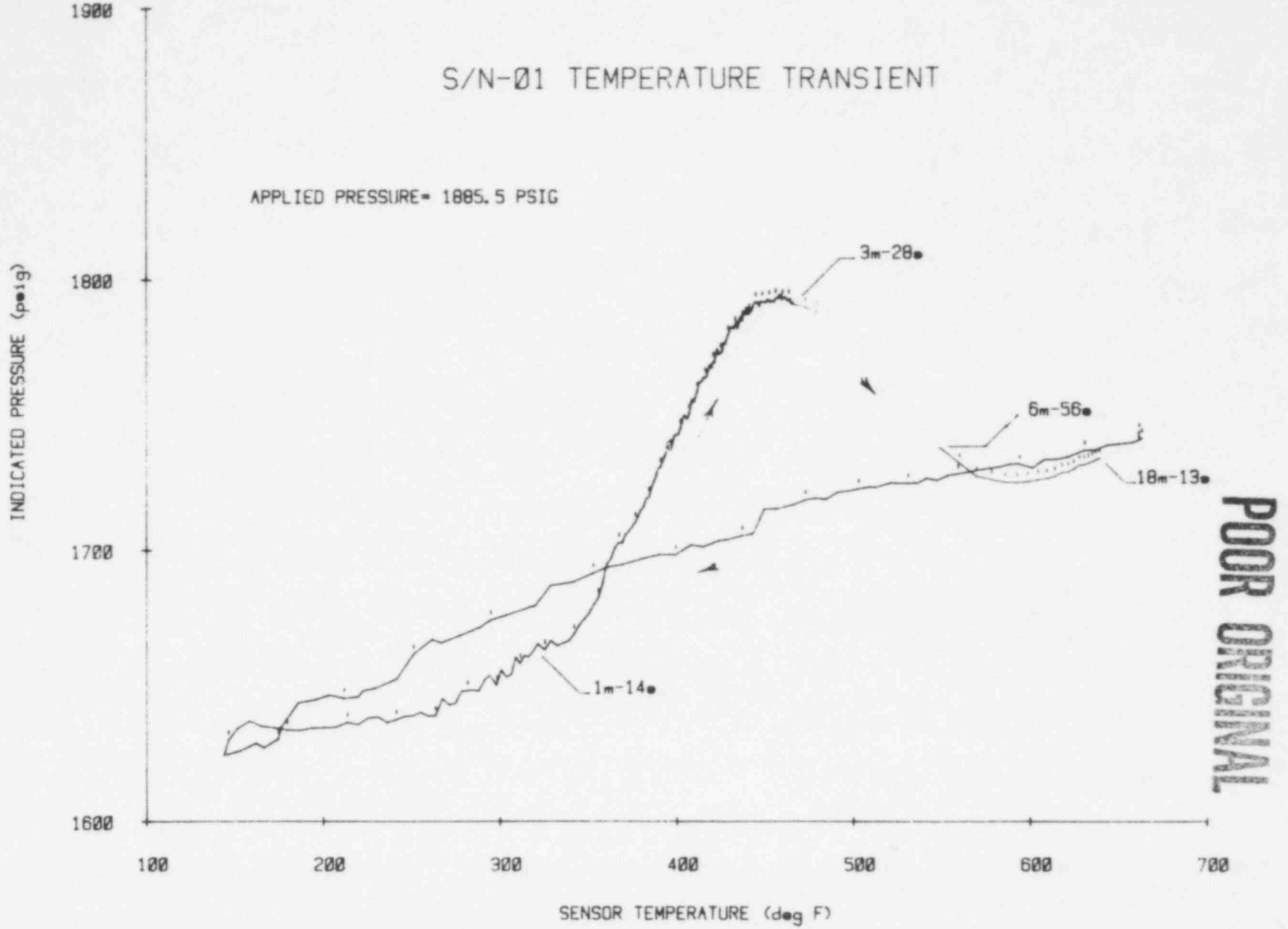

FIGURE VIII.31 Sensor Response for Rapid Cooling (Elapsed Time Shown).

FIGURE VIII.32 Sensor Response for Rapid Cooling (Elapsed Time Shown).

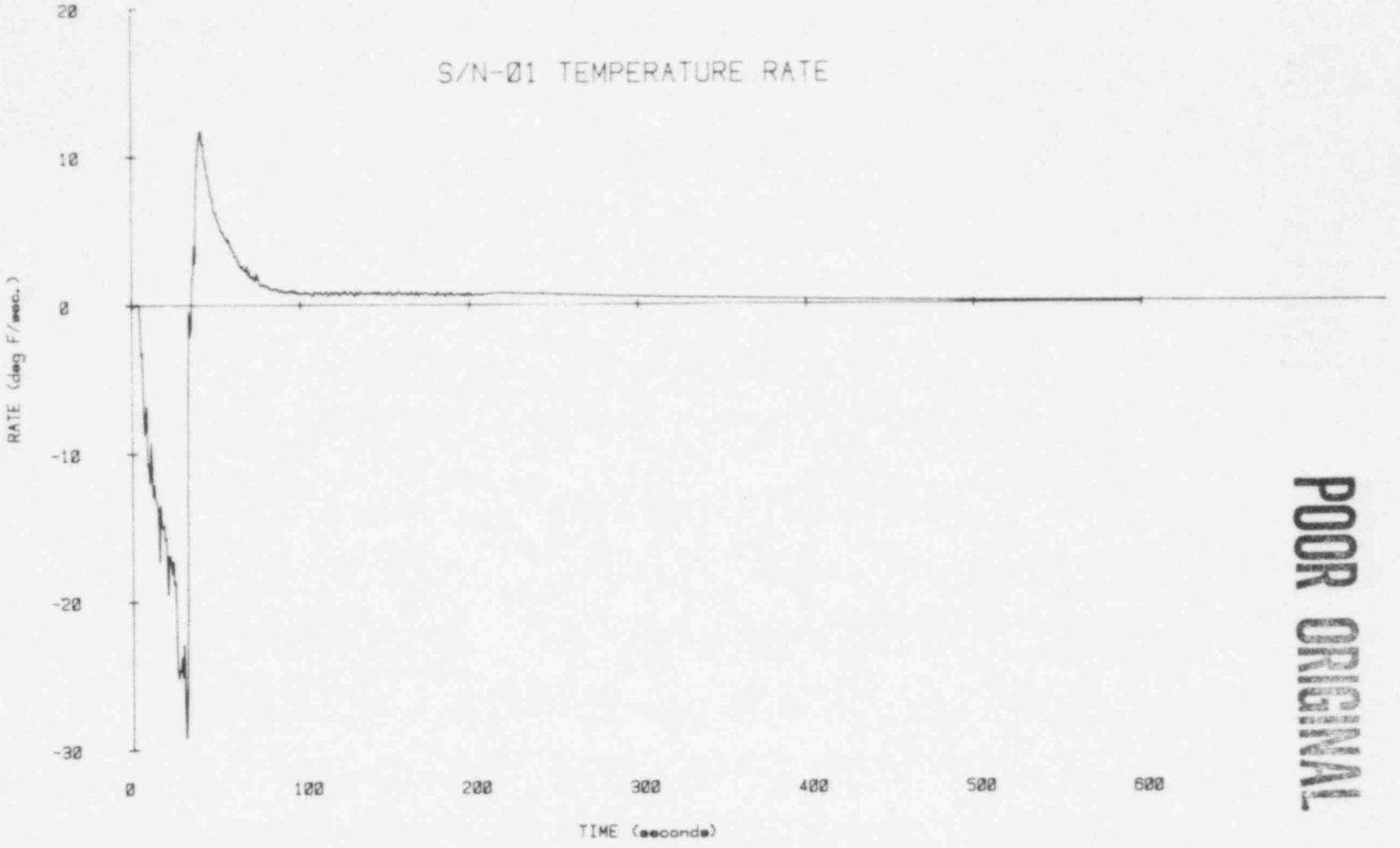

FIGURE VIII.33 Rate of Temperature Change During Transient of Figure VIII.32.

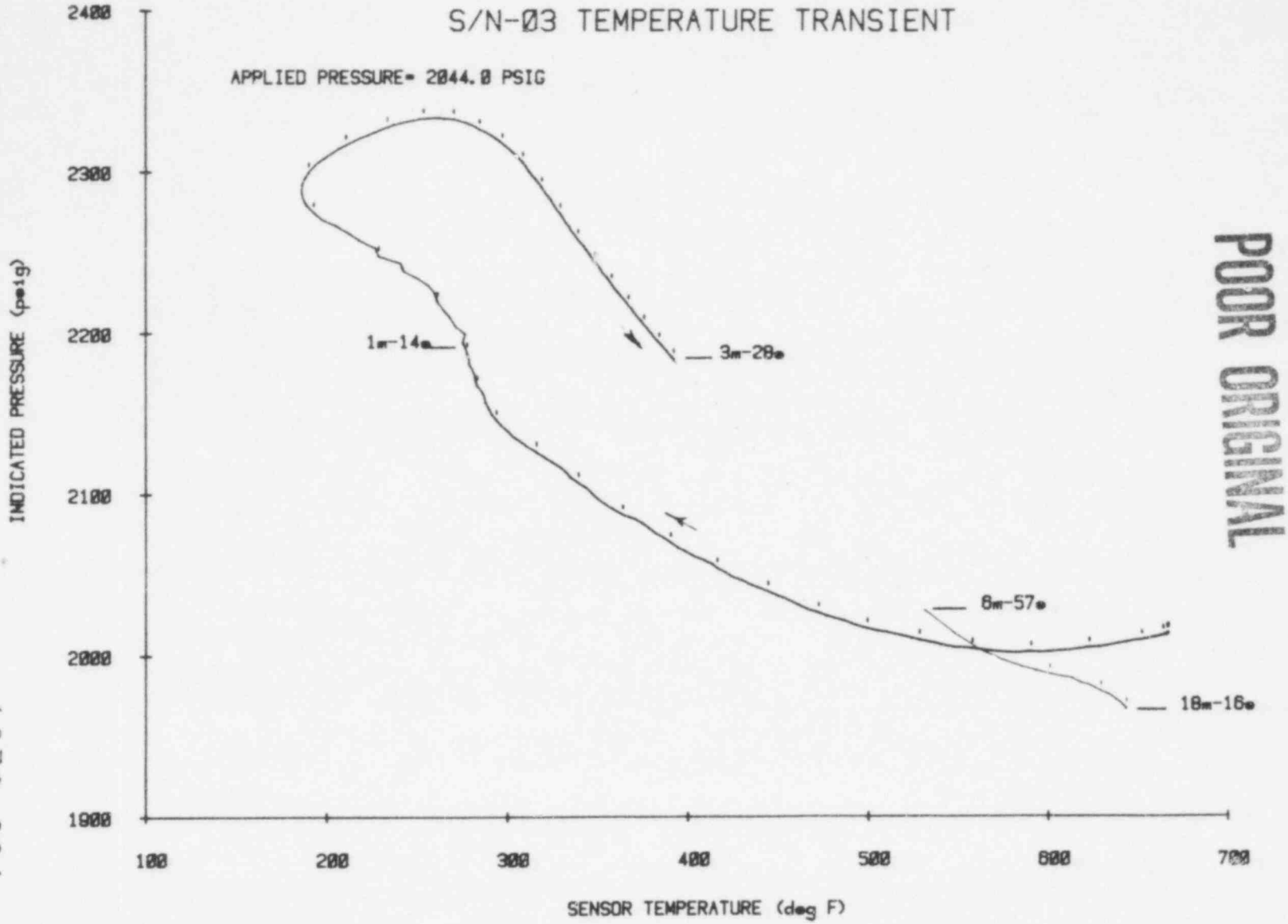

FIGURE VIII.34 Sensor Response for Rapid Cooling (Elapsed Time Shown).

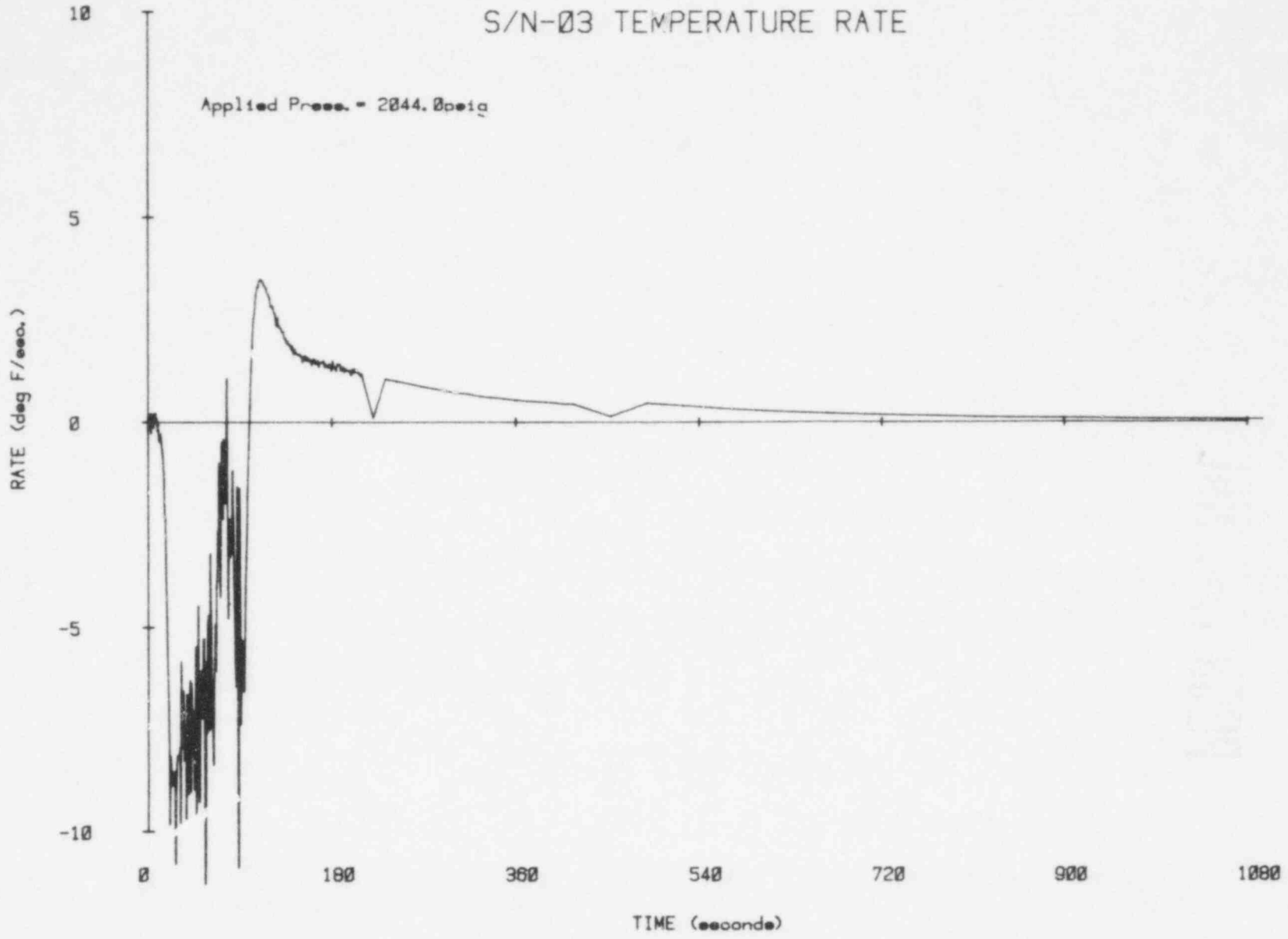

FIGURE VIII.35 Rate of Temperature Change During Transient of Figure VIII.34.

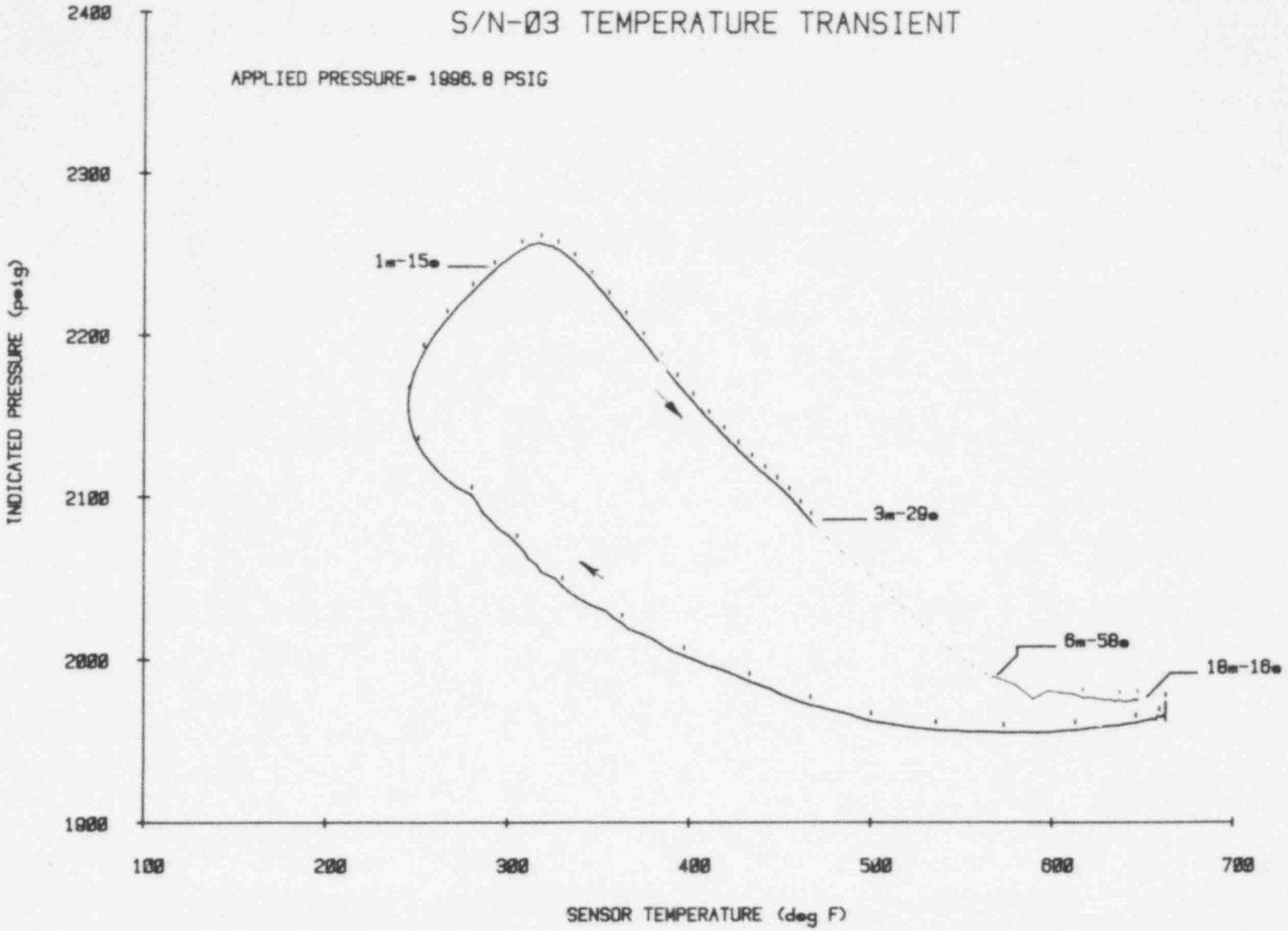

FIGURE VIII.36 Sensor Response for Rapid Cooling (Elapsed Time Shown).

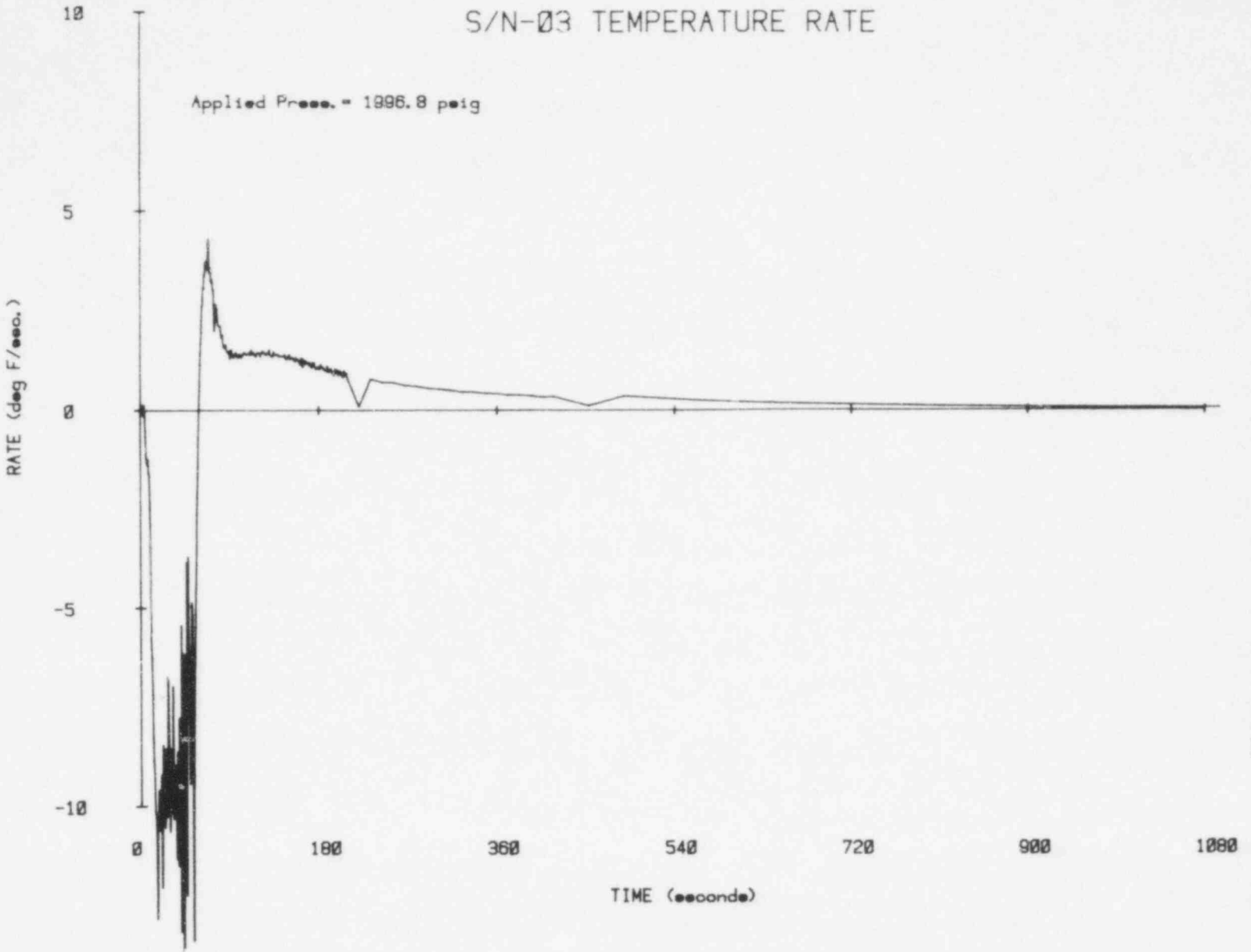

FIGURE VIII.37 Rate of Temperature Change During Transient of Figure VIII.36.

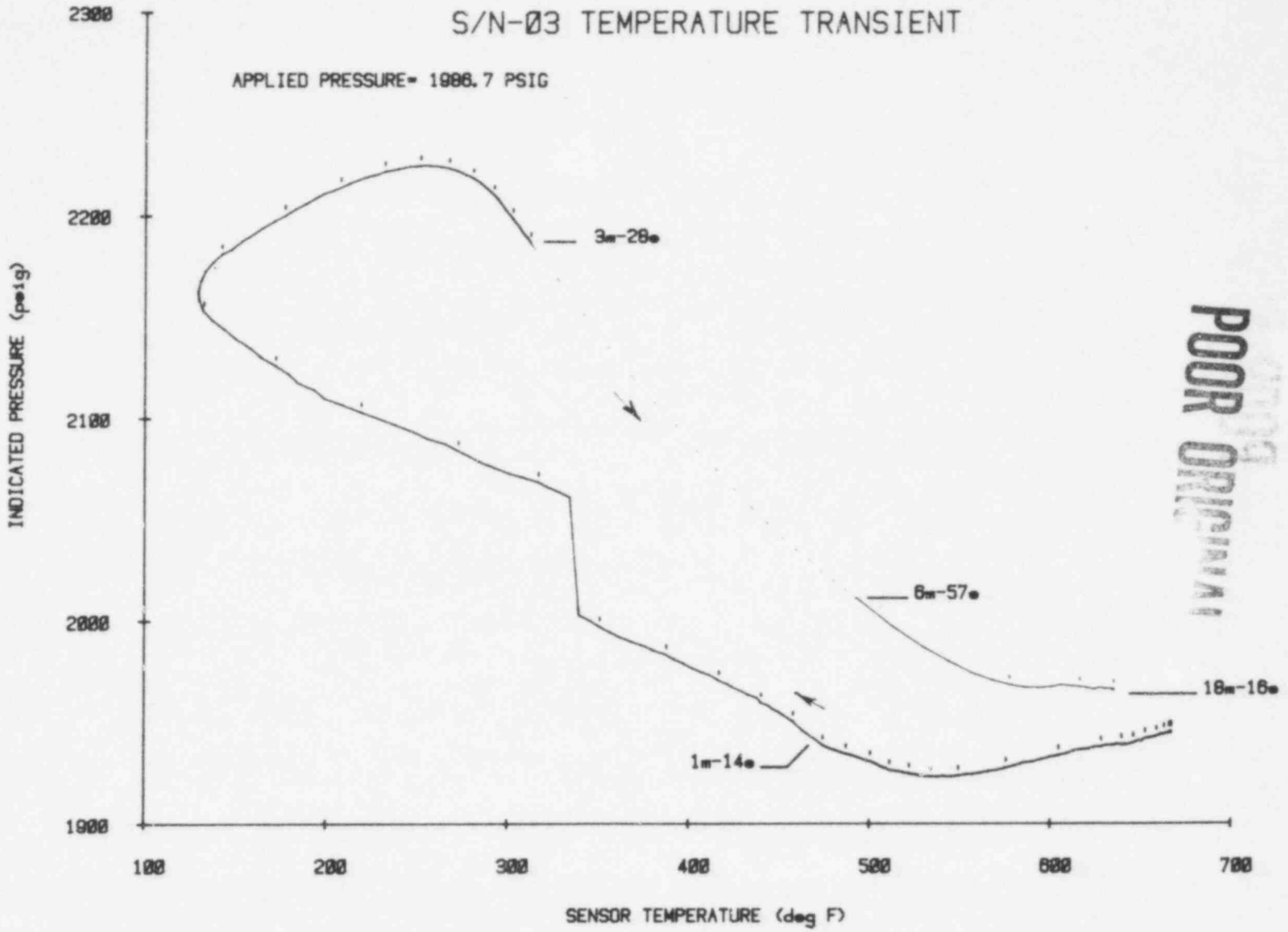

FIGURE VIII.38 Sensor Response for Rapid Cooling (Elapsed Time Shown).

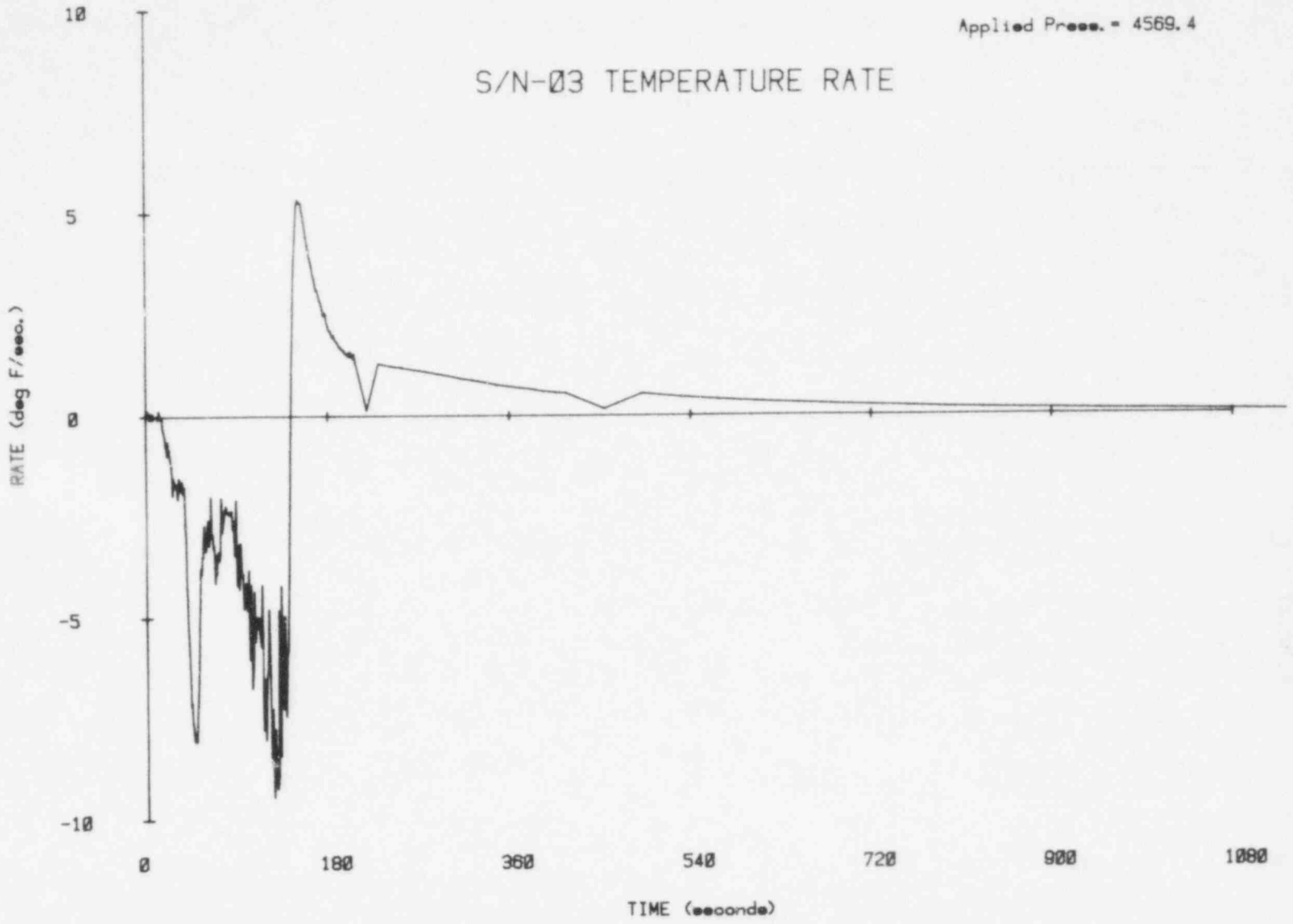

FIGURE VIII.39 Rate of Temperature Change for Transient of Figure VIII.38.

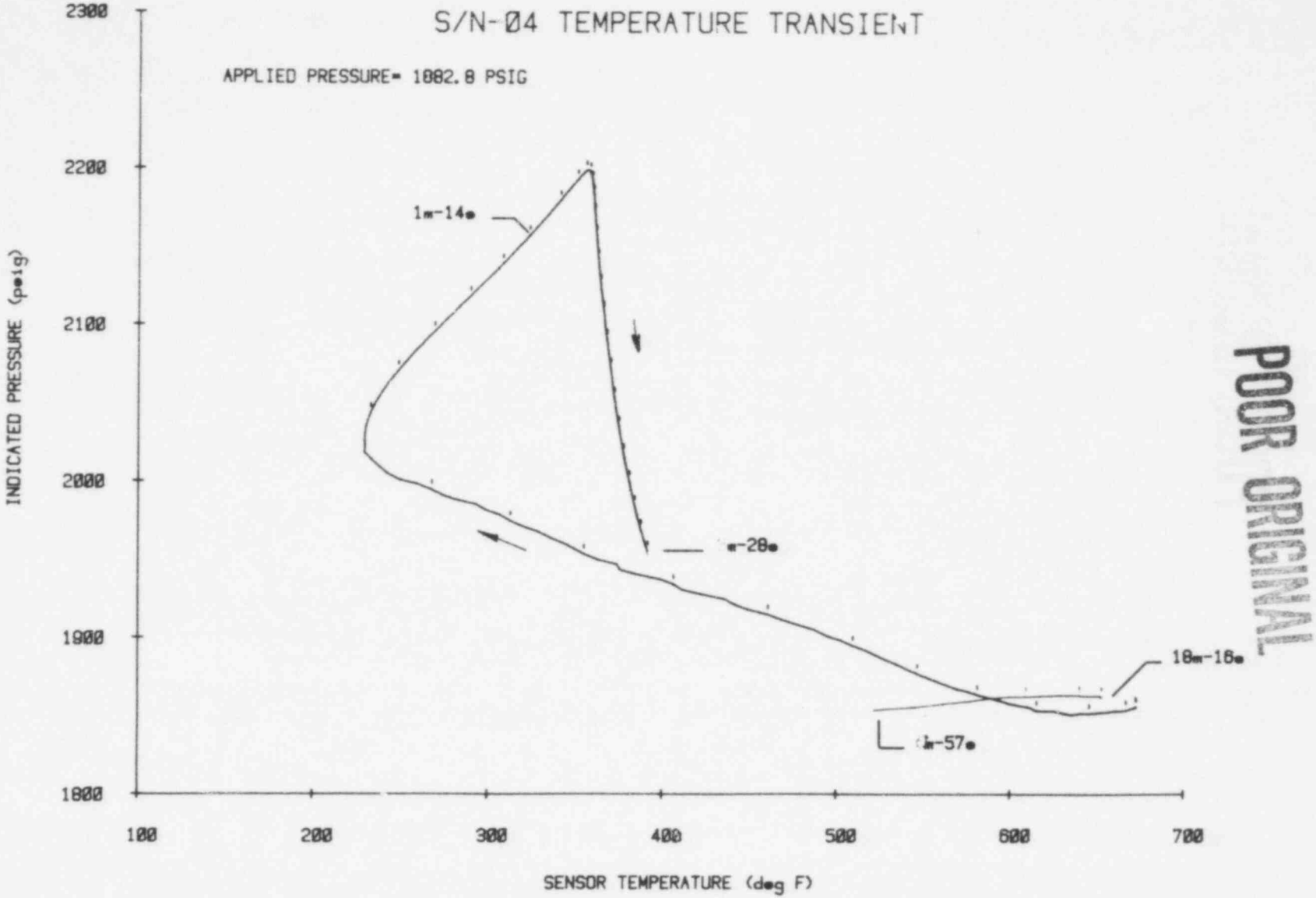

FIGURE VIII.40 Sensor Response for Rapid Cooling (Elapsed Time Shown).

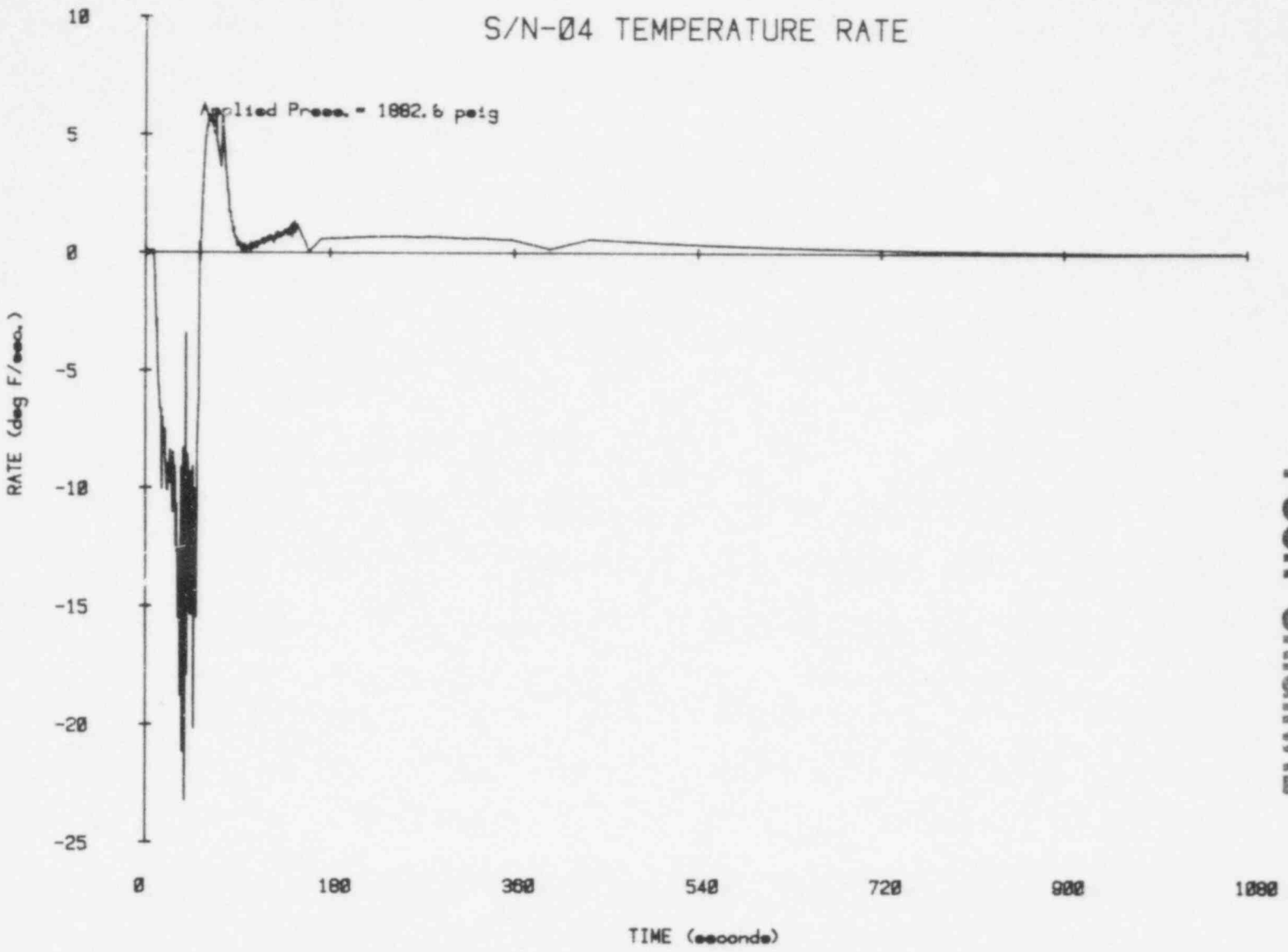

FIGURE VIII.41 Rate of Temperature Change for Transient of Figure VIII.40.

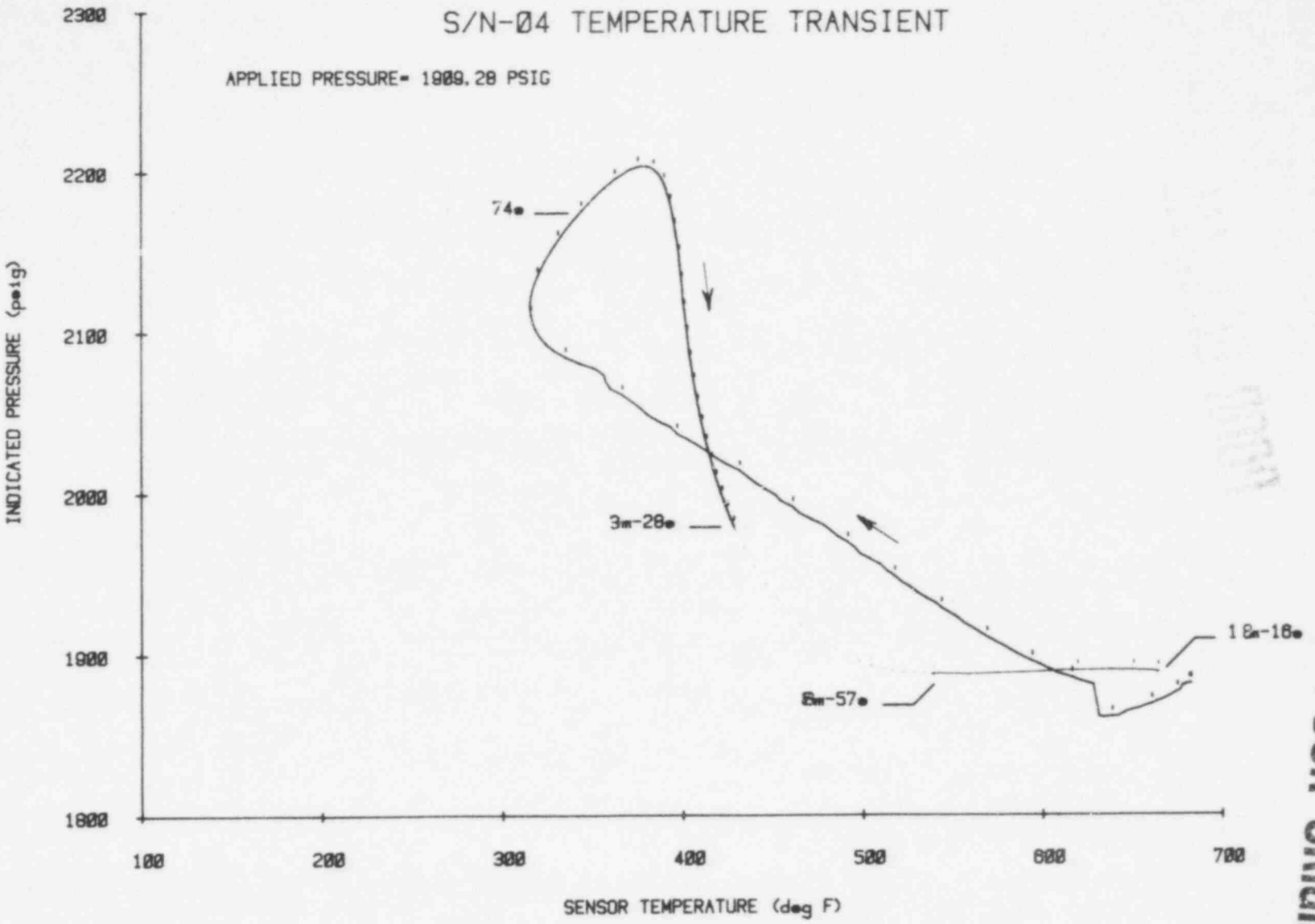

FIGURE VIII.42 Sensor Response for Rapid Cooling (Elapsed Time Shown).

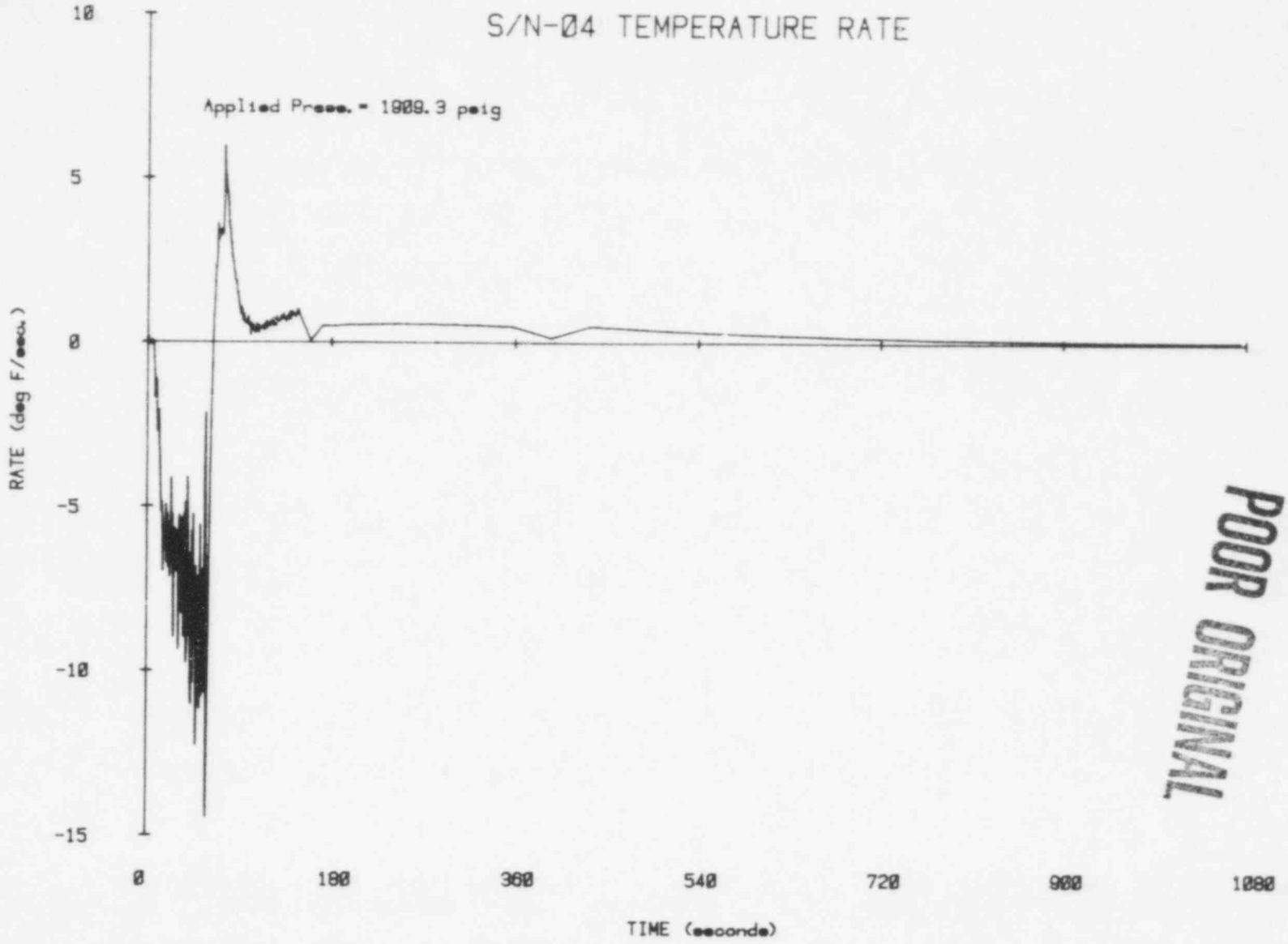

FIGURE VIII.43 Rate of Temperature Change for Transient of Figure VIII.42.

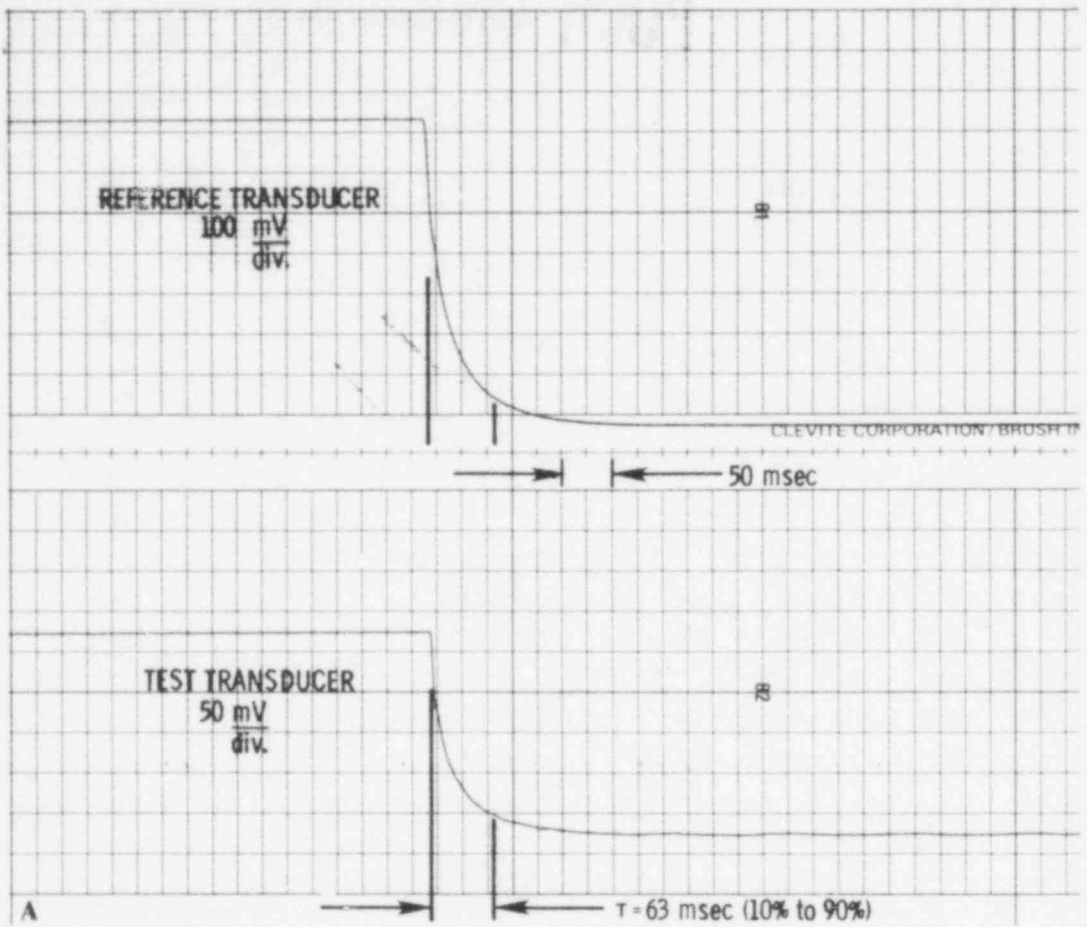

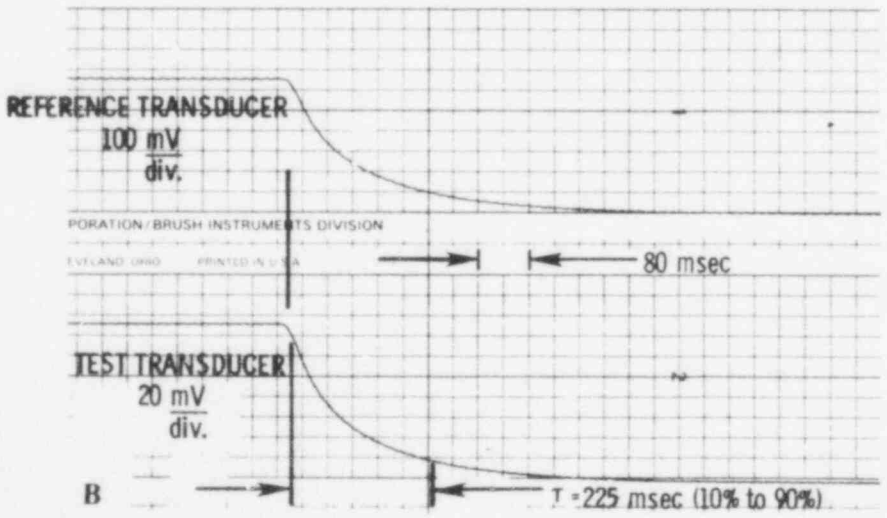

HEDL 7905-09L.1

FIGURE VIII.44 Time Response of Pressure Sensor for Depressurization via (a) Burst disk and (b) Manually operated valve.

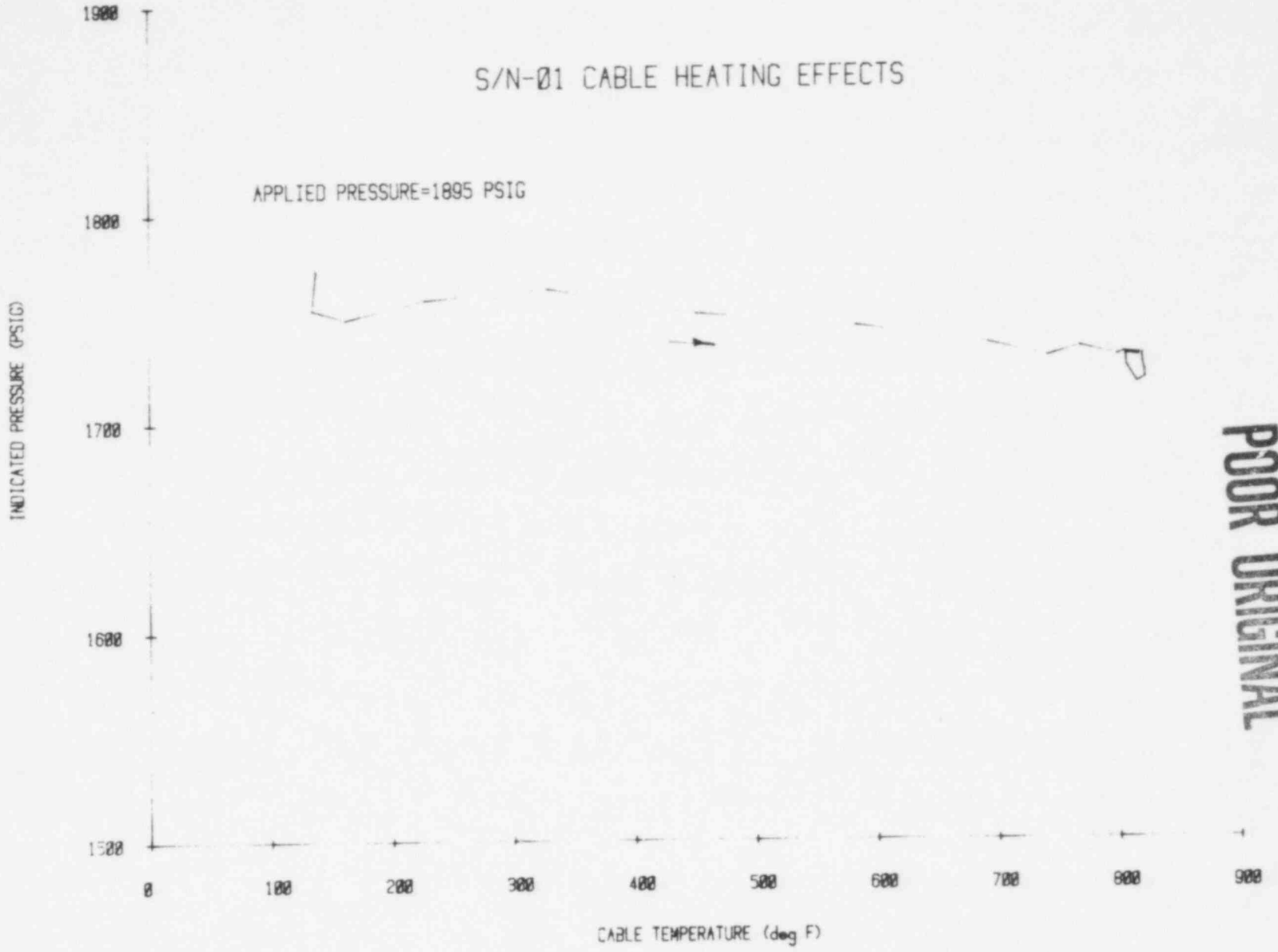

FIG. VIII.45 Effect Upon Sensor Signal Output of Heating 16 Feet of Signal Cable.

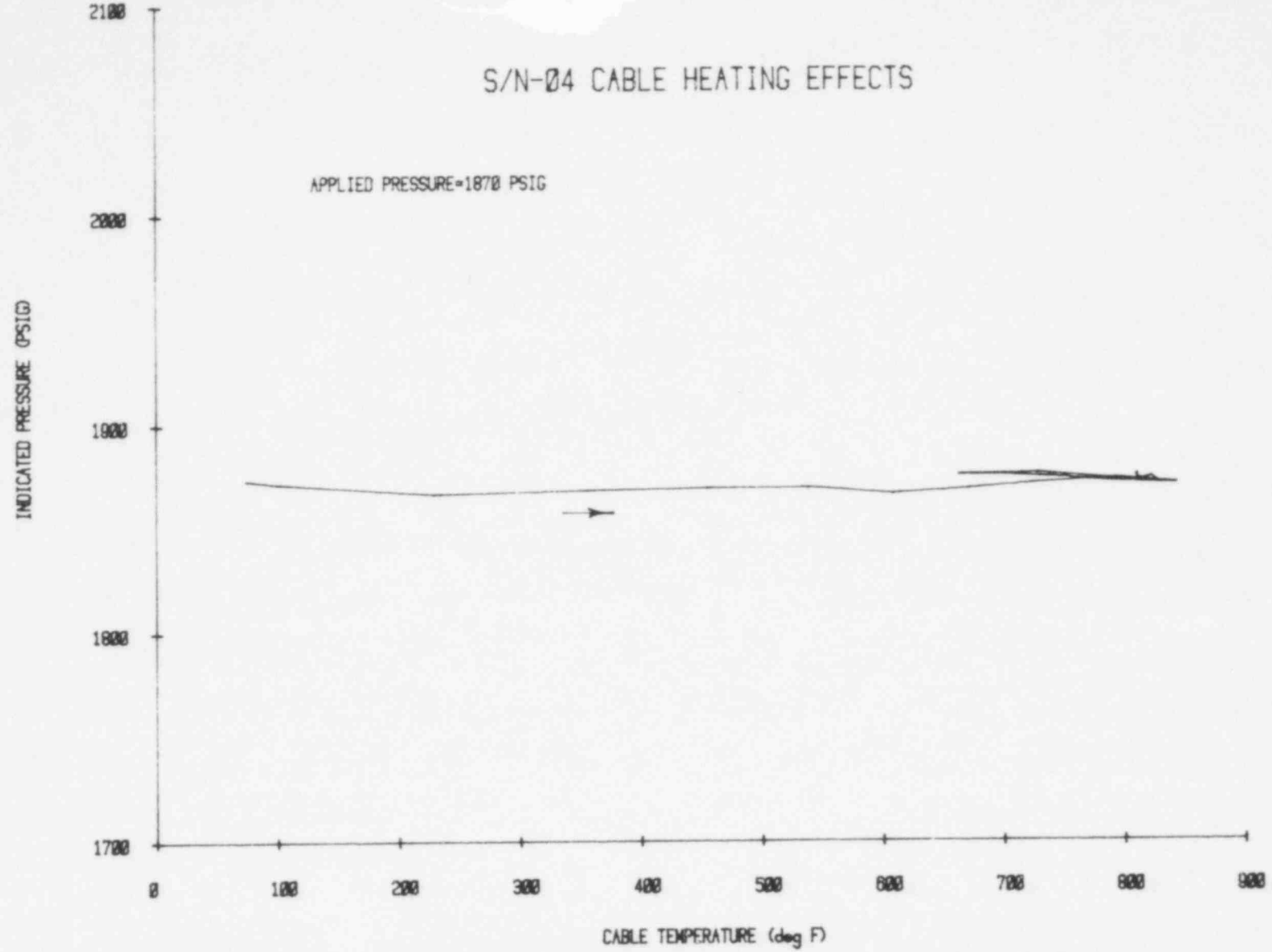

FIGURE VIII.46 Effect Upon Sensor Signal Output of Heating 16 Feet of Signal Cable.

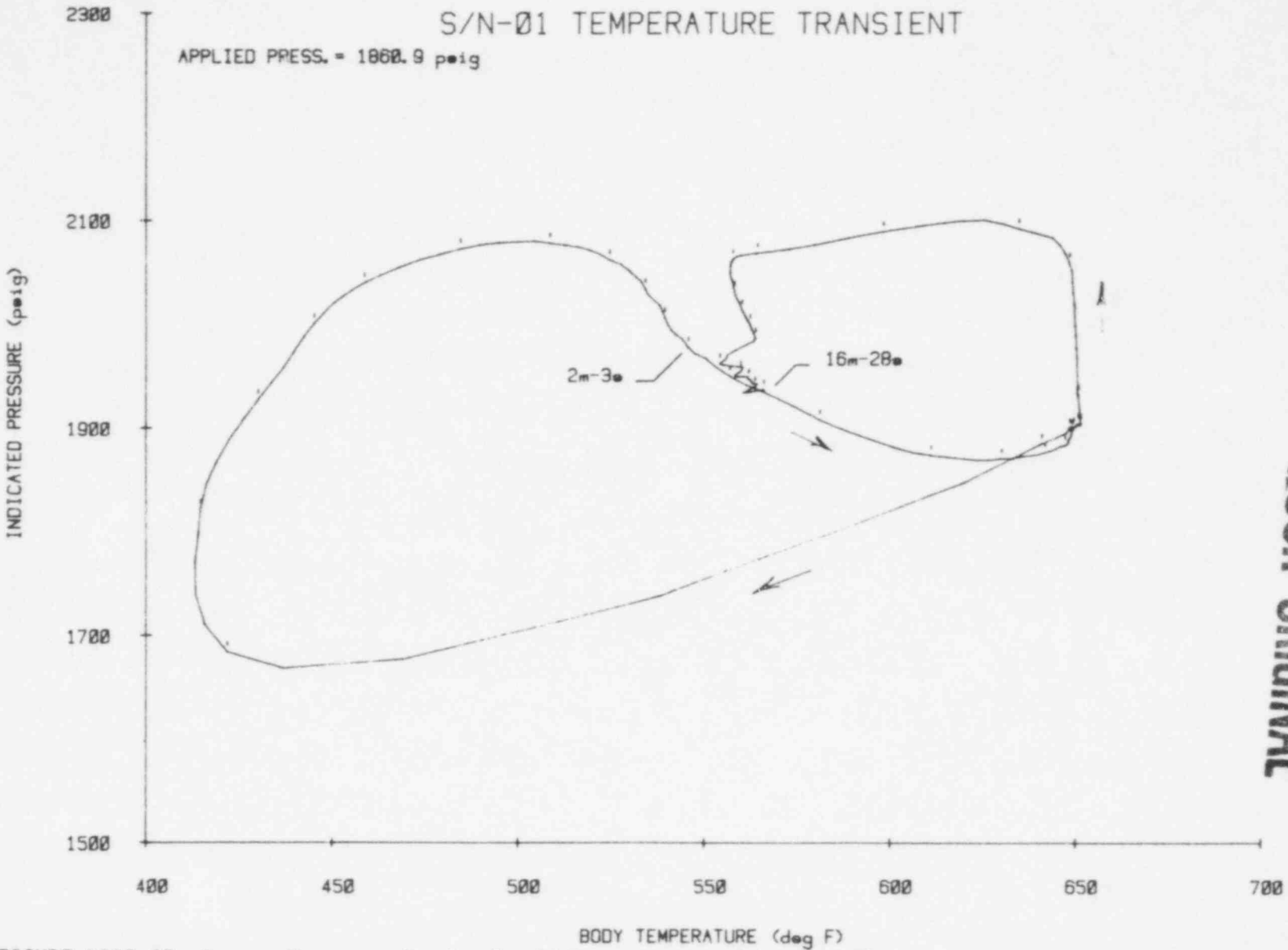

FIGURE VIII.47 Sensor Response During Rapid Depressurization of 650°F Water in Autoclave.

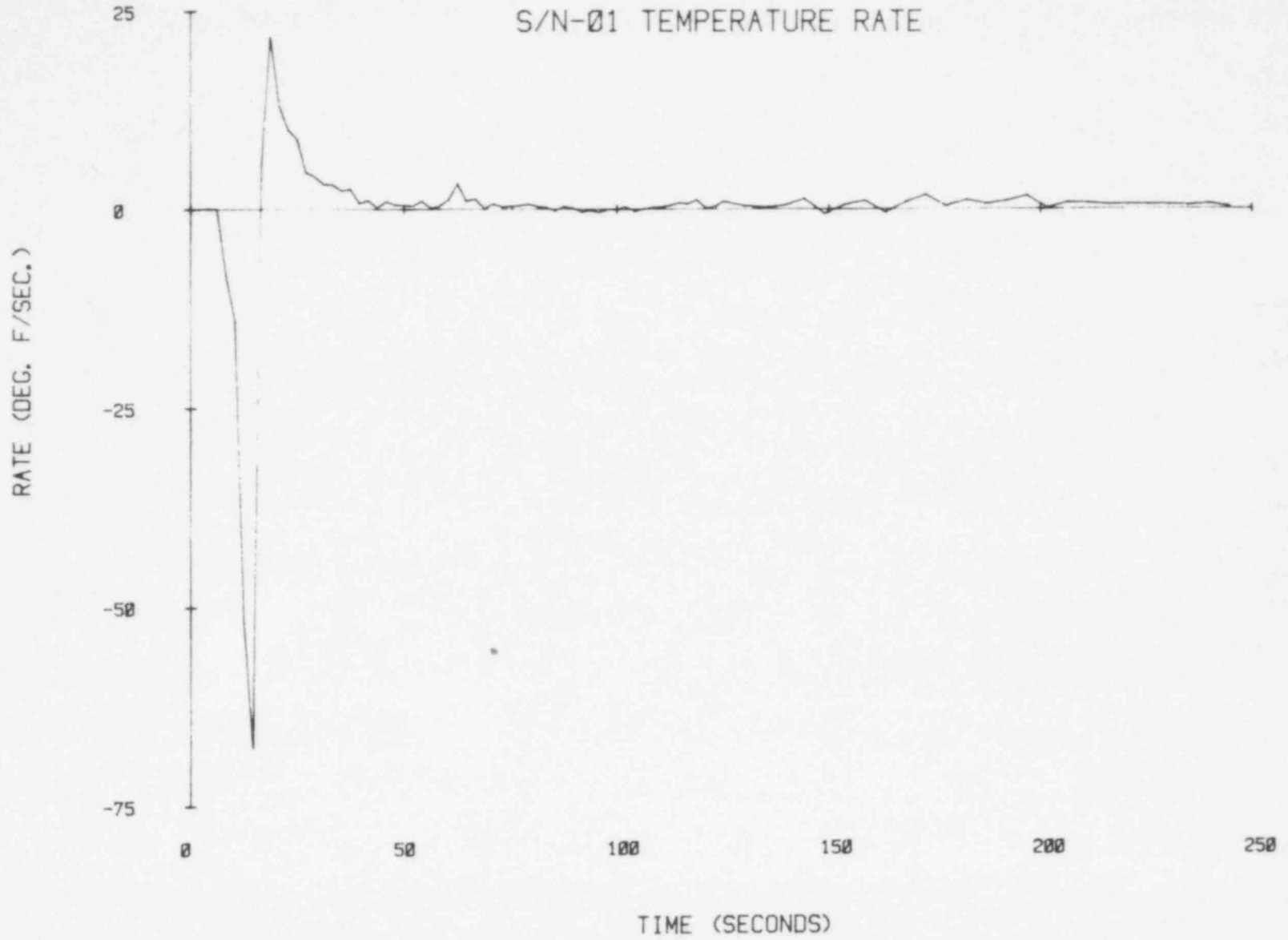

FIGURE VIII.48 Rate of Temperature Change for Blowdown of Figure VIII.47.

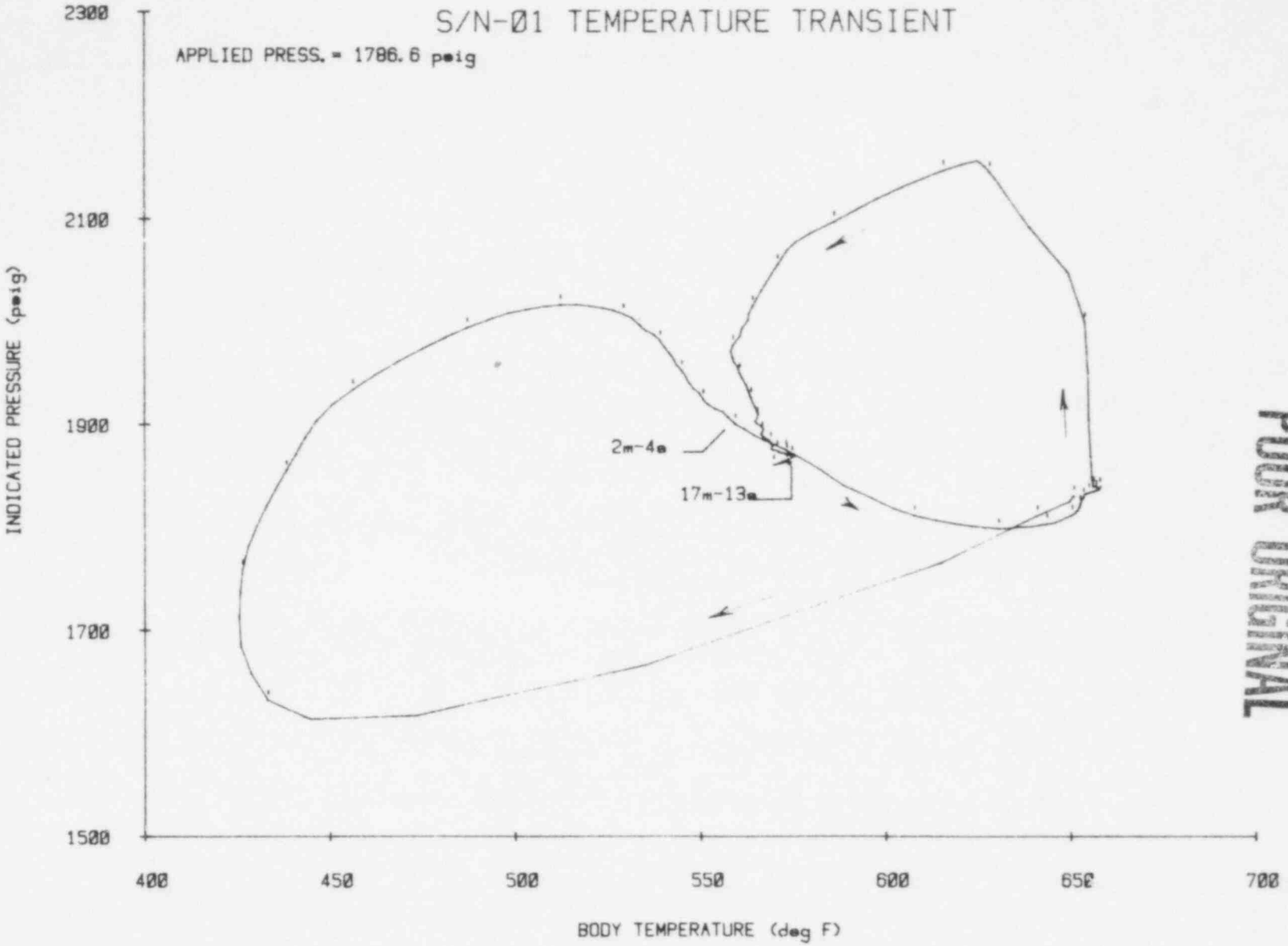

FIGURE VIII.49 Sensor Response During Rapid Depressurization of 650°F Water in Autoclave.

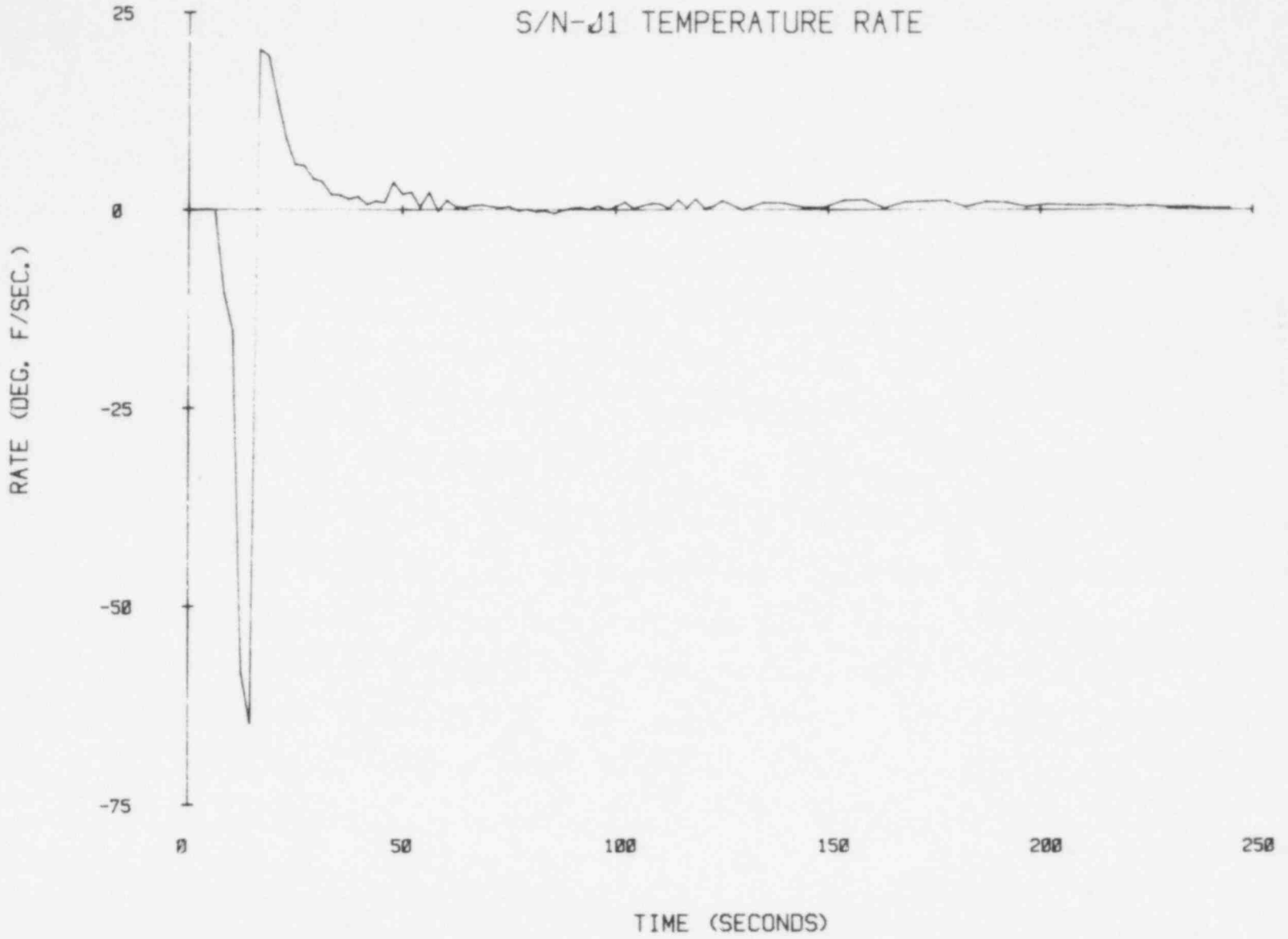

FIGURE VIII.50 Rate of Temperature Change for Blowdown of Figure VIII.49.

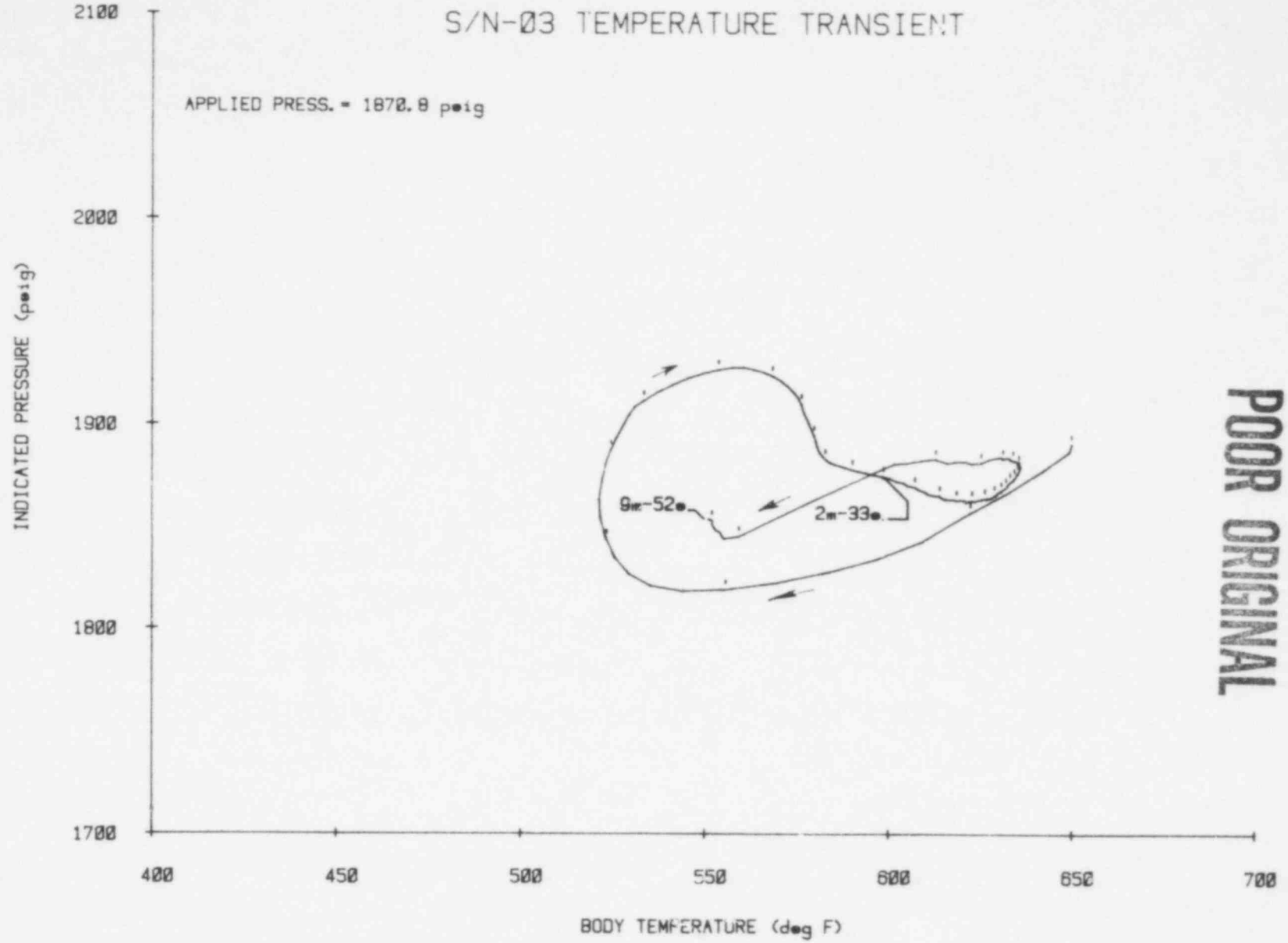

FIGURE VIII.51 Sensor Response During Rapid Depressurization of 650°F Water in Autoclave.

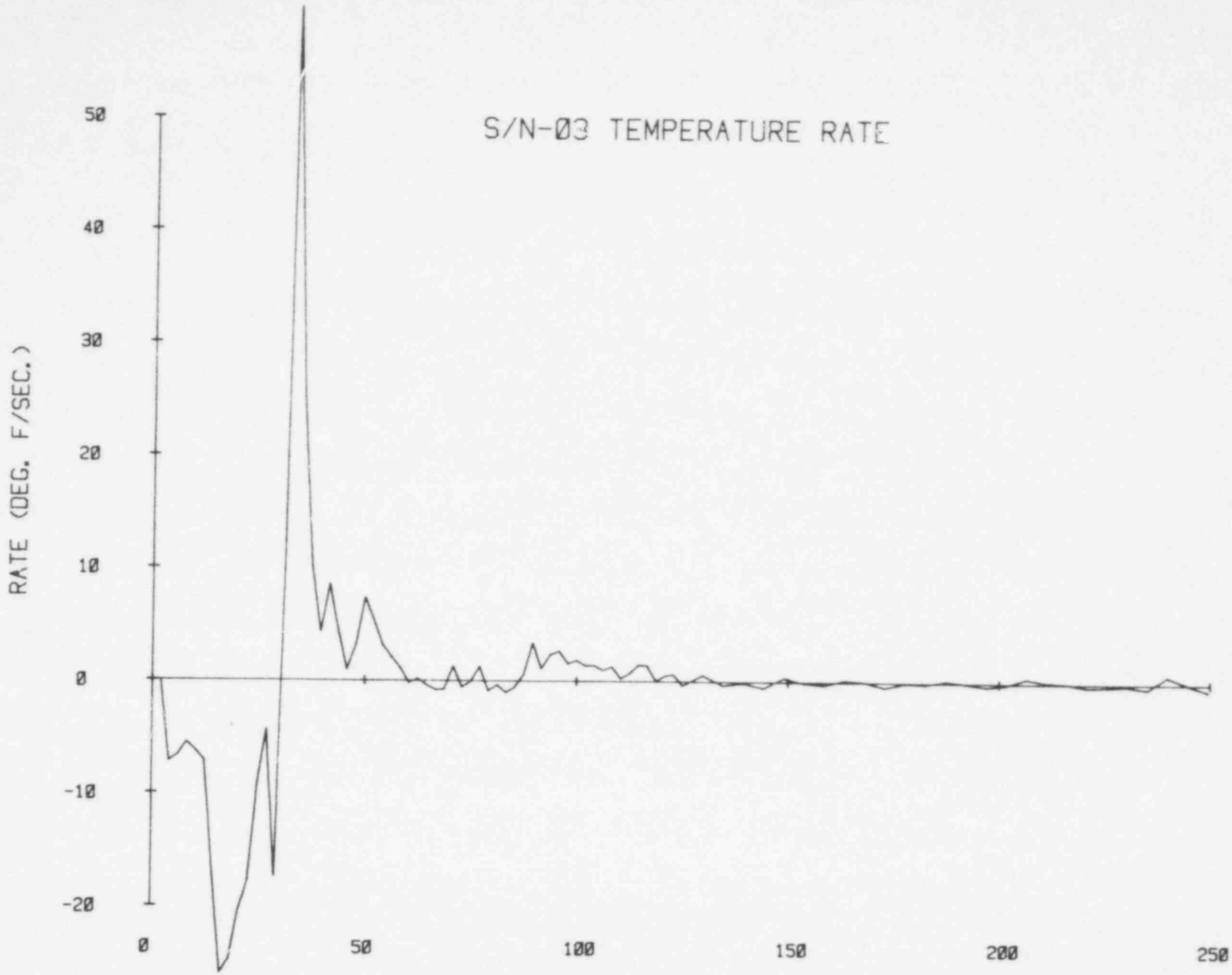

FIGURE VIII.52 Rate of Temperature Change for Blowdown of Figure VIII.51.

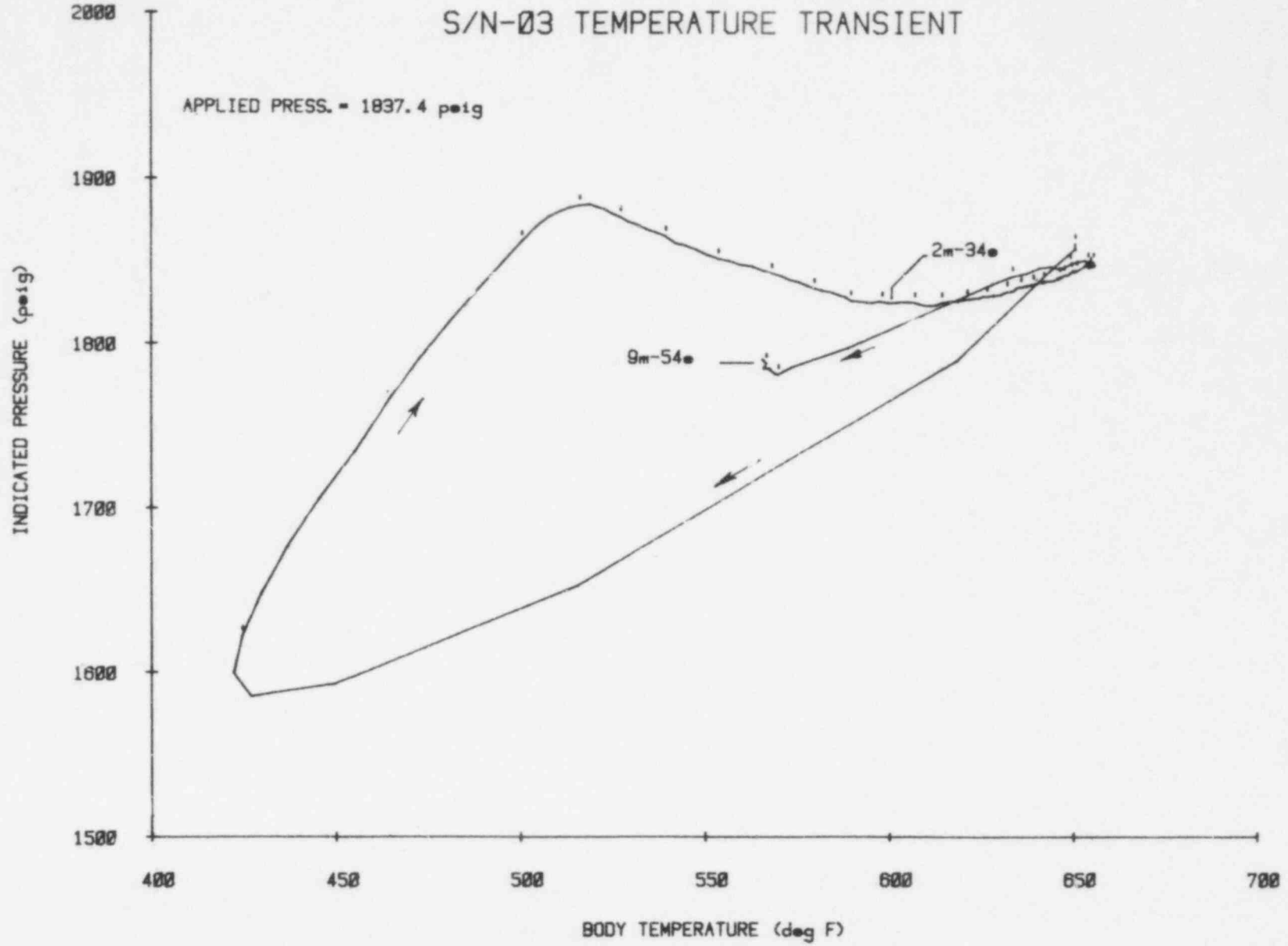

FIGURE VIII.53 Sensor Response During Rapid Depressurization of 650°F Water in Autoclave.

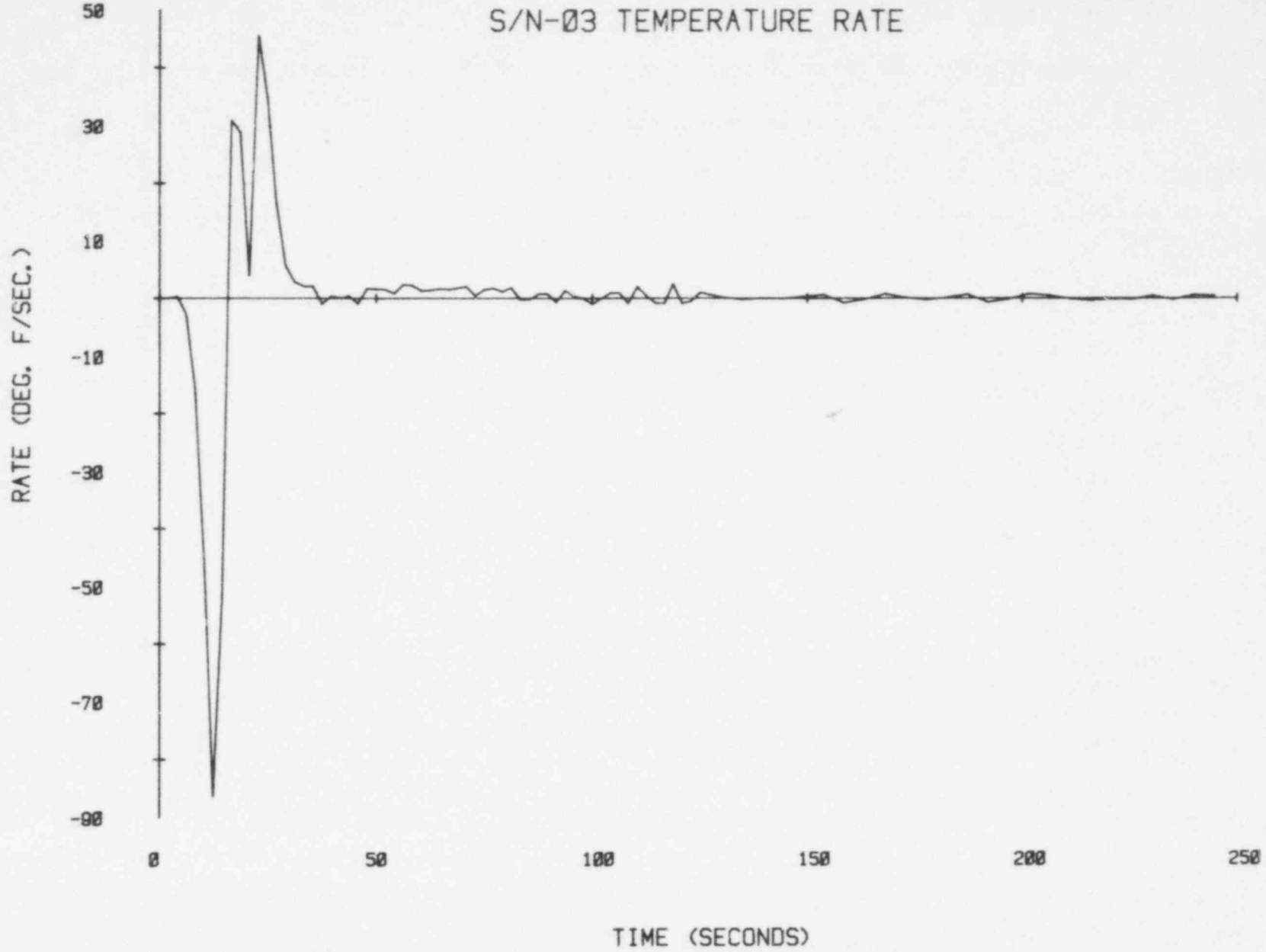

FIGURE VIII.54 Rate of Temperature Change for Blowdown of Figure VIII.53.

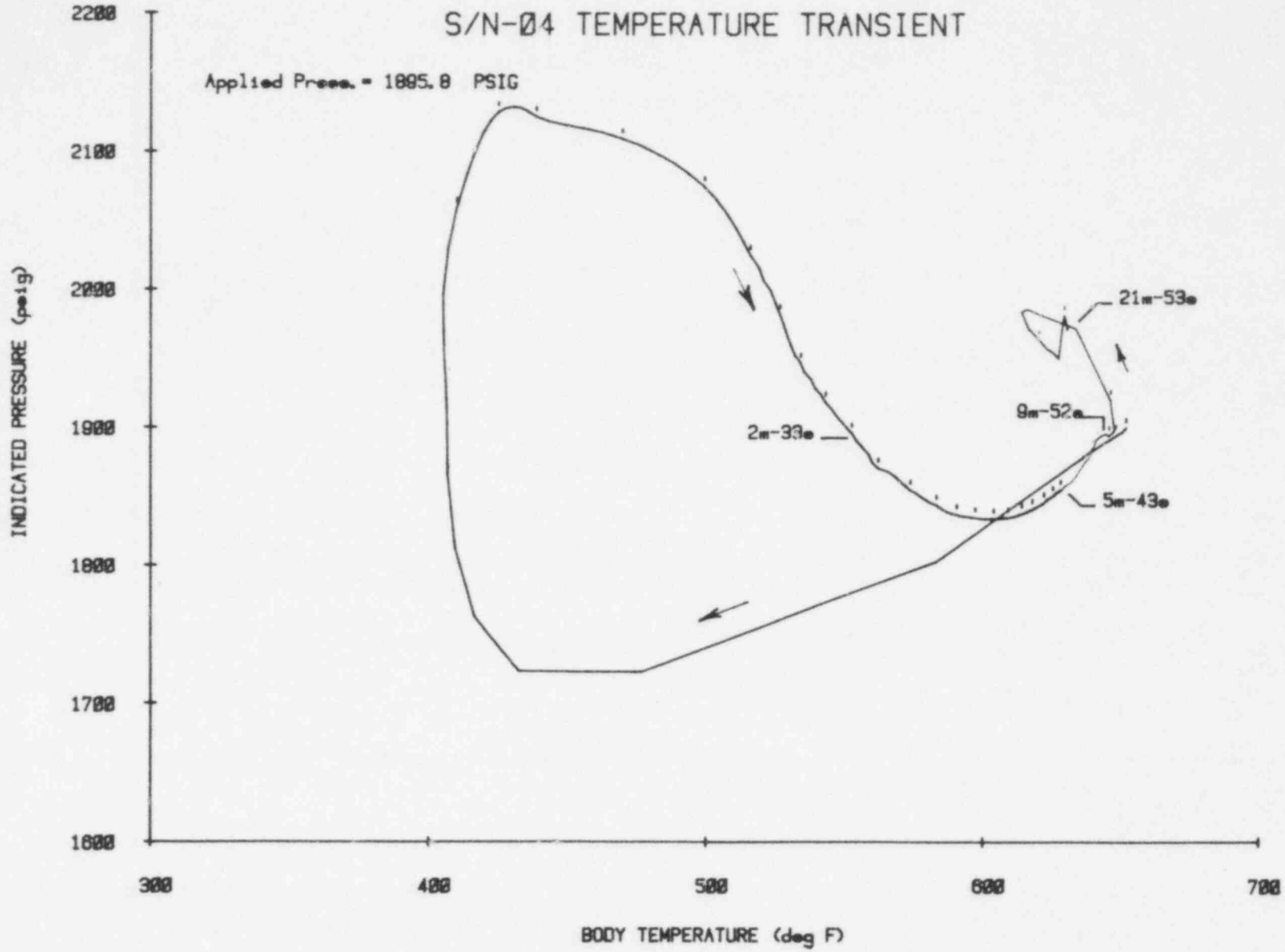

FIGURE VIII.55 Sensor Response During Rapid Depressurization of 650°F Water in Autoclave.

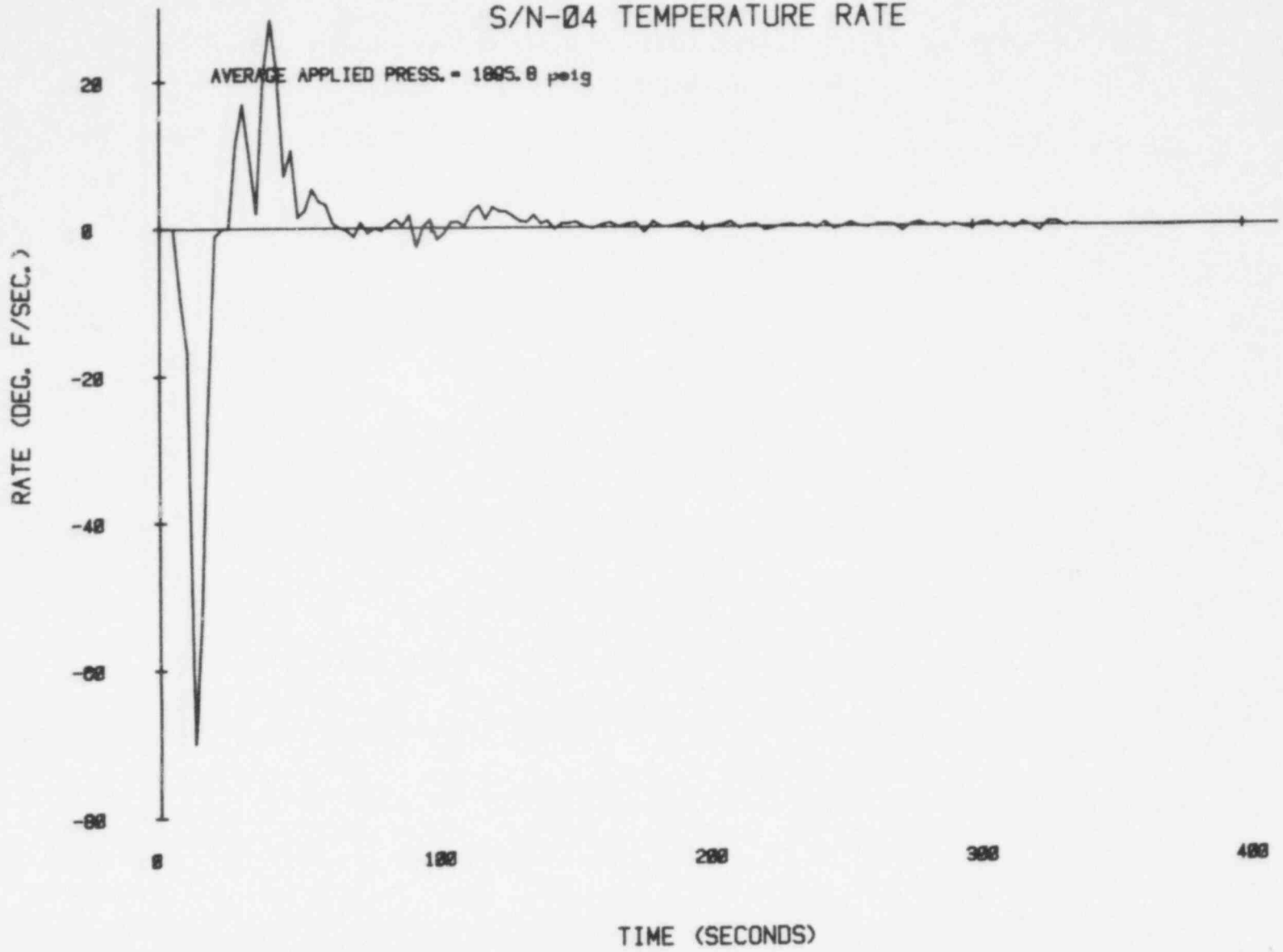

FIGURE VIII.56 Rate of Temperature Change for Blowdown of Figure VIII.55.

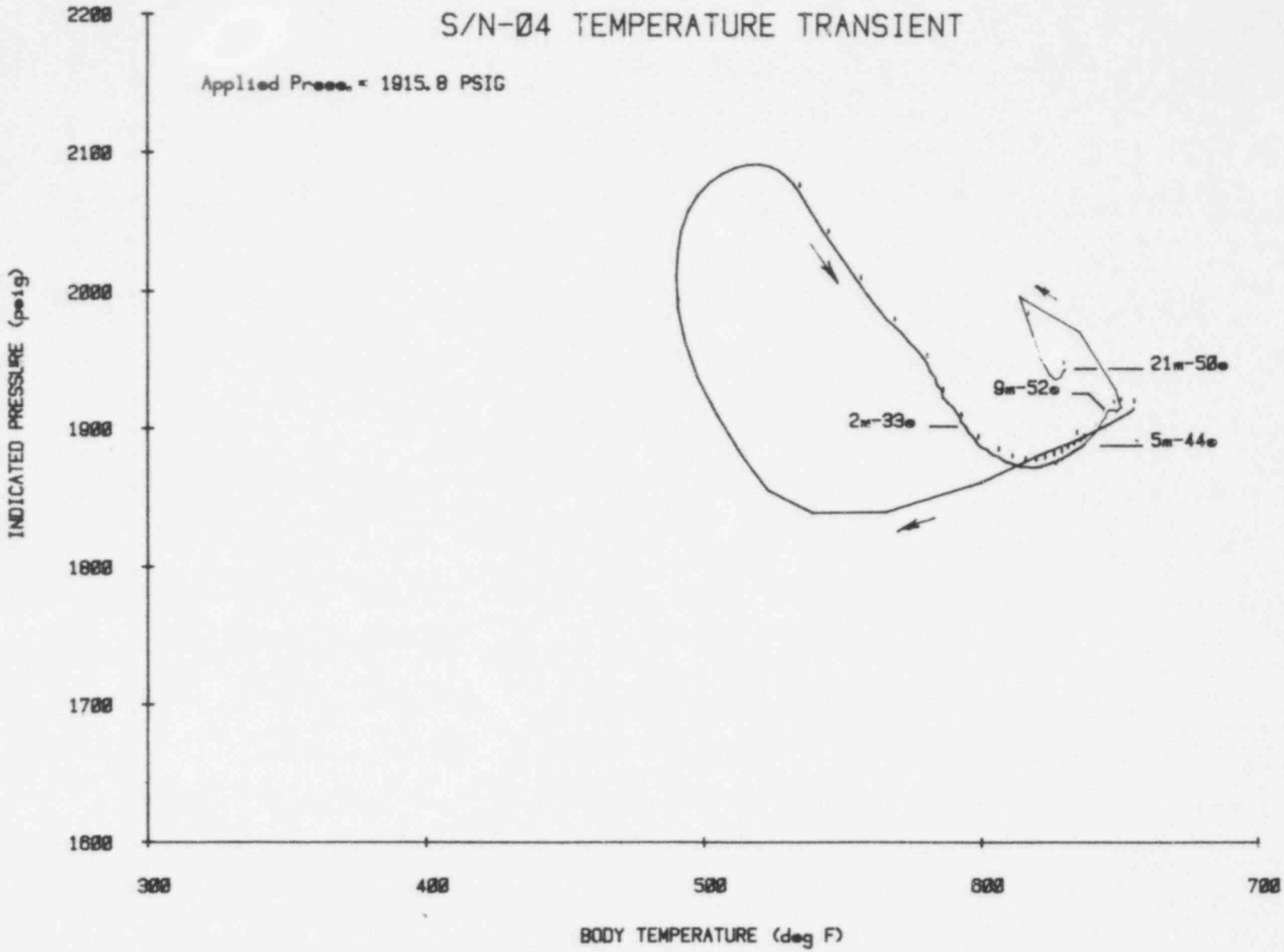

FIGURE VIII.57 Sensor Response During Rapid Depressurization of 650°F Water in Autoclave.

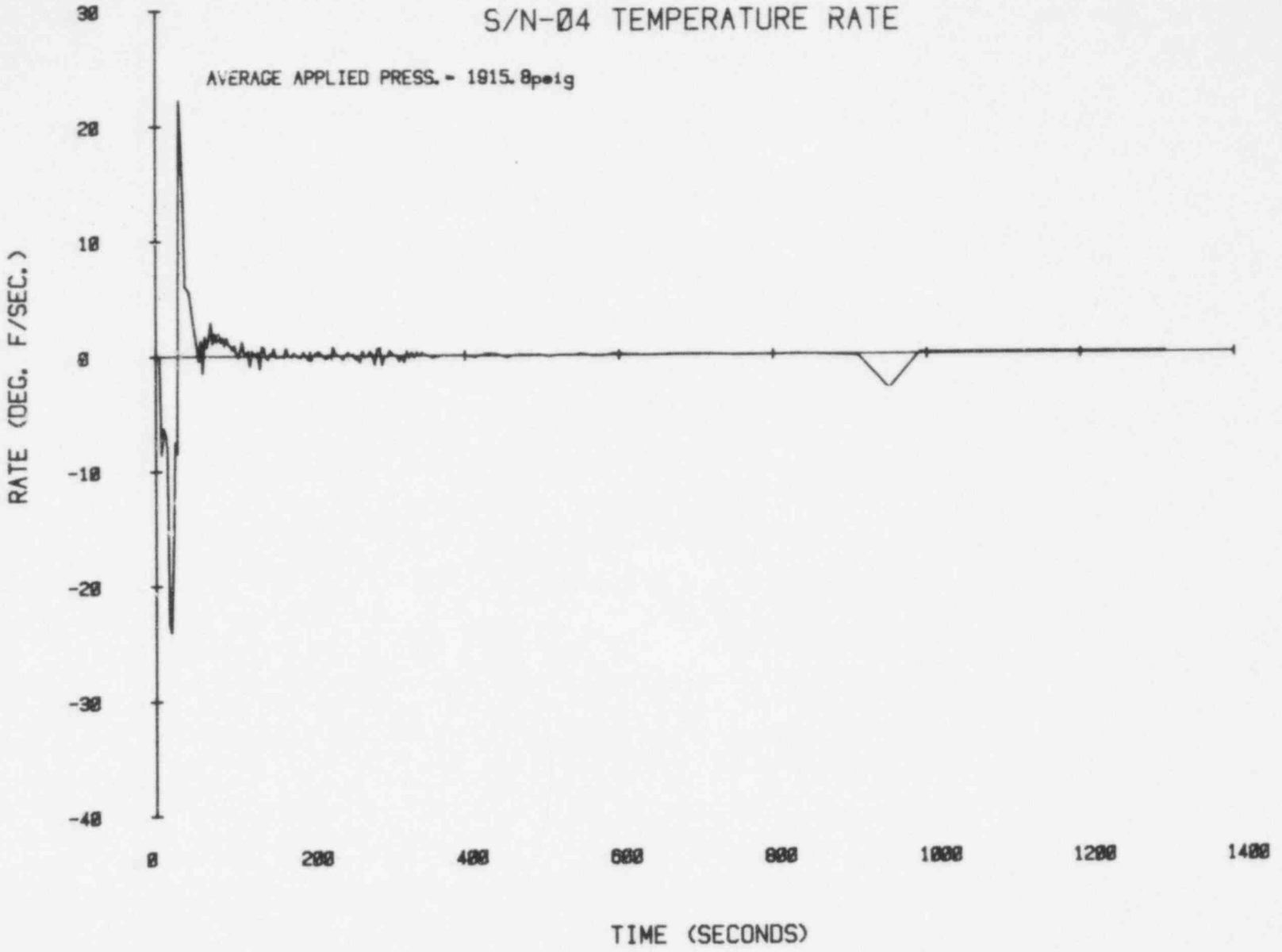

FIGURE VIII.58 Rate of Temperature Change for Blowdown of Figure VIII.57.

NUREG/CR-0836
HEDL-TME 79-33
R3

DISTRIBUTION

R3 (381)

DOE/RL (3)

Manager
Chief Patent Attorney
W. A. Burns

DOE/FFTFPO (1)

R. A. Graham

EG&G
P.O. Box 1625
Idaho Falls, ID 83401 (8)

R. E. Williams (7)
T. G. Faucett

EXXON Nuclear Co. Inc.
2955 Geo Wash Way
Richland, WA 99352 (1)

B. S. Flora

HEDL
c/o P. A. Thurman
Supervisor, Document Processing
P.O. Box 1970
Richland, WA 99352 (22)

T. R. Billeter	(2)	W/A-56	
C. P. Cannon		W/A-56	
A. I. Y. Chan		W/A-56	
T. T. Claudson		W/C-15	
G. B. Vondruska		W/C-115	
C. T. Schaedel		W/B-126	
E. M. Sheen		W/A-56	
J. L. Stringer		W/A-56	
J. M. Yatabe		W/C-22	
Central Files	(10)	W/C-110	
Publ. Services	(2)	W/C-115	

Los Alamos Scientific Laboratory
P.O. Box 1663
Los Alamos, New Mexico 87545 (1)

NRC/HQ (3)

R. VanHouten
W. V. Johnston
G. D. McPherson

NRC/ID (1)

P. O. Strom

Kaman Sciences
1500 Garden of the Gods Road
Colorado Springs, CO 80933

Bruce DuVall

NRC FORM 335 (7-77)

U.S. NUCLEAR REGULATORY COMMISSION

BIBLIOGRAPHIC DATA SHEET

1. REPORT NUMBER *(Assigned by DDC)*
NUREG/CR-0836

TITLE AND SUBTITLE *(Add Volume No., if appropriate)*
Pressure Sensor for Use in the Loss-of-Fluid-Test (LOFT) Reactor

2. *(Leave blank)*

3. RECIPIENT'S ACCESSION NO.

AUTHOR(S)
T. R. Billeter

5. DATE REPORT COMPLETED
MONTH: July YEAR: 1979

PERFORMING ORGANIZATION NAME AND MAILING ADDRESS *(Include Zip Code)*
Hanford Engineering Development Lab
P. O. Box 1970
Richland, WA 99352

DATE REPORT ISSUED
MONTH: September YEAR: 1979

6. *(Leave blank)*

8. *(Leave blank)*

SPONSORING ORGANIZATION NAME AND MAILING ADDRESS *(Include Zip Code)*
Office of Nuclear Regulatory Research
U. S. Nuclear Regulatory Commission
Washington, D. C. 20555

10. PROJECT/TASK/WORK UNIT NO.

11. CONTRACT NO.
NRC FIN No. B6228

13. TYPE OF REPORT

PERIOD COVERED *(Inclusive dates)*

15. SUPPLEMENTARY NOTES

14. *(Leave blank)*

16. ABSTRACT *(200 words or less)*

This report summarizes development and qualification testing of pressure measurement instrumentation intended for use in the loss-of-fluid-test (LOFT) reactor. Tests at temperatures up to 800° F and pressures up to 2500 psig were conducted at Hanford Engineering Development Laboratory in the Loss-of-Fluid-Test (LOFT) reactor. Operational characteristics of the selected pressure transducers are summarized for a series of static, quasi-static, and transient tests conducted for a period of about 700 hours.

17. KEY WORDS AND DOCUMENT ANALYSIS

17a. DESCRIPTORS

17b. IDENTIFIERS/OPEN-ENDED TERMS

18. AVAILABILITY STATEMENT
Unlimited

19. SECURITY CLASS *(This report)*
Unclassified

21. NO. OF PAGES

20. SECUPITY CLASS *(This page)*
Unclassified

22. PRICE
$

NRC FORM 335 (7-77)